Danno da radiazione in rivelatori al silicio

Mara Bruzzi

INFN, University of Florence, Italy

- ✓Richiami sui rivelatori a semiconduttore
- ✓Ambienti operativi e livelli di irraggiamento
- ✓Danno da radiazione microscopico
- ✓Danno da radiazione macroscopico
- ✓Aumento della resistenza al danno da radiazione
    - ✓ Material Engineering
    - ✓ Device Engineering
- ✓Conclusioni

Principio di funzionamento di un rivelatore

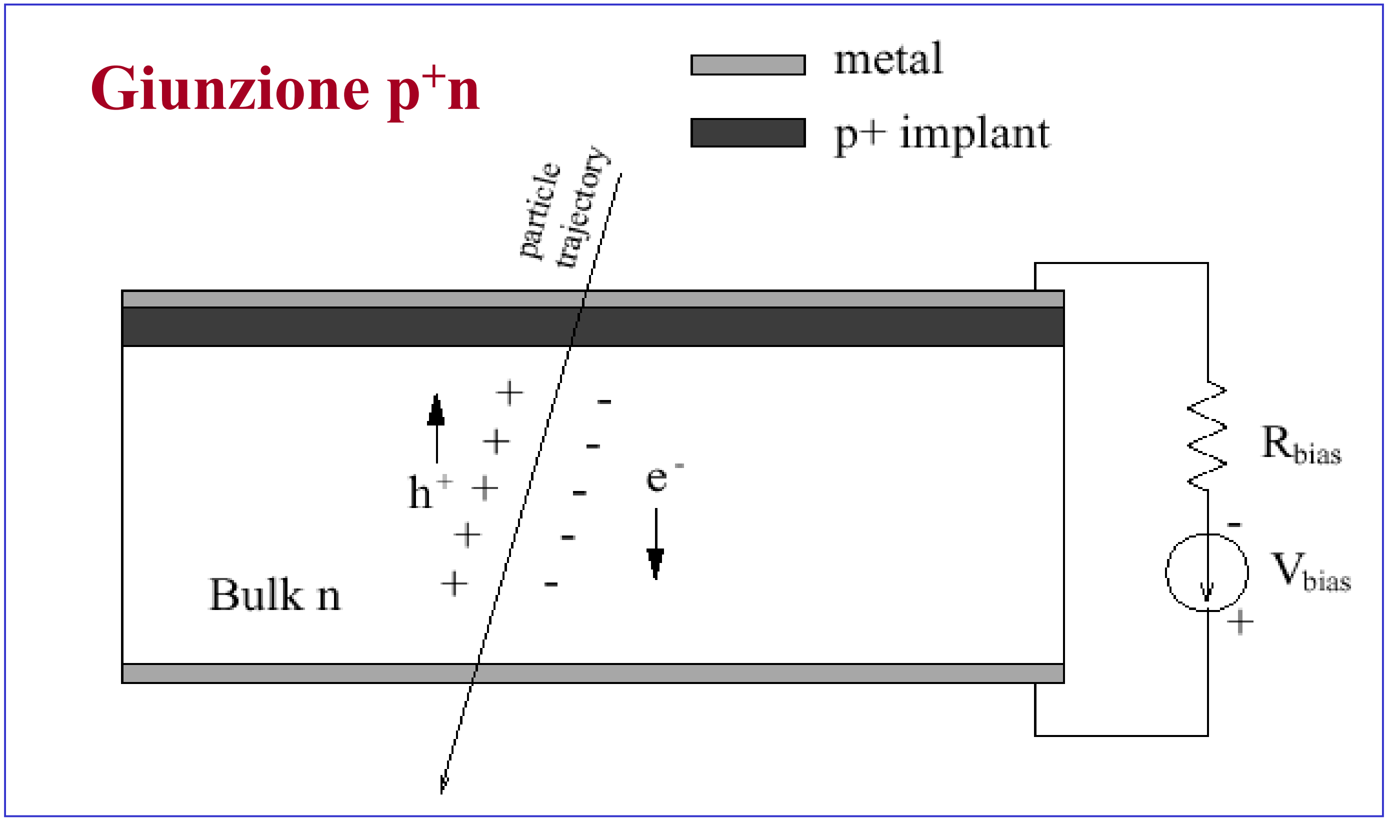

Giunzione p^+n

Contatto ohmico

Isolante $\rho > 10^{10}\Omega$cm

Contatto ohmico

Contatto Schottky

Semiconduttore tipo n o p

Contatto ohmico

Materiali semiconduttori / isolanti per la rivelazione di radiazione

Property	Diamond	4H SiC	Si
Bandgap [eV]	5.5	3.3	1.12
Breakdown Field [V/cm]	10^7	$4 \cdot 10^6$	$3 \cdot 10^5$
Electron mobility [cm^2/Vs]	1800	800	1450
Hole mobility [cm^2/Vs]	1200	115	450
Saturation velocity [cm/s]	$2.2 \cdot 10^7$	$2 \cdot 10^7$	$0.8 \cdot 10^7$
Effective atomic number Z_{eff}	6	~10	14
Dielectric constant ε_r	5.7	9.7	11.9
e-h creation energy [eV]	13	8.4	3.6
minority carrier lifetime [s]	10^{-9}	$5 \cdot 10^{-7}$	$2.5 \cdot 10^{-3}$
Wigner Energy [eV]	43	25	13-20

Bassa corrente di fuga

Elevata resistenza al danno da radiazione?

Sensibilità elevata

Generalita' sui materiali conduttori ed isolanti

Struttura cristallina del diamante (C, Ge, Si, etc.):
due reticoli cubici FCC traslati lungo la diagonale di corpo

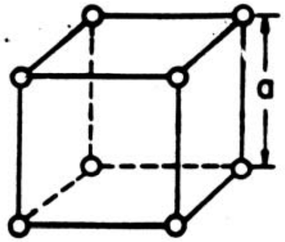

Cubico semplice

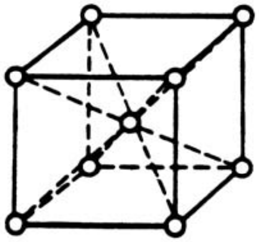

Cubico a corpo centrato

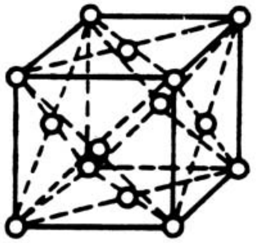

Cubico a facce centrate

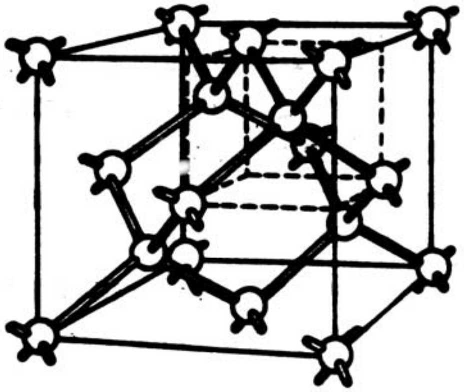

Diamante (C, Ge, Si, ..)

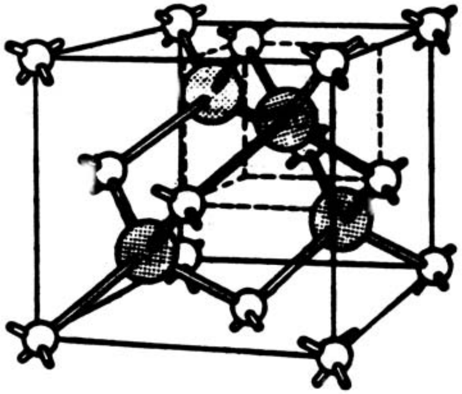

Zincoblenda (GaAs, GaP, ..)

Struttura cristallina polimorfa del SiC

La struttura reticolare del diamante è basata sul legame tetraedrico: un atomo centrale è circondato da 4 atomi primi vicini che giacciono ai vertici di un tetraedro. GaAs, Si, diamante hanno struttura Zincoblenda (b). CdS, ZnS hanno struttura wurtzite, esagonale dove ancora il legame è tetraedrico ma lo strato superiore di atomi non è ruotato di 60° come nella zincoblenda (a).

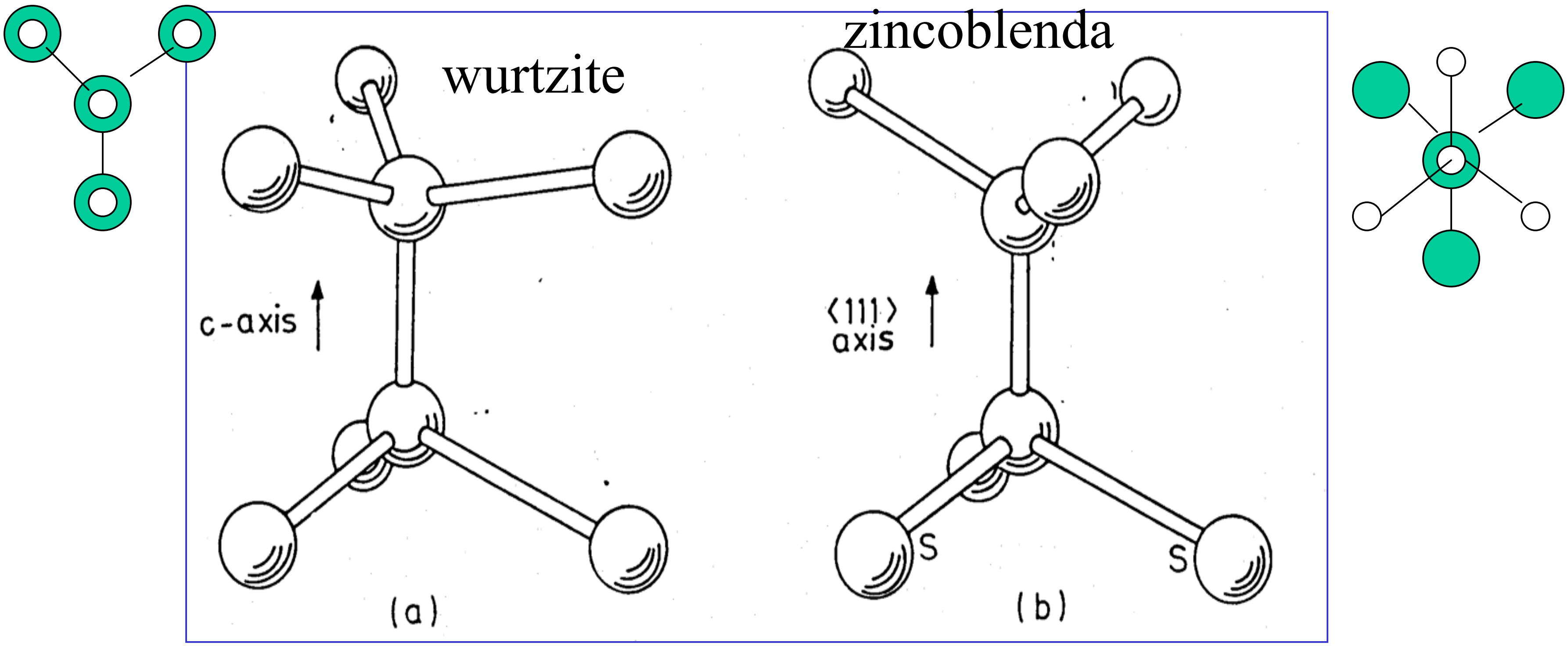

Politipismo del SiC

Si hanno vari arrangiamenti con diversa percentuale di esagonalità a seconda di come si dispongono le sequenze di atomi si e C lungo l’asse c. La struttura che si ottiene può essere cubica, esagonale o romboedrica.

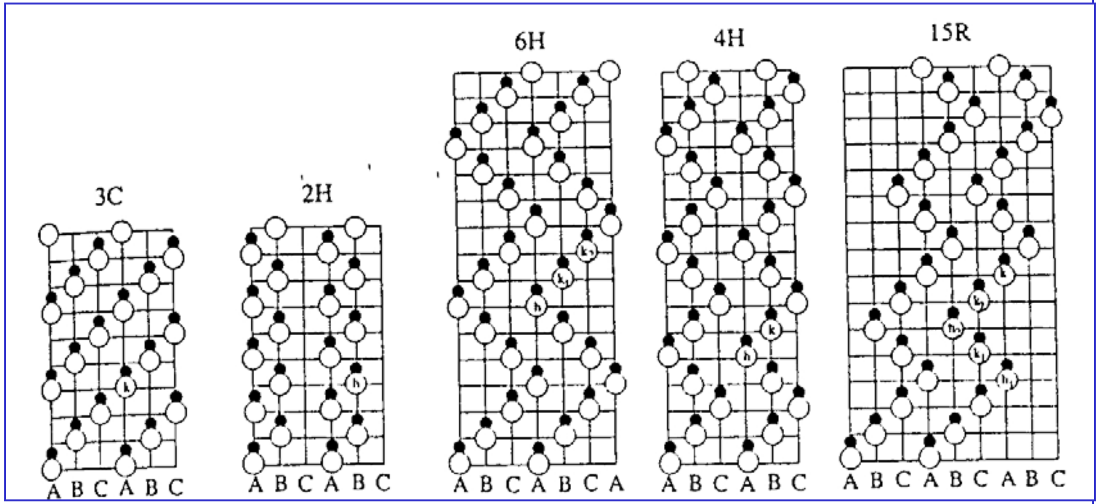

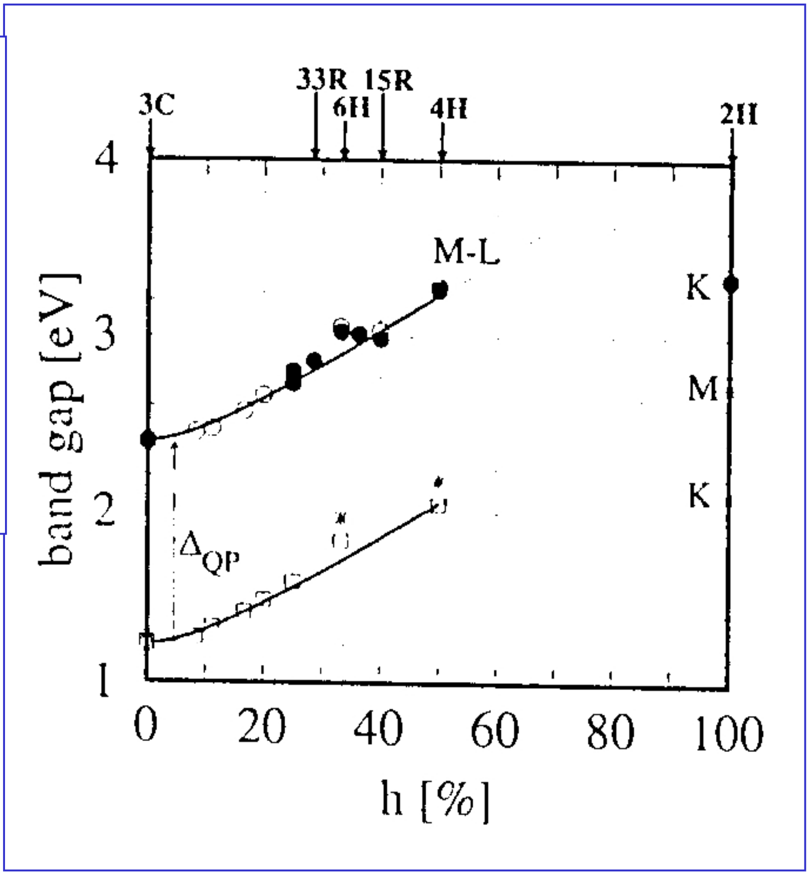

Il gap dipende dalla percentuale di esagonalità

Giunzione p-n

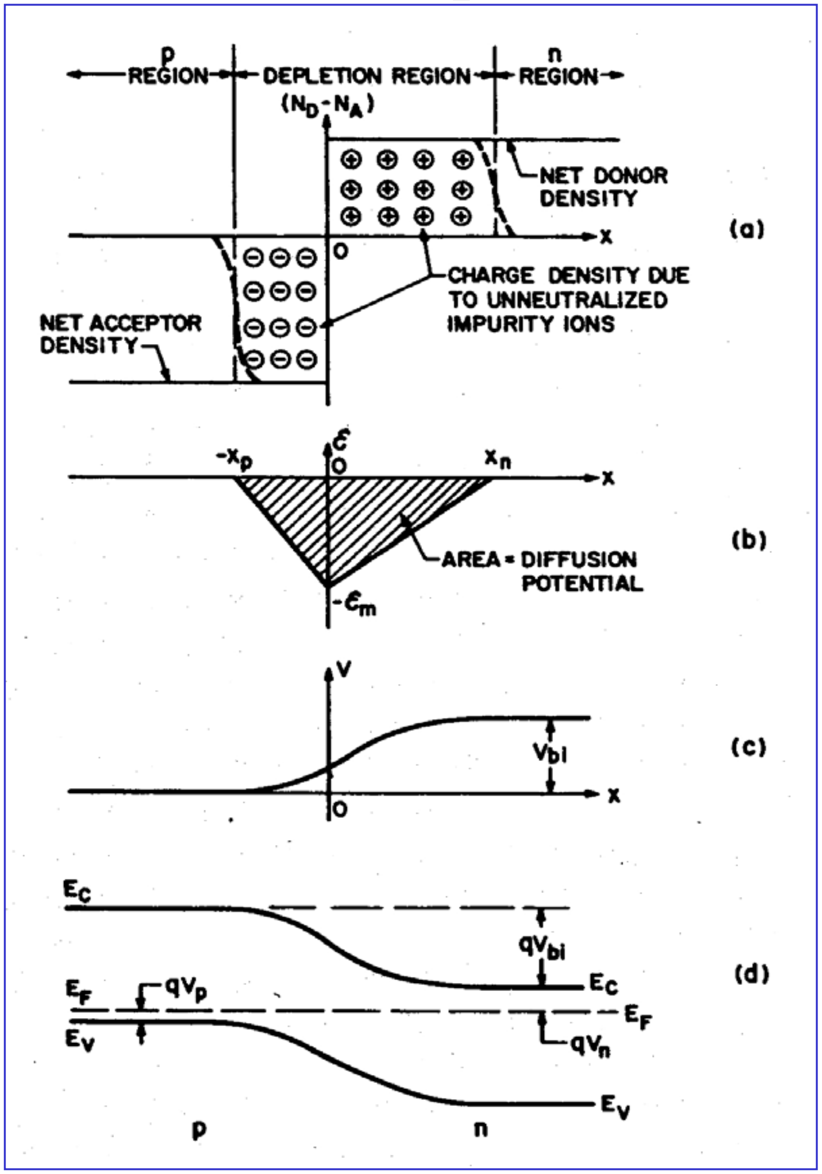

Giunzione Schottky

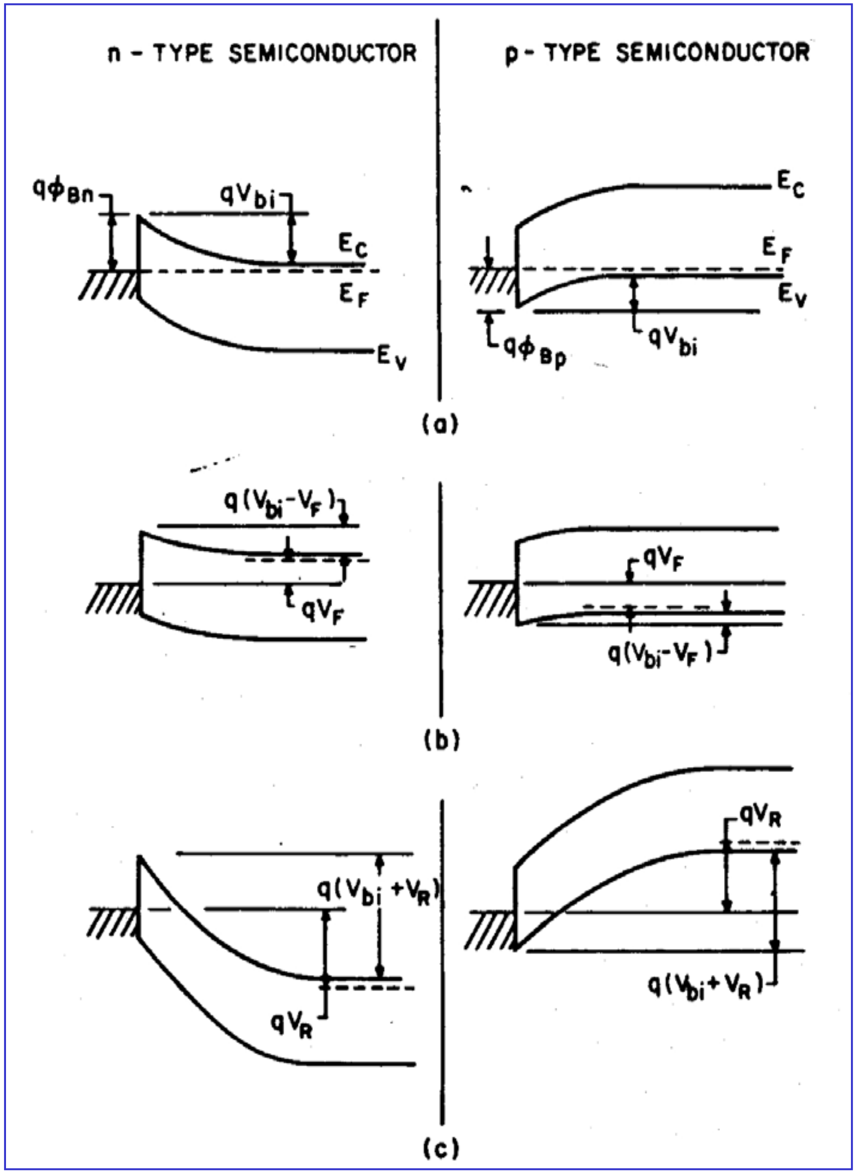

Grandezze fisiche di rilievo per la giunzione Schottky o p-n

Corrente di fuga

$$J_{inversa} = \frac{1}{2} q \frac{n_i}{\tau_0} W \alpha \sqrt{V_{rev}}$$

Corrente diretta

$$J_{diretta} \alpha \qquad e^{qV/nKT}$$

Capacita'

$$C = \frac{\varepsilon \cdot Area}{d}$$

spessore della regione svuotata

$$d = \sqrt{\frac{2\varepsilon}{qN_{eff}}(V_{rev} + V_{built-in})}$$

Concentrazione di carica fissa nella regione svuotata

$$N_{eff} = \frac{2 \cdot \varepsilon \cdot V_{dep}}{q \cdot W^2}$$

Resistivita'

$$\rho = \frac{1}{q \cdot \mu \cdot N_{eff}}$$

Corrente Inversa

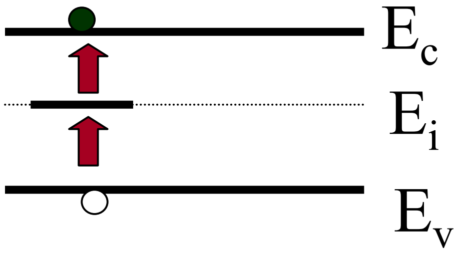

dovuta principalmente alla presenza di centri di generazione/ricombinazione a meta' gap

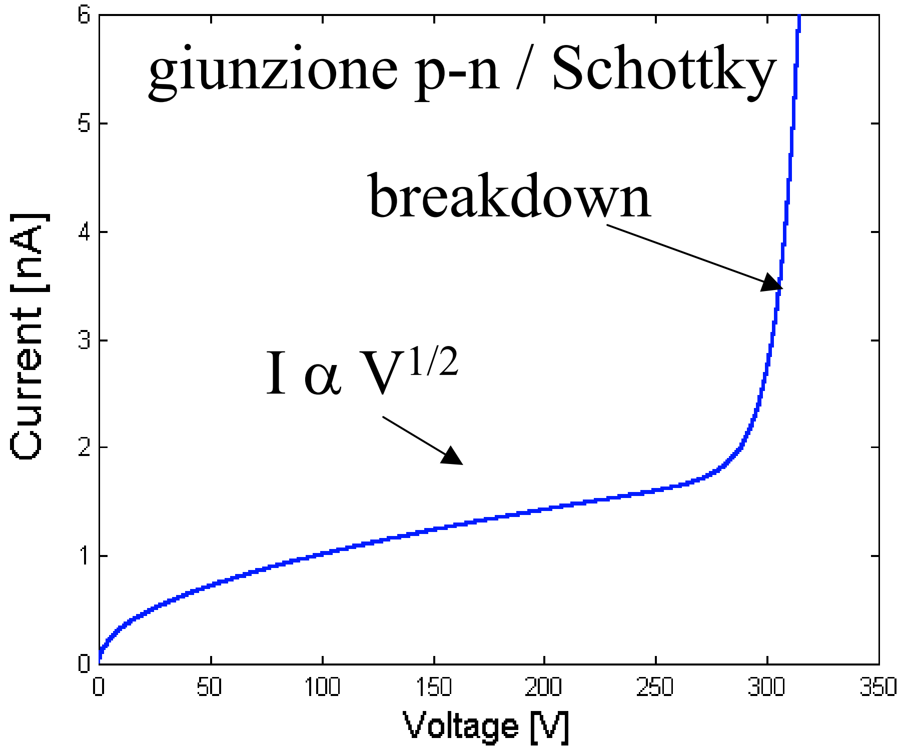

$$J_{gen} \alpha T^2 \cdot e^{-E_g/2kT}$$

La corrente di fuga varia di ordini di grandezza al variare del gap del materiale. Per SiC e diamante densita' tipiche di corrente < 1pA/cm^2

Capacità della giunzione

bassa tensione di completo svuotamento → basso valore di N$_{eff}$ → elevata resistivita' di bulk

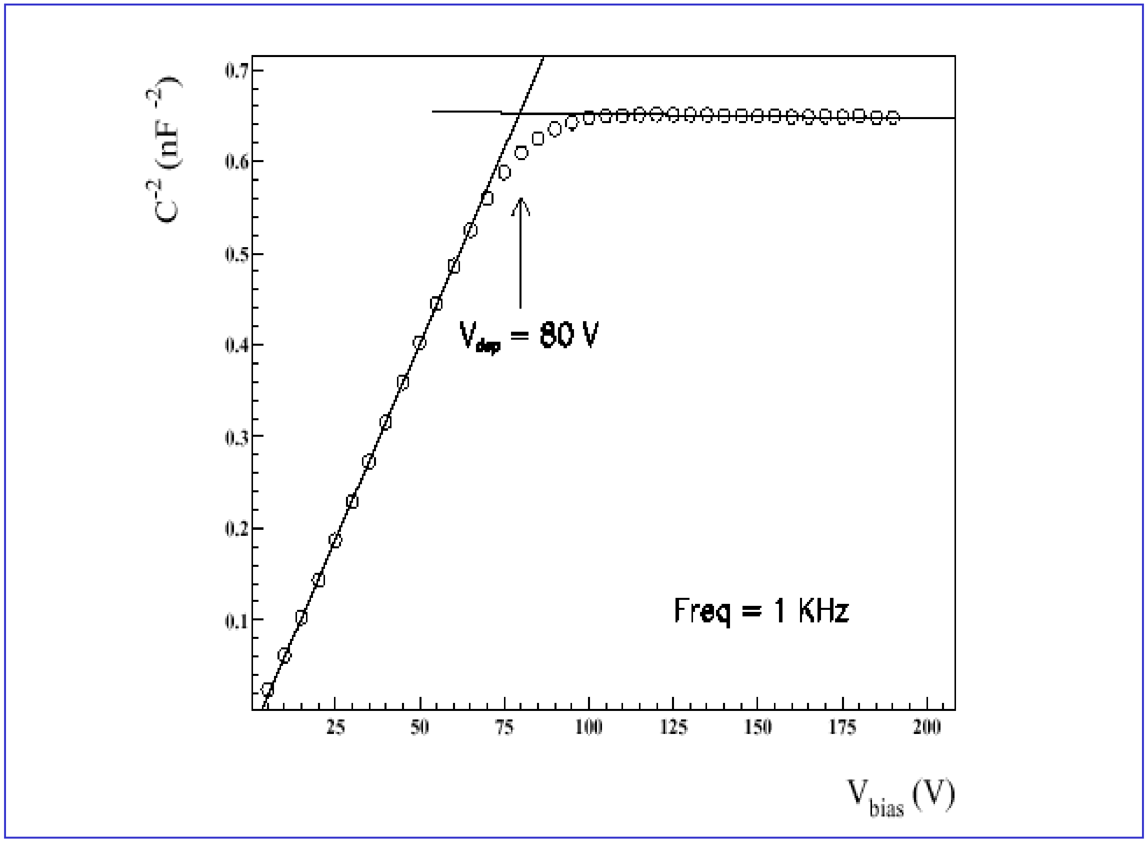

$$N_{eff} = \frac{2\varepsilon V_{dep}}{qd^2}$$

$$C(V) = \frac{\varepsilon A}{W(V)} = \sqrt{\frac{\varepsilon \cdot N_{eff}}{2V_{rev}}} A$$

Regione attiva del rivelatore

W = larghezza di svuotamento $\quad$ R_p = range della particella

L = lunghezza di diffusione minoritari

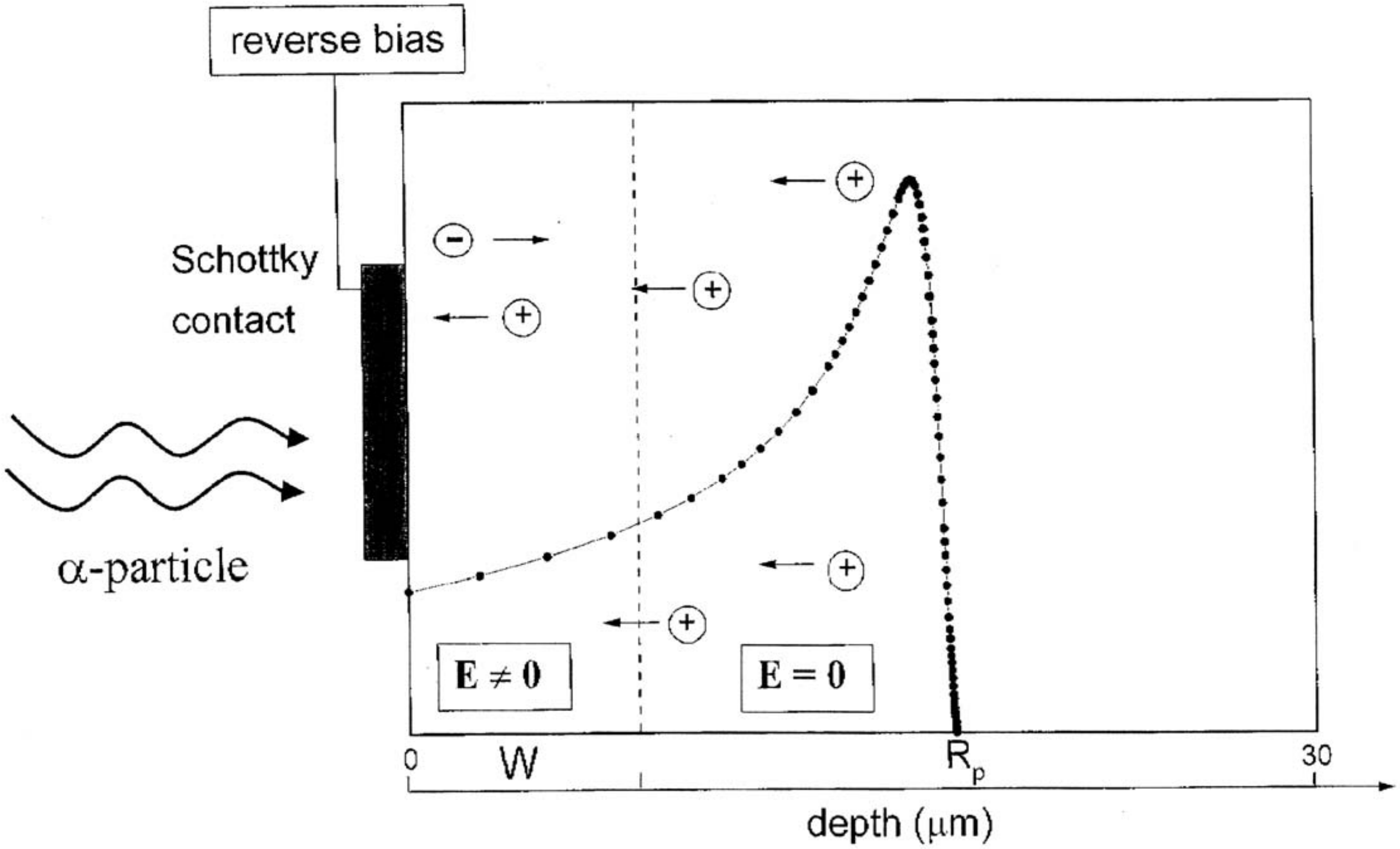

Si puo' avere contributo al segnale per la diffusione dei portatori minoritari che vengono creati in R_p all'interno della regione neutra

Caratteristiche importanti in un rivelatore di radiazione

- Elevato segnale / sensibilita' (corrente / carica)
- Basso rumore
- minimo ingombro spaziale / massimo volume attivo
- Elevata velocita' di risposta: v =μE
- Stabilita' con la dose accumulata

- Bassa energia per creazione coppia e-h → gap piccolo
- Bassa corrente di buio → gap elevato
- Bassa tensione di completo svuotamento
- Elevata mobilita'
- Elevata resistenza al danno da radiazione

Energia necessaria per creare una coppia e-h

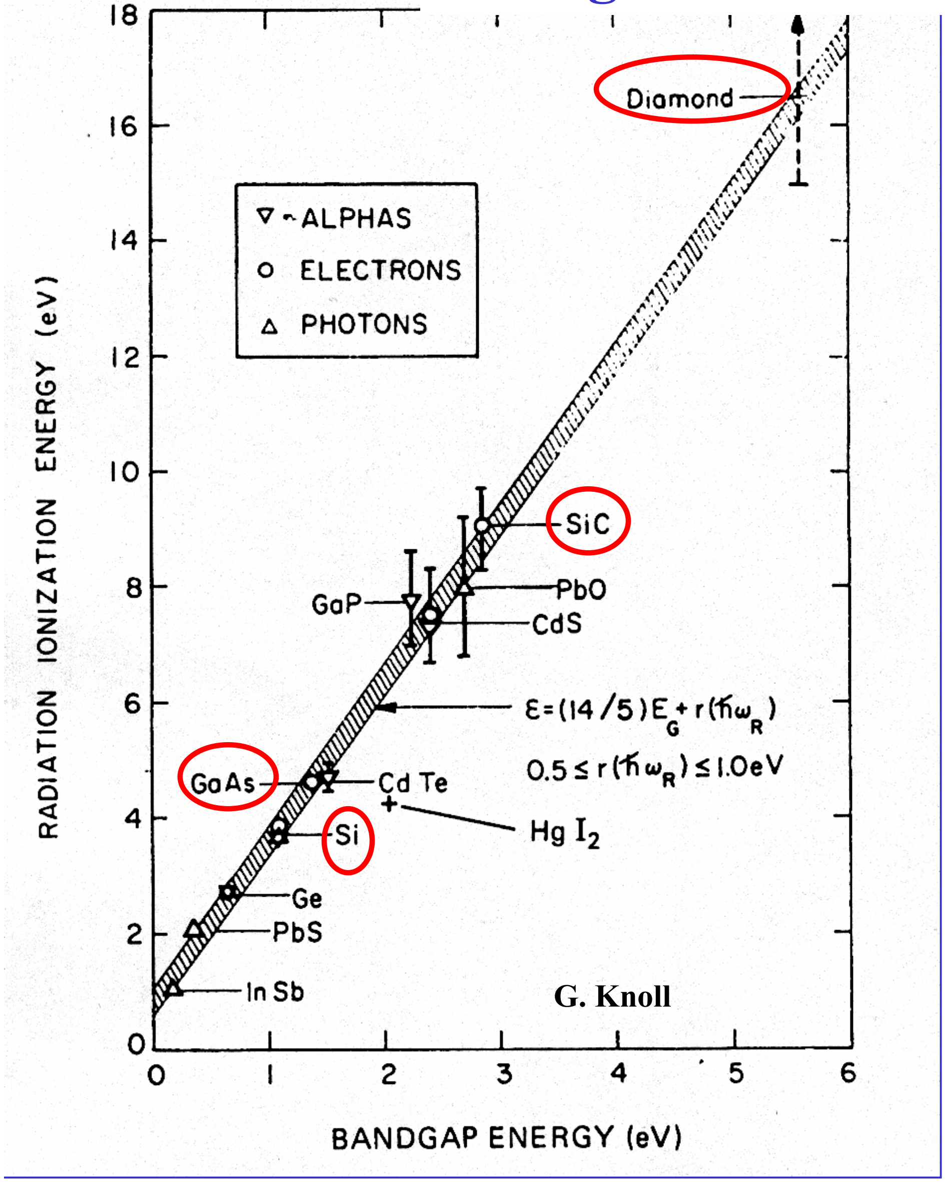

G. Knoll

$$E = 1.76eV + 1.84 \cdot E_g$$

Particella al minimo di ionizzazione (mip)

Coppie e-h per 300μm:

Silicio:	24.000
SiC :	15.300
Diamante :	10.800

Rivelatore di posizione a microstrip

Float Zone Silicon ρ = 1-6 kΩcm
Orientazione <111>, <100>
thickness ~ 300μm module length ≈ 10cm strip width *w* ≈15 μm, pitch *p* ≈ 50-200μm.

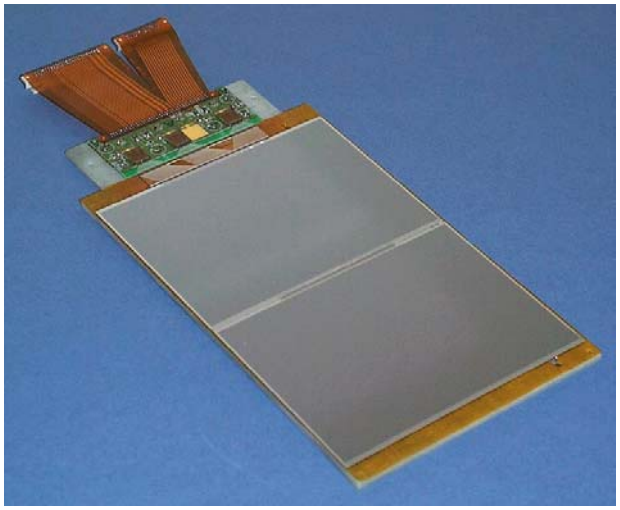

🟦 Al
🟪 B p^+
🟩 P n^+
⬛ n-type Si
🟨 $SiO_2 + Si_3N_4$

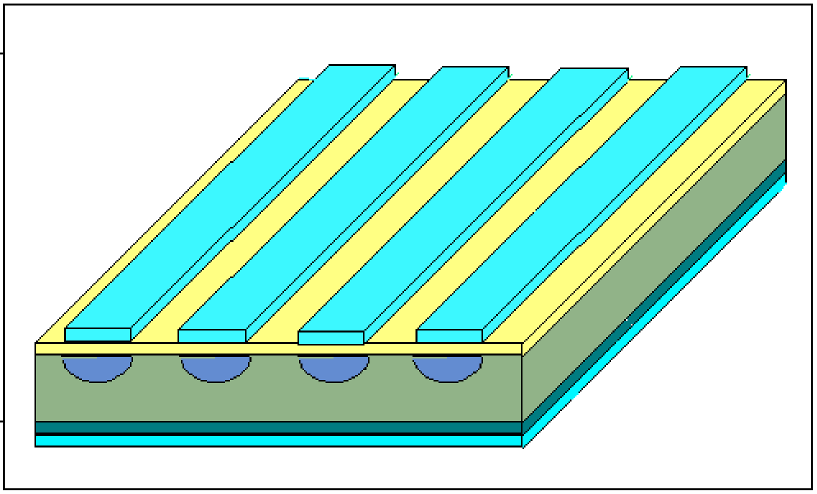

Ambienti operativi e livelli di irraggiamento

High energy Physics experiments at Large Hadron Collider (LHC)

p-p collision $E_{cm} = 14 \text{TeV}$

$\boldsymbol{L} \sim 10^{34}\ \text{cm}^{-2}\ \text{s}^{-1}$

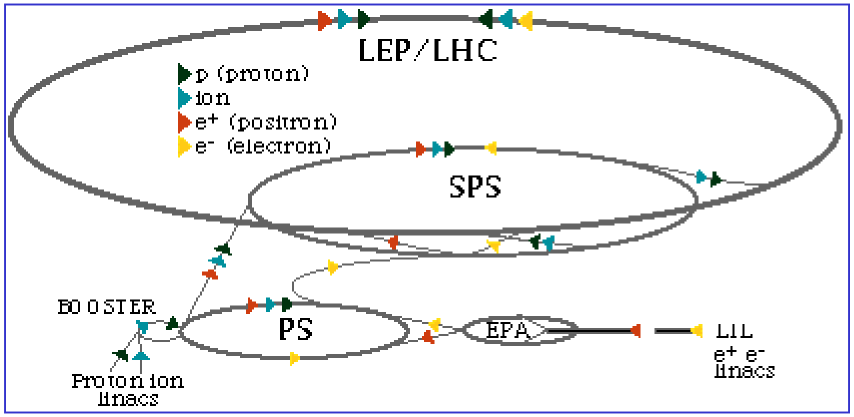

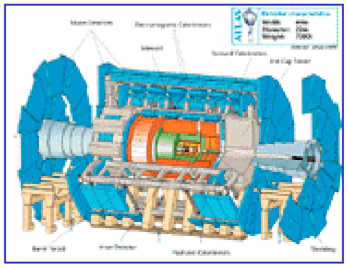

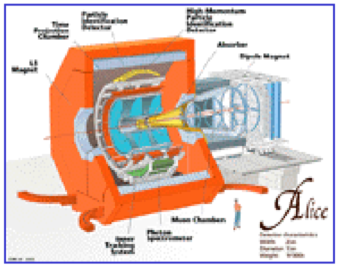

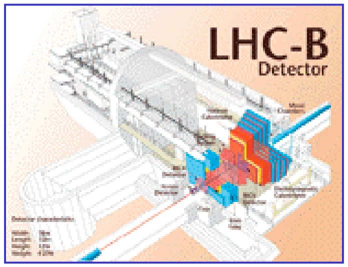

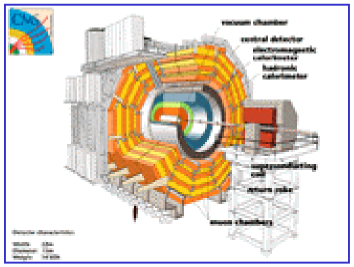

Livelli di radiazione in LHC

- Requirement: To operate the detector up to 10 years of LHC with a S/N > 10
- Major issue: Radiation hardness

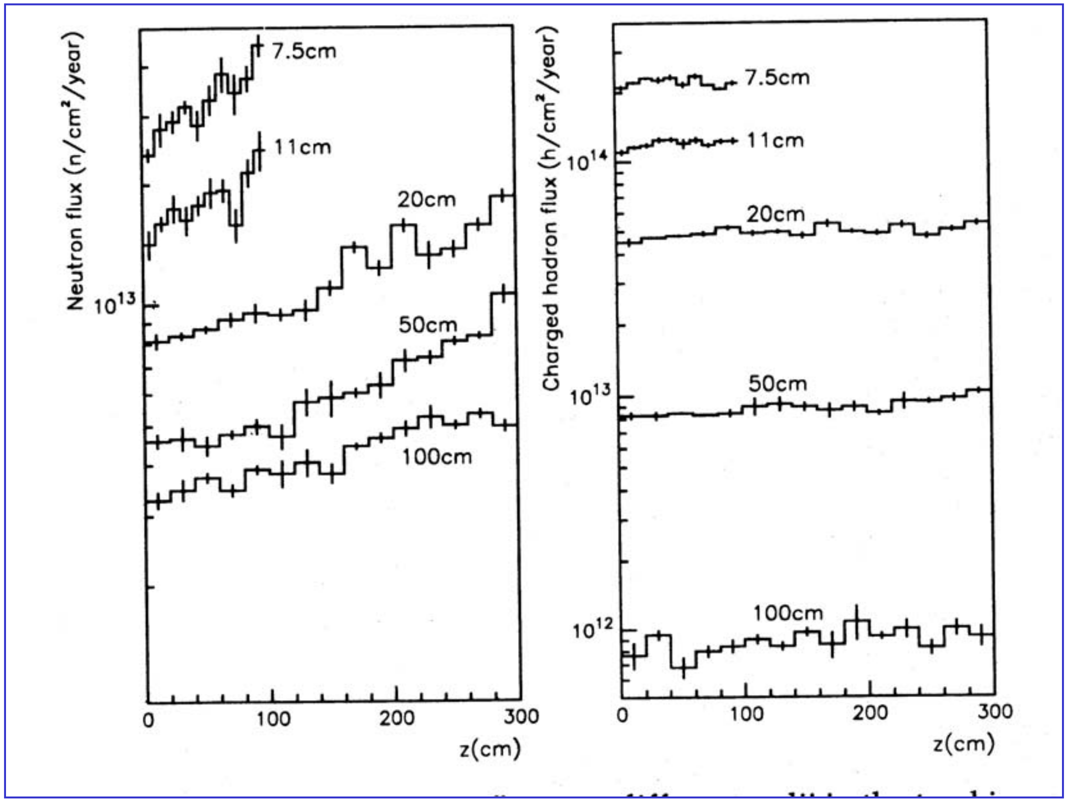

10 years-lifetime

p, n, π, e irradiation

f ~ 10^{14} cm^{-2} microstrips

f ~ 10^{15} cm^{-2} pixels

Possible upgrade of LHC
SuperLHC

	LHC	sLHC
√s [TeV]	14	14
Luminosity [cm $^{-2}$s^{-1}]	10^{34}	10^{35}
Bunch spacing Δt [ns]	25	12.5/25
σ_{pp} (inelastic) [mb]	~ 80	~ 80
# interactions/x-ing	~ 20	~ 100/200
$dN_{ch}/d\eta$ per x-ing	~ 150	~ 750/1500
$<E_T>$ charg. Part. [MeV]	~ 450	~ 450
Tracker occupancy *	1	5/10
Dose central region *	1	10
LAr Pileup Noise [MeV]	300	950
μ Counting Rate [kHz]	1	10

* Normalized to LHC values: 10^4 Gy/year R=25 cm

H. Sadrozinski, presented to RESMDD 04 , Florence october 2004

Anticipated Radiation Environment for Super LHC

Hadron fluence and radiation dose in different radial layers of the CMS tracker for an integrated luminosity of 2500fb^{-1}.
(Giannotti et al. CERN-TH/2002-078)

Radius (cm)	Fluence of fast hadrons [cm^{-2}]	Dose [KGy]
4	1.6×10^{16}	4200
11	2.3×10^{15}	940
22	8.0×10^{14}	350
75	1.5×10^{14}	35
115	1.0×10^{14}	9.3

The tracker volume can be split into 3 radial regions:

1.	**R > 60cm**	**improved Si strip technology**
2.	**20cm < R < 60cm**	**improved hybrid pixel technology**
3.	**R < 20cm**	**new approaches and concepts are required**

ATLAS ID Upgrade

H. Sadrozinski, presented to RESMDD 04 , Florence october 2004

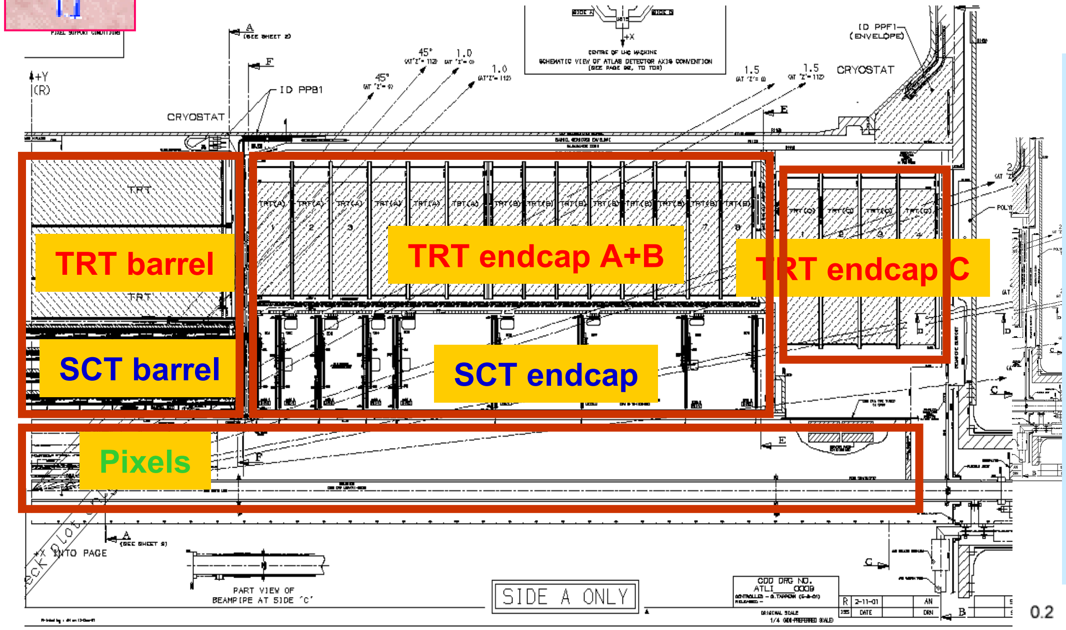

ATLAS Upgrade Steering Group

US-ATLAS Upgrade Program:

- Strip Electronics (SiGe)
- Module Integration
- Short strips (p-type and 2D)
- 3D detectors
- Pixel electronics

Replace entire ID ($200m^2$)

Keep Modularity
-> (Pixels, Barrel, 2 endcaps)
Catch up with CMS:
-> replace gaseous TRT detectors
Find Rad-hard Sensors
Optimize Sensor Geometry
Increase Multiplexing

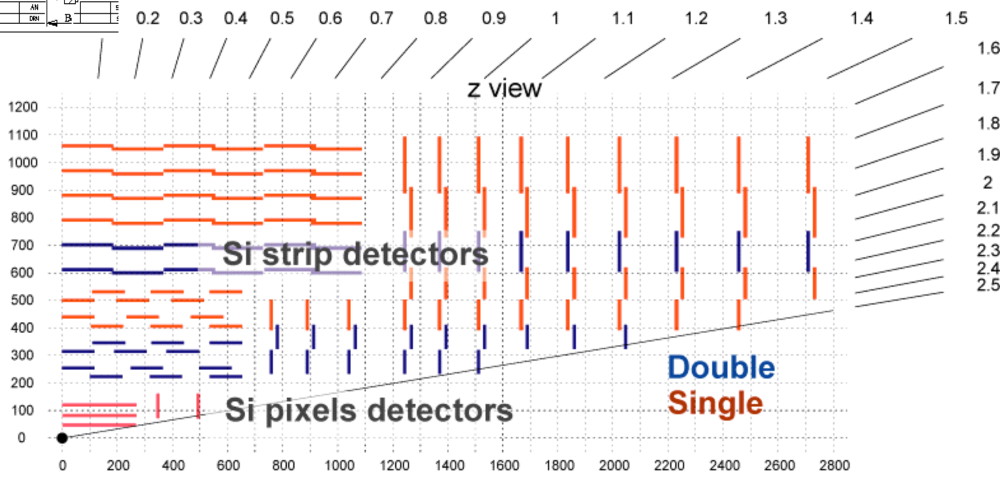

The layout of the CMS inner tracker

sATLAS Tracker Regions

H. Sadrozinski, presented to RESMDD 04 , Florence october 2004

- **Integrated Luminosity**
- **(radiation**

Straw-man layout (Abe Seiden):

Inner:	**6 cm ≤ r ≤ 12 cm** **3 layers pixel** **pixels style readout**
Middle:	**20 cm ≤ r ≤ 55 cm** **4 layers short strips** **space points**
Outer:	**55 cm ≤ r ≤ 1 m** **4 layers “long strips”** **single coordinate**

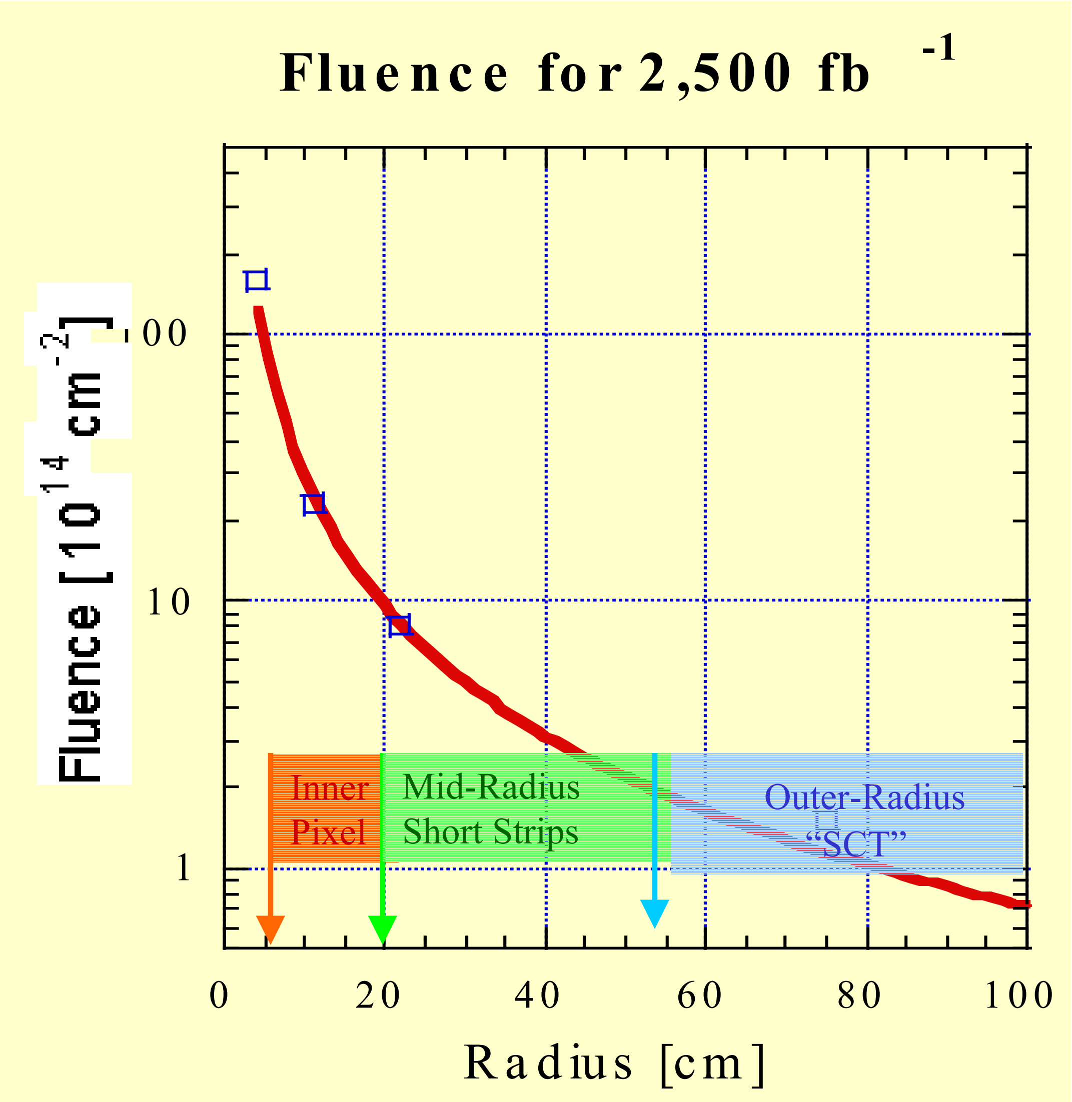

I.N.F.M.

2. Microscopic Radiation damage in Silicon

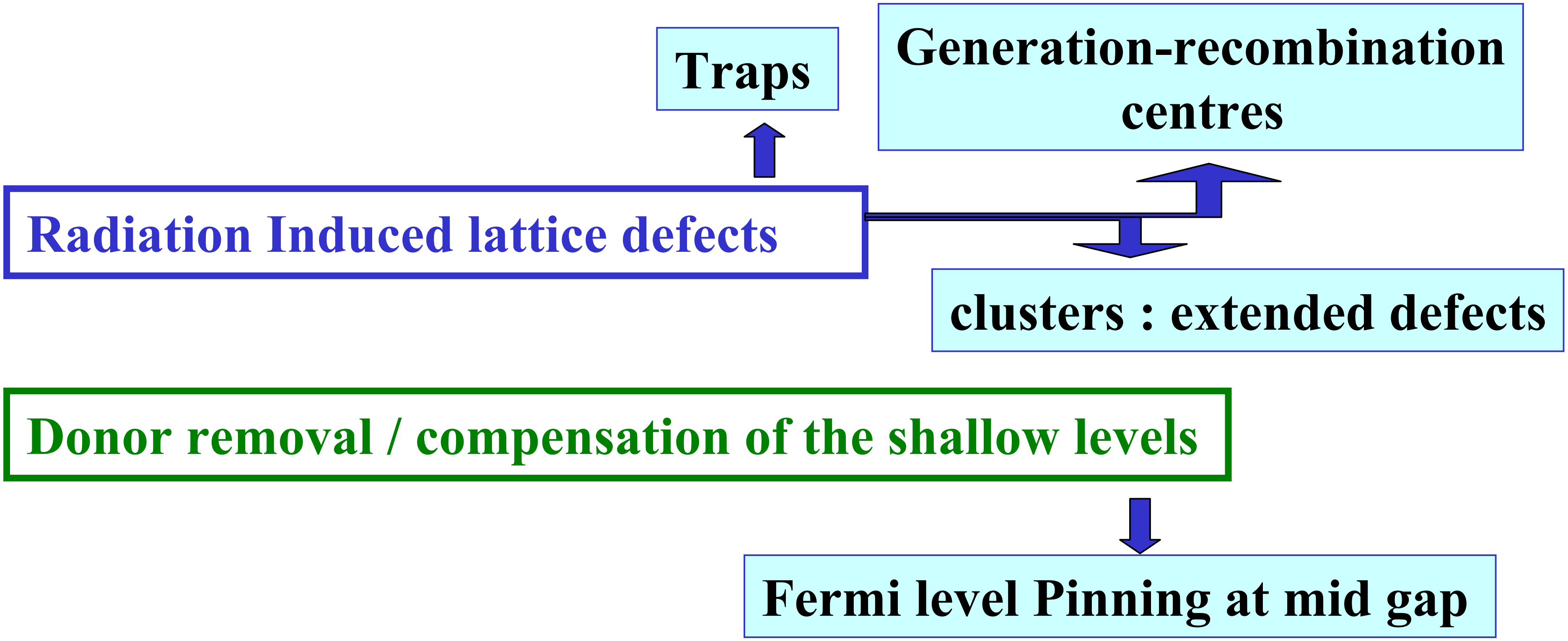

Traps

Generation-recombination centres

Radiation Induced lattice defects

clusters : extended defects

Donor removal / compensation of the shallow levels

Fermi level Pinning at mid gap

Surface damage at the Si/SiO$_2$ interface

Creation of Radiation Induced lattice defects

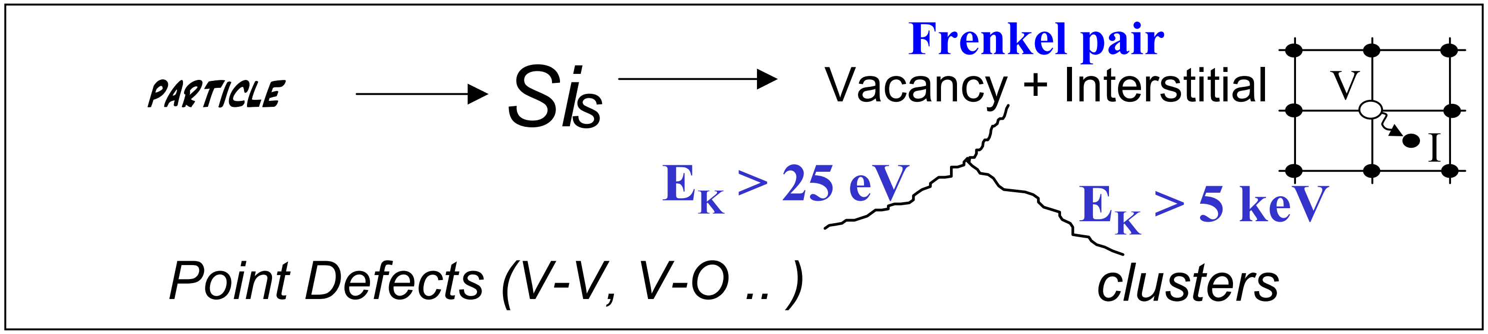

Simulation of Microscopic Damage

- ✓**Generation of hadronic interactions**
- ✓**Transport of the produced heavy recoils**
- ✓**Migration of V and I to form stable defects**

[Mika Huhtinen NIMA 491(2002) 194]

Vacancy amount and distribution depends on particle kind and energy

^{60}Co-gammas

- Compton Electrons with max. $E_{\gamma} \approx 1$ MeV (<u>no cluster production</u>)

Electrons

- $E_e > 255$ keV for displacement
- $E_e > 8$ MeV for cluster

Neutrons (elastic scattering)

- $E_n > 185$ eV for displacement
- $E_n > 35$ keV for cluster

Only point defects ↔ point defects & clusters ↔ Mainly clusters

Initial distribution of vacancies in (1μm)^{3}after 10^{14} particles/cm^2

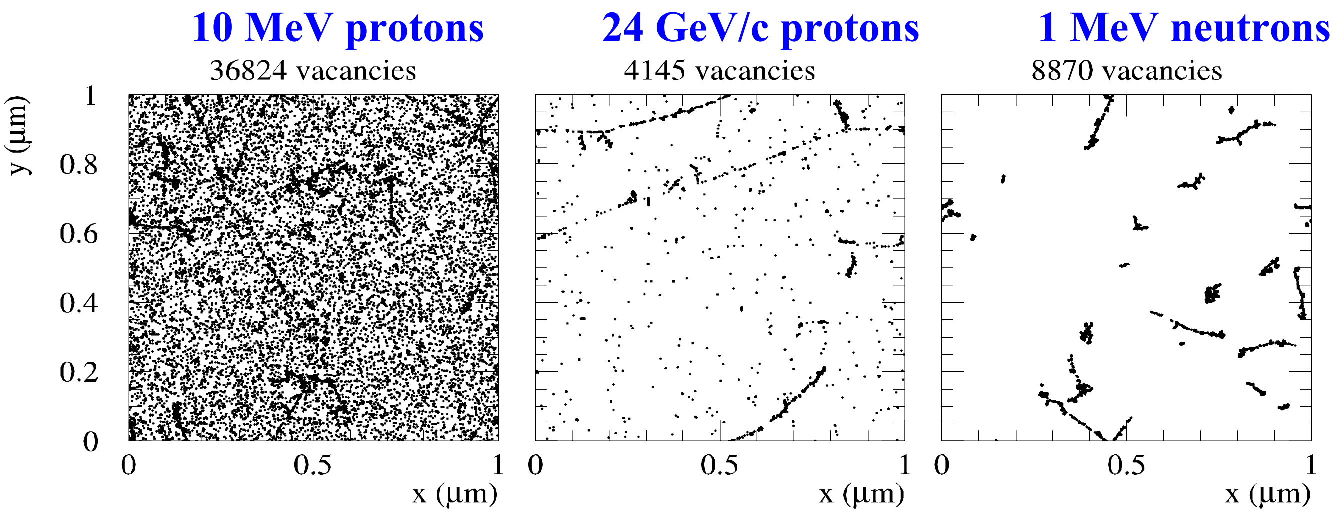

[Mika Huhtinen NIMA 491(2002) 194]

RD50 Primary Damage and secondary defect formation

- **Two basic defects**

I - Silicon Interstitial V - Vacancy

- **Primary defect generation**

I, I_2 higher order I (?)
$\Rightarrow$ **I** -CLUSTER (?) ⇐
V, V_2, higher order V (?) **Damage?!**
$\Rightarrow$ V -CLUSTER (?) ⇐

- **Secondary defect generation**

Main impurities in silicon: Carbon (C_s)
Oxygen (O_i)

$I+C_s \rightarrow C_i \Rightarrow C_i+C_s \rightarrow C_iC_s$
$C_i+O_i \rightarrow C_iO_i$
$C_i+P_s \rightarrow C_iP_s$

$V+V \rightarrow V_2$ $V+V_2 \rightarrow V_3$
$V+O_i \rightarrow VO_i \Rightarrow V+VO_i \rightarrow \underline{V_2O_i}$
$V+P_s \rightarrow VP_s$

$I+V_2 \rightarrow V$ $I+VO_i \rightarrow O_i$

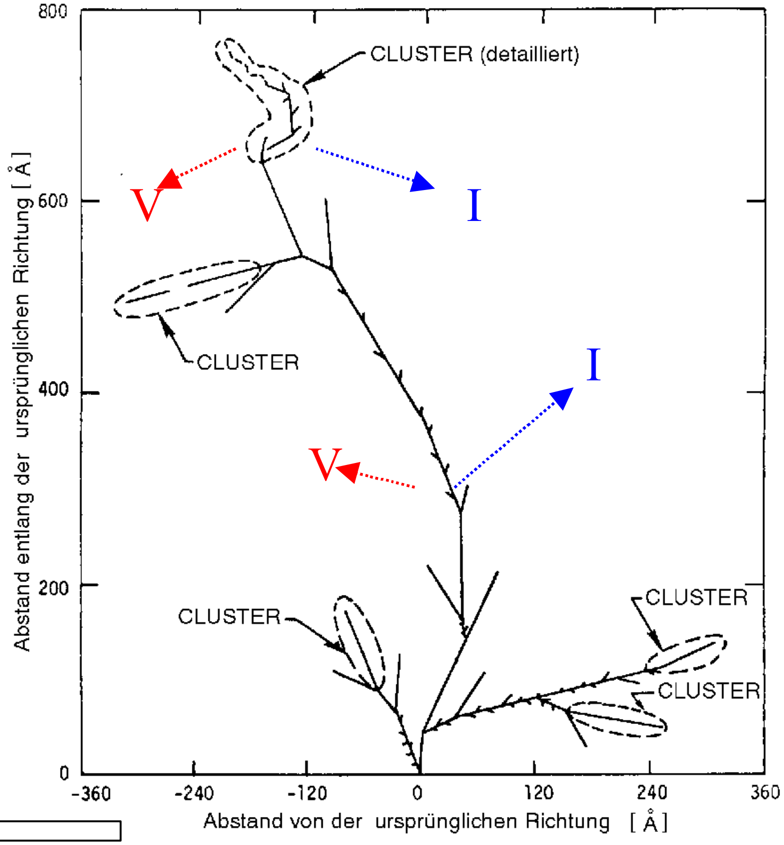

Damage?! (“V_2O-model”)

Radiation Induced defects related to the lattice vacancy

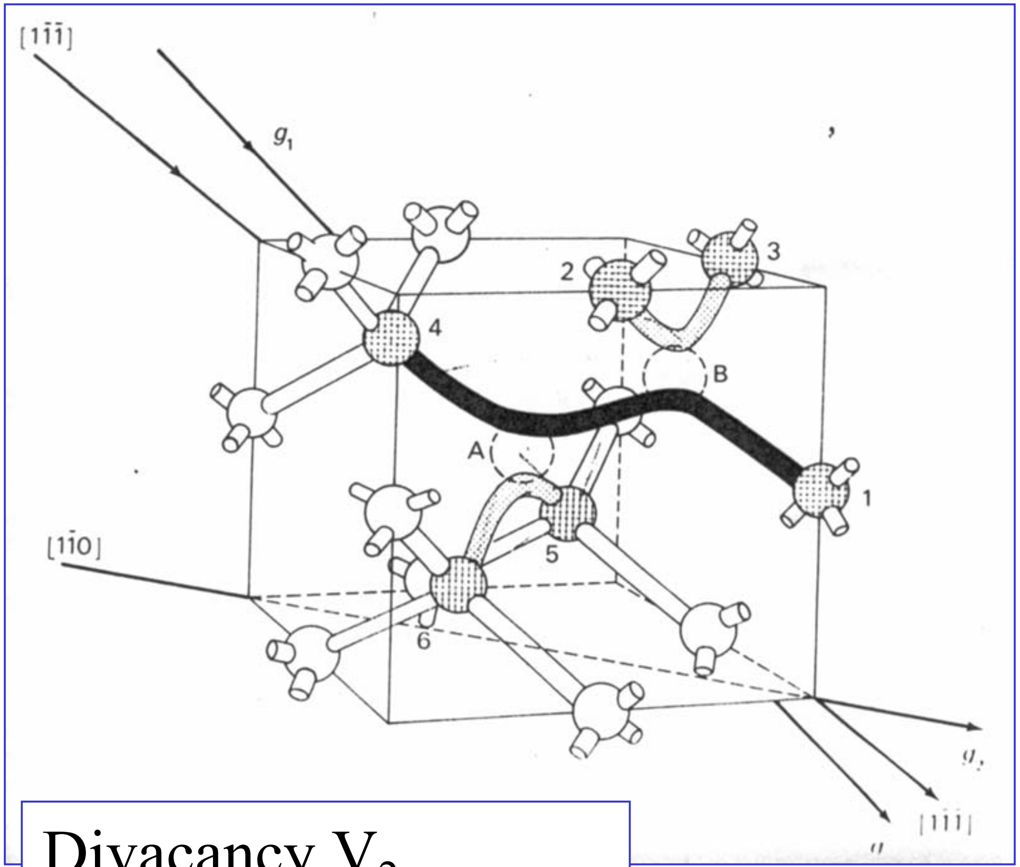

Divacancy V_2

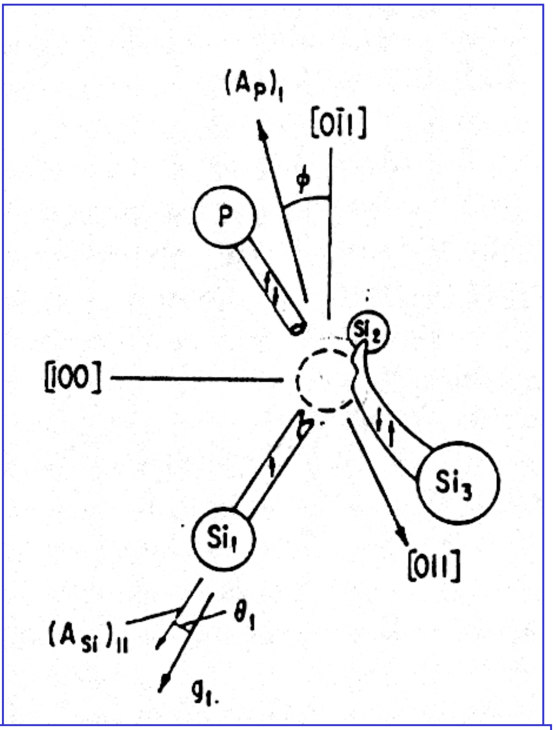

Phosphorous-Vacancy
P-V (E centre)

Corbett, Watkins et al, PRB, 60s

Radiation Induced Defects related to Carbon

$[C_s] \sim 10^{15}\ cm^{-3}$

C_iO_i

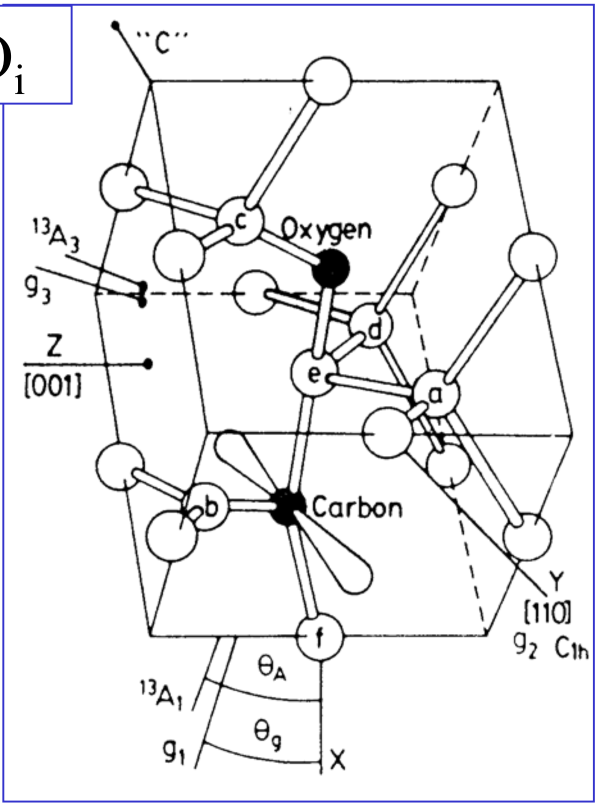

C_i

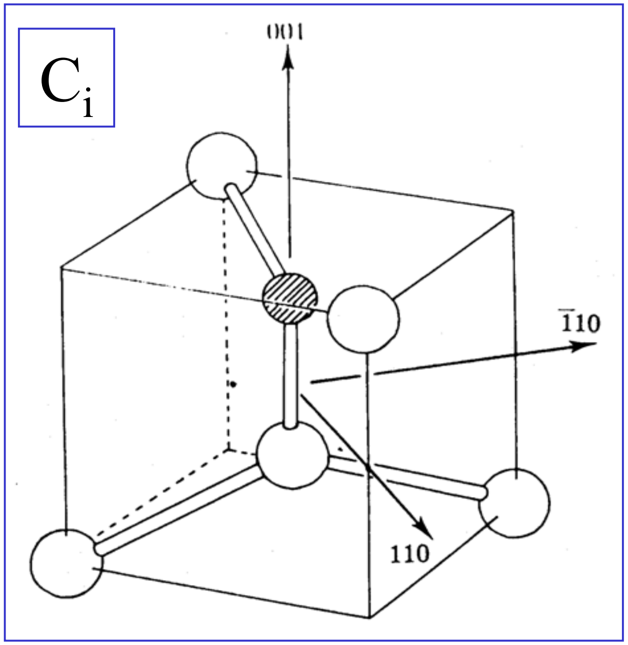

Watkins replacement mechanism:

$$Si_i + C_s \longrightarrow C_i$$

C_i mobile at 300K

$$C_i + O_i \longrightarrow C_i\,O_i$$

Radiation Induced Defects related to Oxygen

FZ Si $[O_i] \sim 10^{15}$ cm^{-3} ; CZ Si $[O_i] \sim 10^{18}$ cm^{-3}

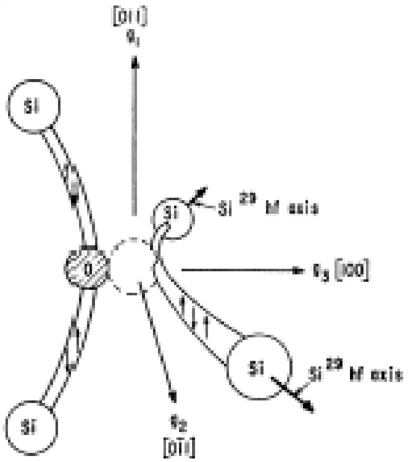

FIG. 5. Model of the *A* center as a substitutional oxygen atom. The oxygen atom bonds between two of the four neighboring silicon atoms, and the remaining two silicon atoms pull together to form a covalent bond. Spin resonance arises from an additional electron which is trapped in the Si–Si molecular bond as shown. The *g* tensor and hyperfine axes are indicated.

V-O defect (A centre)

Watkins, Corbett: Phys.Rev.,121,4, (1961),1001

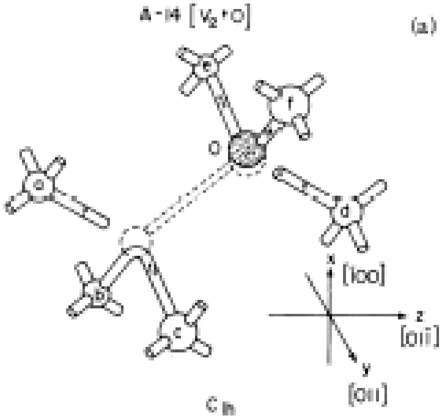

V_2O defect

Lee, Corbett: Phys.Rev.B,13,6, (1976),2653

I.N.F.M

Energy Levels related to traps

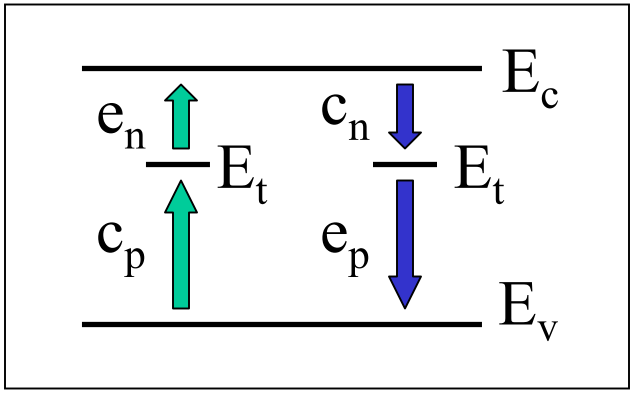

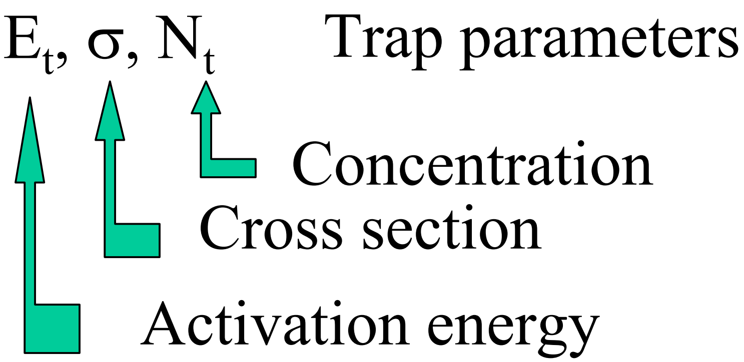

E_t, σ, N_t Trap parameters

Concentration

Cross section

Activation energy

Emission coefficient:

$$e_n = N_c \sigma_n v_{th} \cdot e^{-\frac{E_c - E_t}{KT}}$$

Capture coefficient :

$$c_n = n \sigma_n v_{th}$$

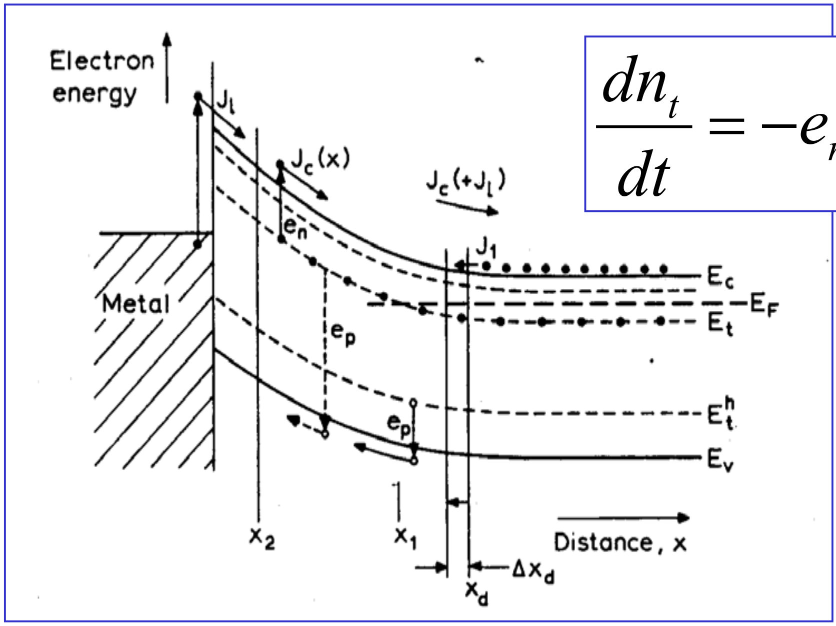

$$\frac{dn_t}{dt} = -e_n \cdot n_t$$

Tecniche per l'analisi dei difetti in materiali semiconduttori

1. Thermally Stimulated Currents TSC
2. Deep Level Transient Spectroscopy DLTS
3. Photo Induced Current Transient Spectroscopy PICTS

Livelli energetici profondi in regione svuotata

$$\frac{dn_t}{dt} = -e_n \cdot n_t$$

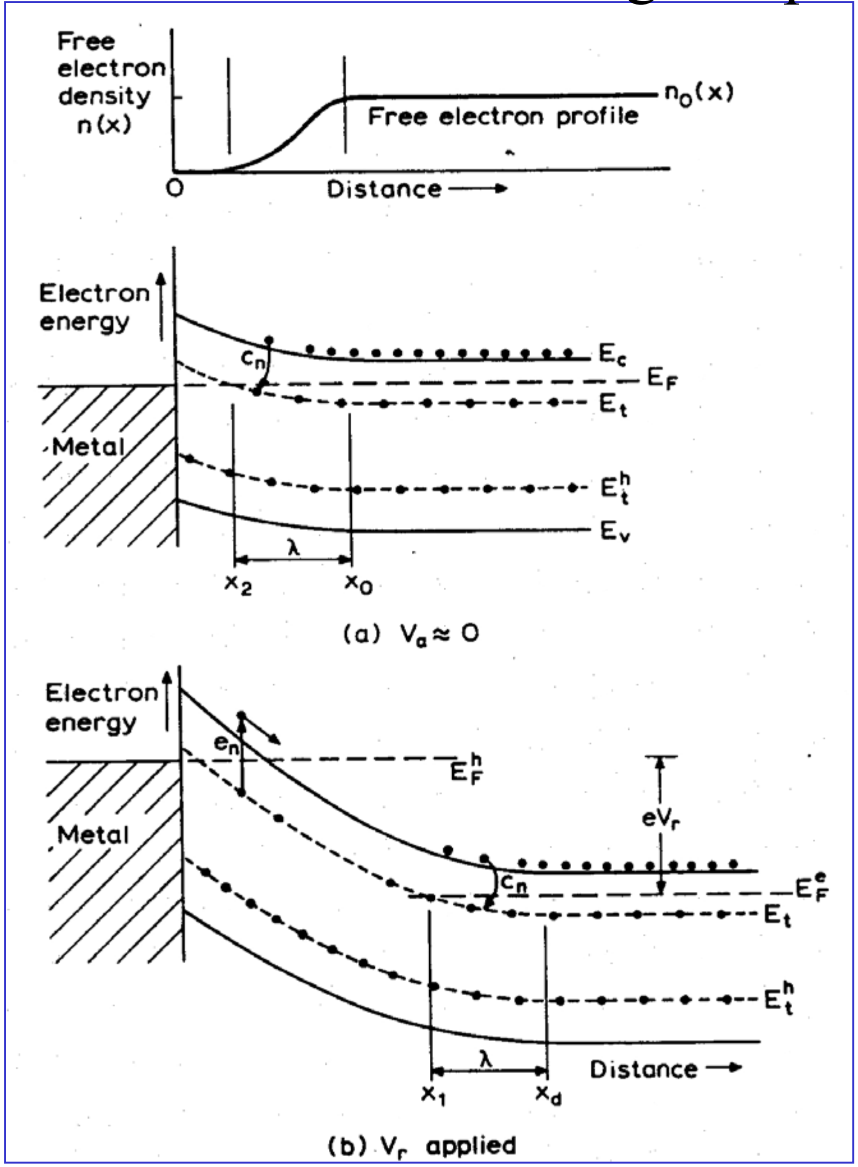

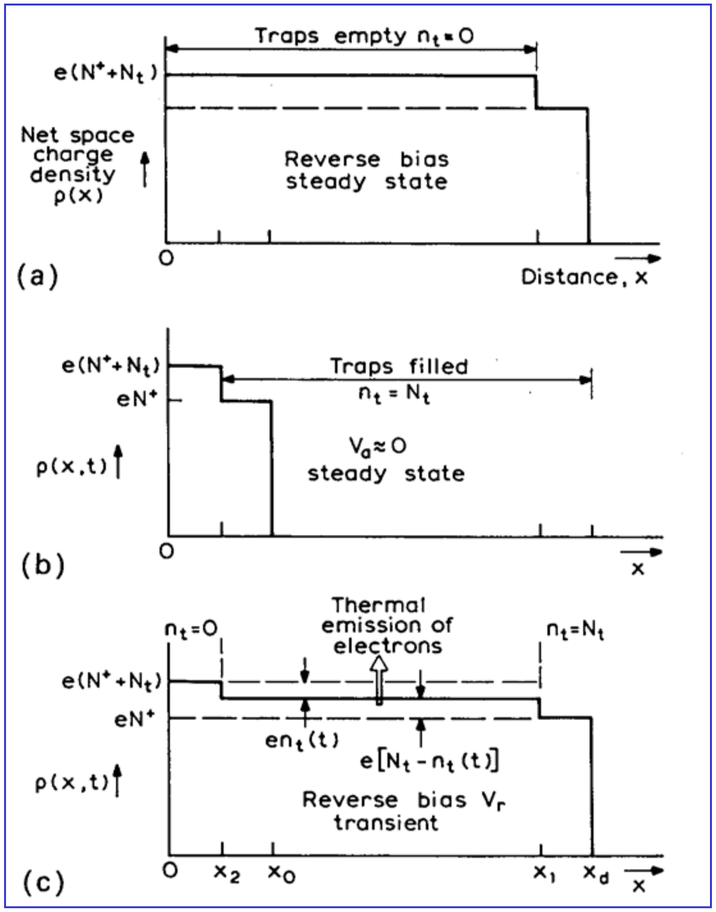

Orton & Blood, The electrical characterization of semiconductors, Academic Press, 1990

Thermally Stimulated Current TSC

$$J_{TSC} = J_c + \frac{\partial D}{\partial t} = -\frac{1}{2} q W_d e_n n_t$$

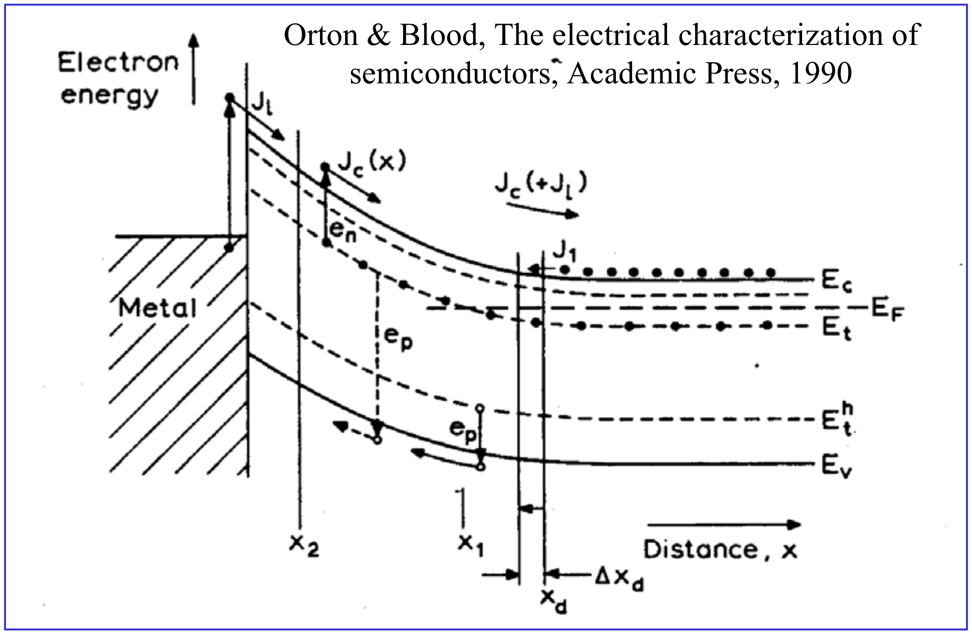

Orton & Blood, The electrical characterization of semiconductors, Academic Press, 1990

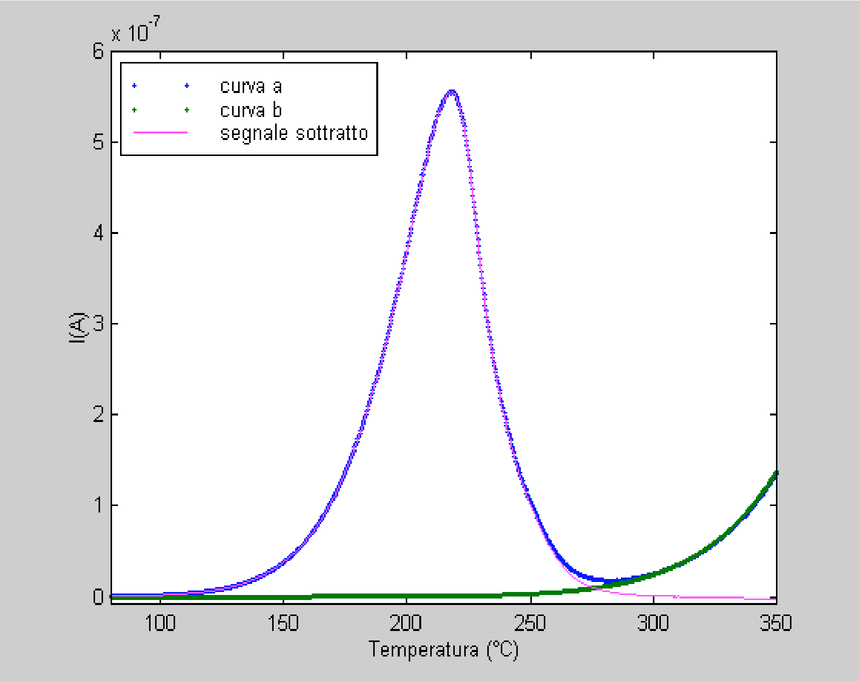

Esempio di TSC in diamante: S. Pini, tesi di laurea in Fisica

$$I_{TSC}(T) = -\frac{1}{2} q\cdot A\cdot N_t \cdot W \cdot e_n(T)\exp\left(-\frac{1}{b}\int_{Ti}^{T} e_n(T)\,dT\right)$$

I.N.F.M

Deep Level Transient Spectroscopy DLTS

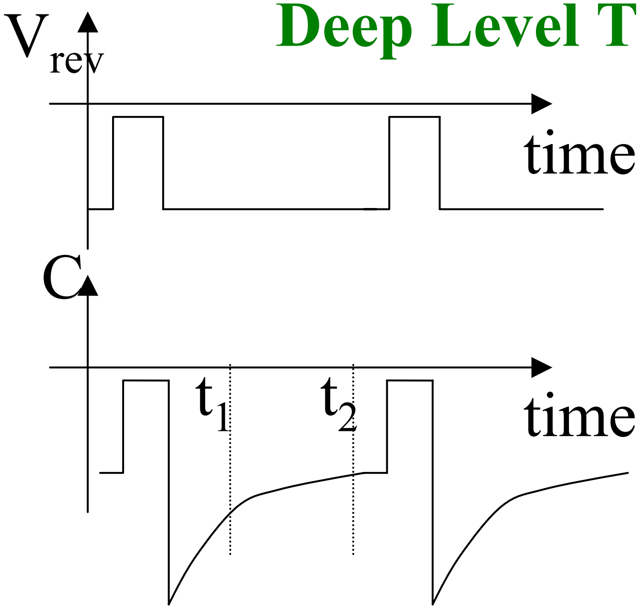

$$S = \Delta C_0 \left(e^{-e_n(T)t_1} - e^{-e_n(T)t_2} \right)$$

$$e_n(T_{max}) = \frac{t_2 - t_1}{\ln(t_2 / t_1)} \alpha T_{max}^2 \cdot e^{-E_t / KT_{max}}$$

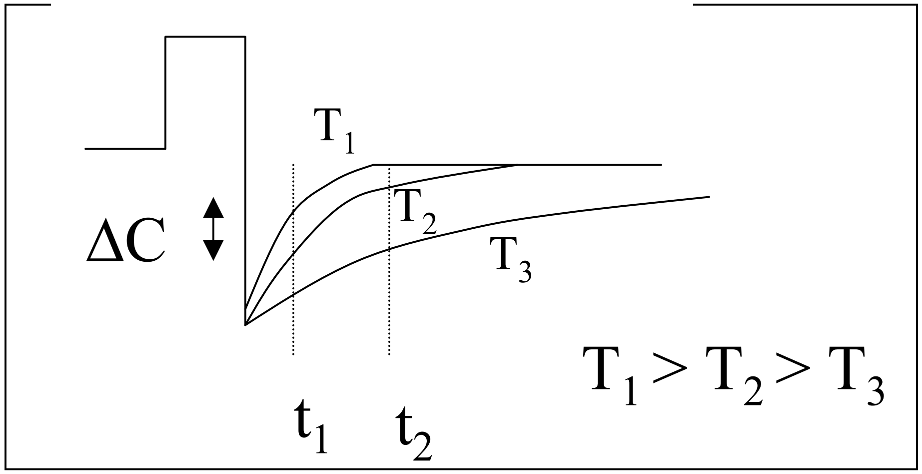

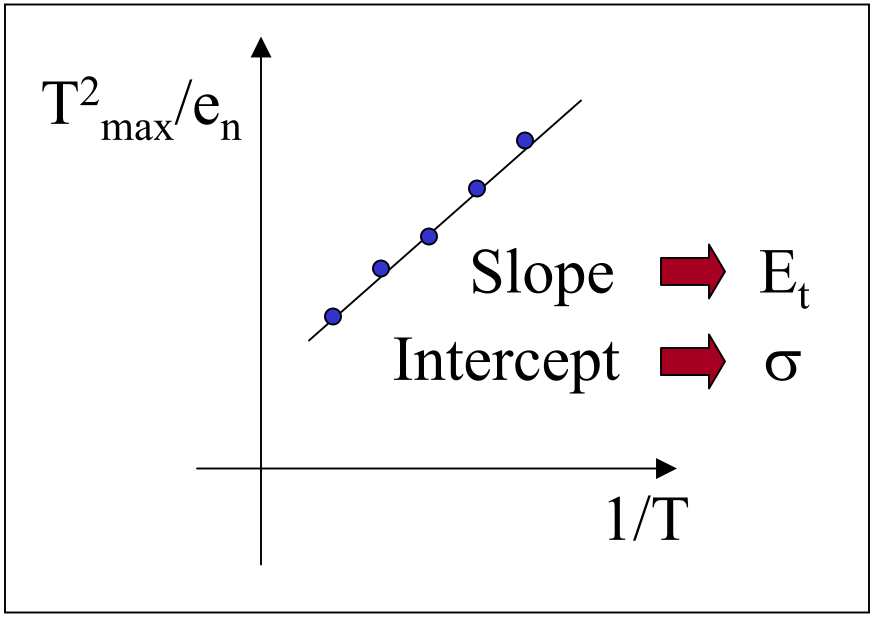

Segnale DLTS misurato con giunzione p^+n di Si irraggiato con e^-

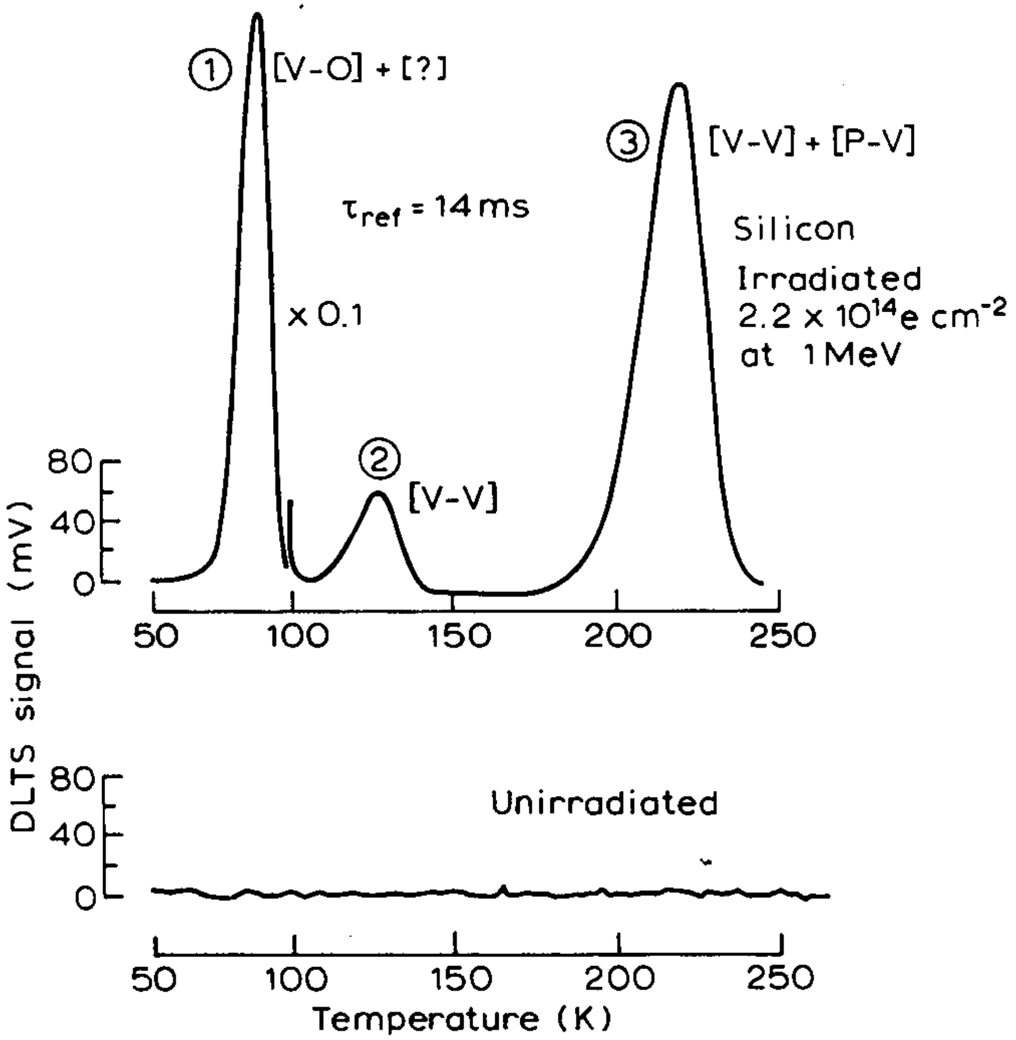

Orton & Blood, The electrical characterization of semiconductors, Academic Press, 1990

Photo Induced Current Transient Spectroscopy PICTS

Orton & Blood, The electrical characterization of semiconductors, Academic Press, 1990

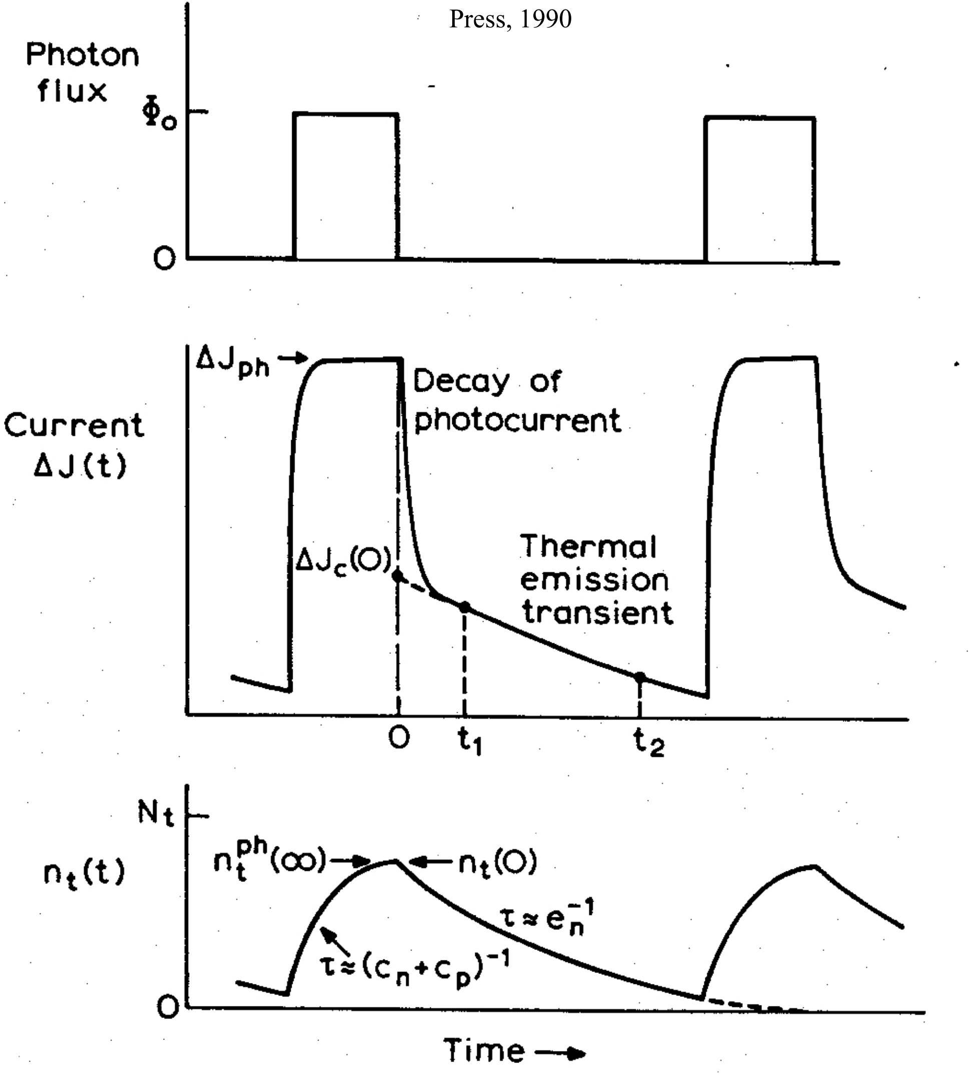

Simile alla DLTS, l'eccitazione delle trappole viene effettuata mediante un flusso di fotoni con $h\nu > E_g$ e viene misurato il transiente in corrente

PICTS: Difetti nativi presenti in SI LEC GaAs

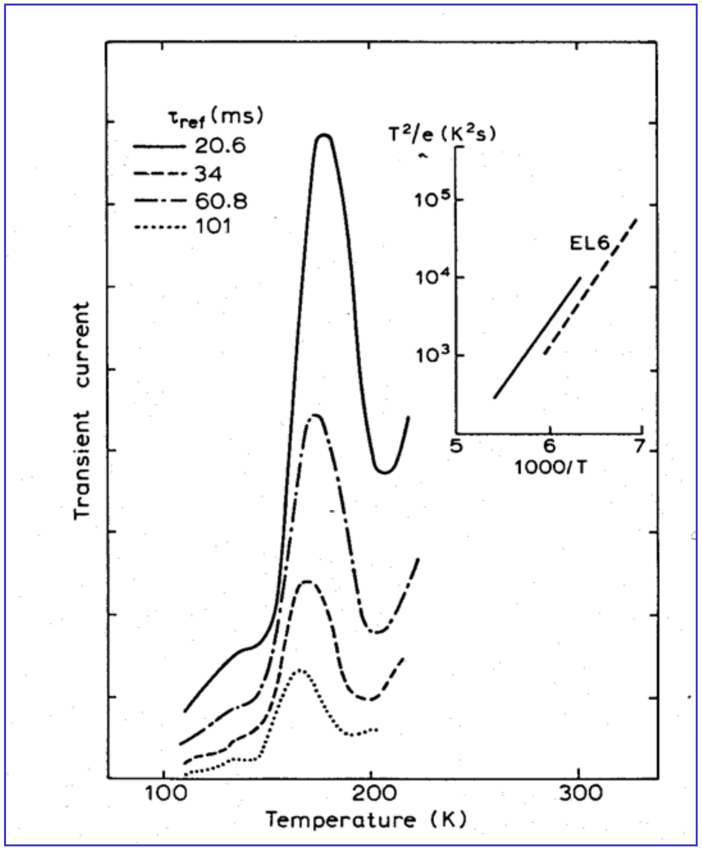

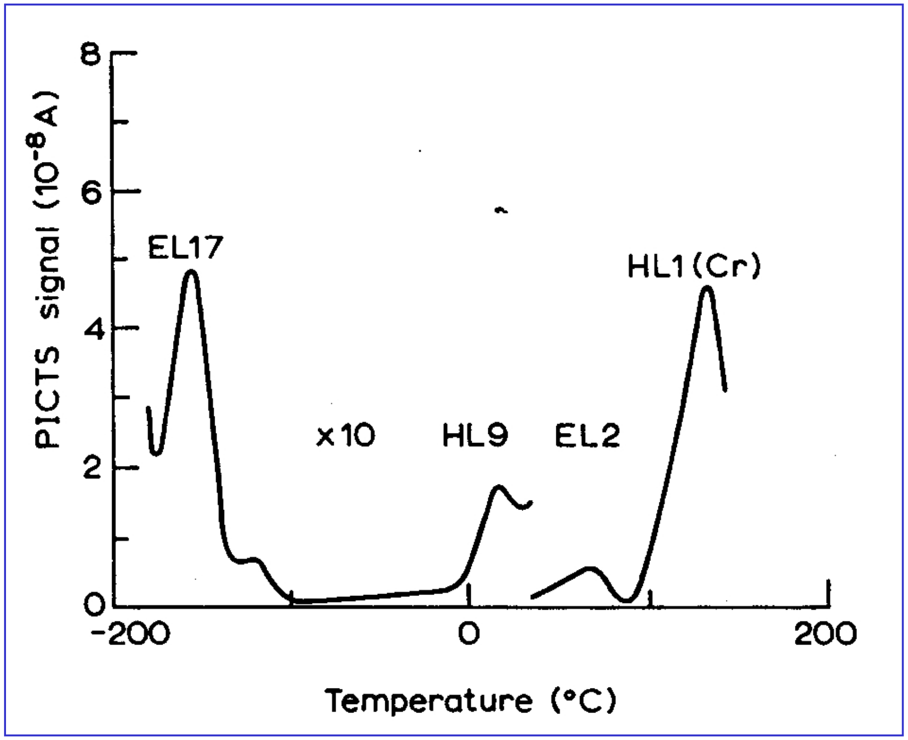

Orton & Blood, The electrical characterization of semiconductors, Academic Press, 1990

Visualizzazione dei clusters (difetti estesi) con tecniche DLTS

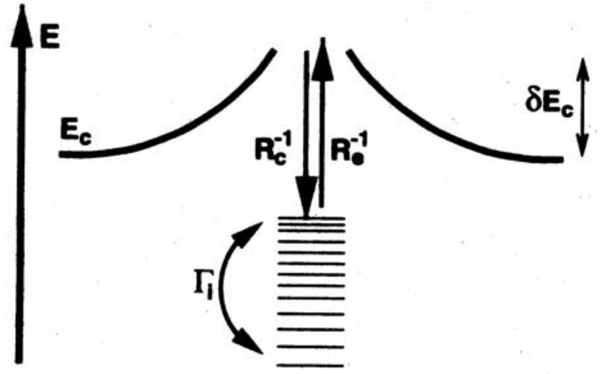

Una barriera di potenziale scherma il difetto esteso alterando il segnale DLTS

$$R_c(E,t) = \sigma_n v_{th} n\left[1 - f(E,t)\right]\exp\left[\frac{-\delta E_c}{kT}\right]$$

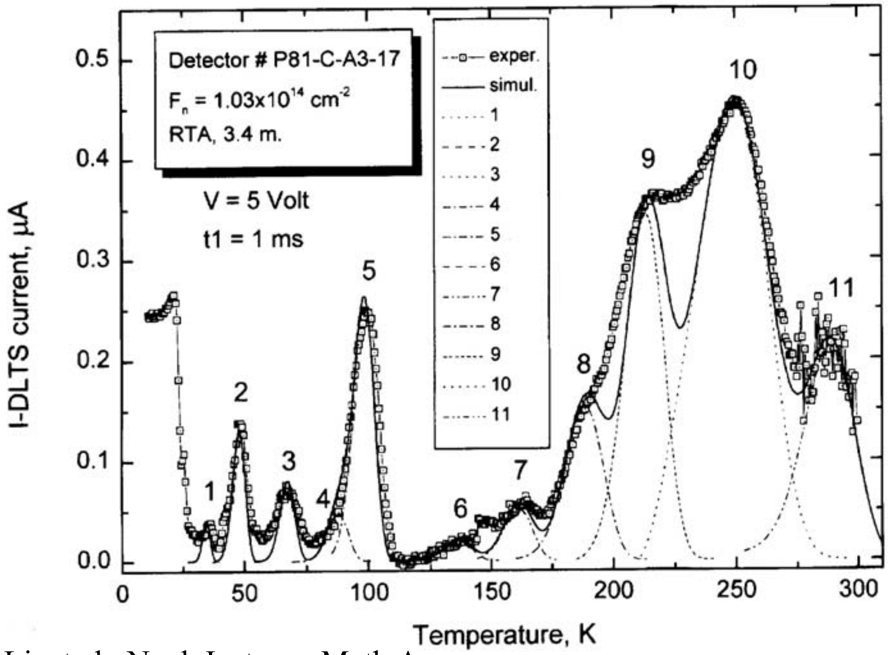

Z. Li et al., Nucl. Instrum. Meth A

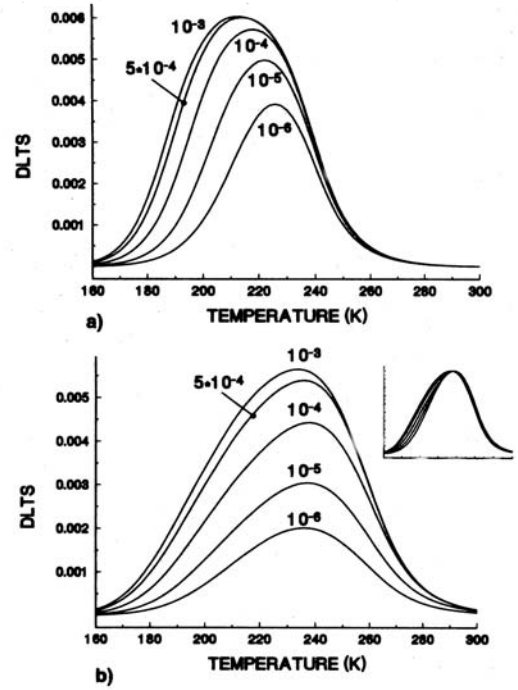

W. Schroeter et al., PRB

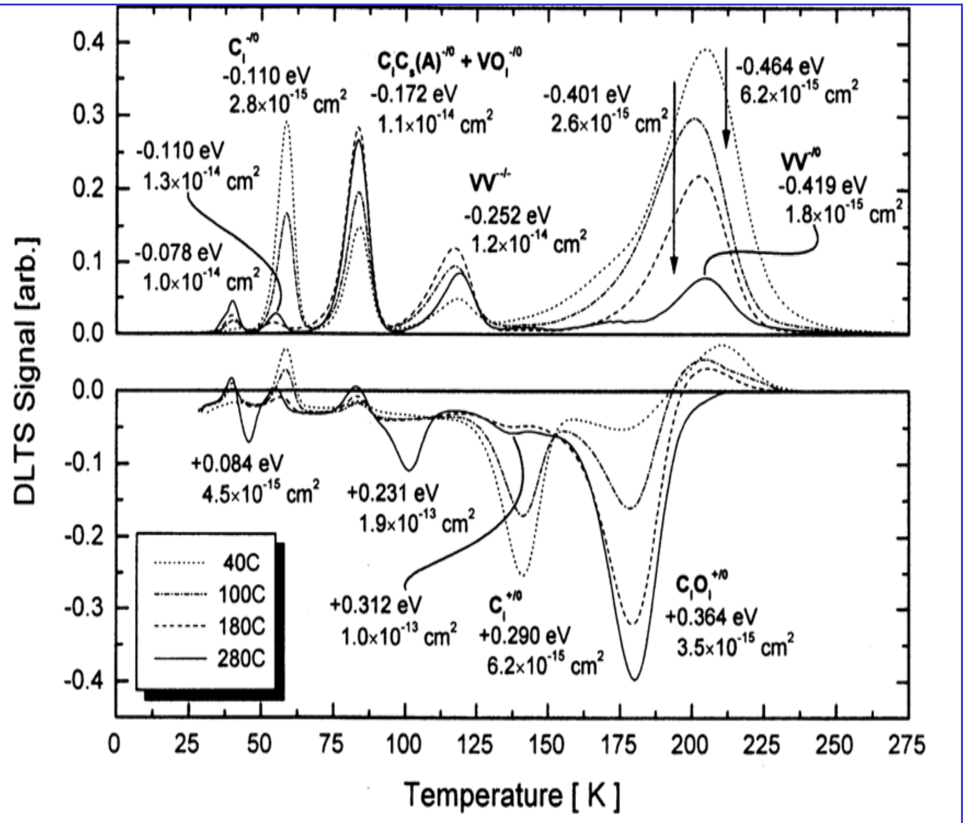

Low fluence range

DLTS - f =10^{11} cm^{-2}

5.3MeV neutrons

ROSE Coll. NIM A 466 (2001) 308-326

Broaden peaks

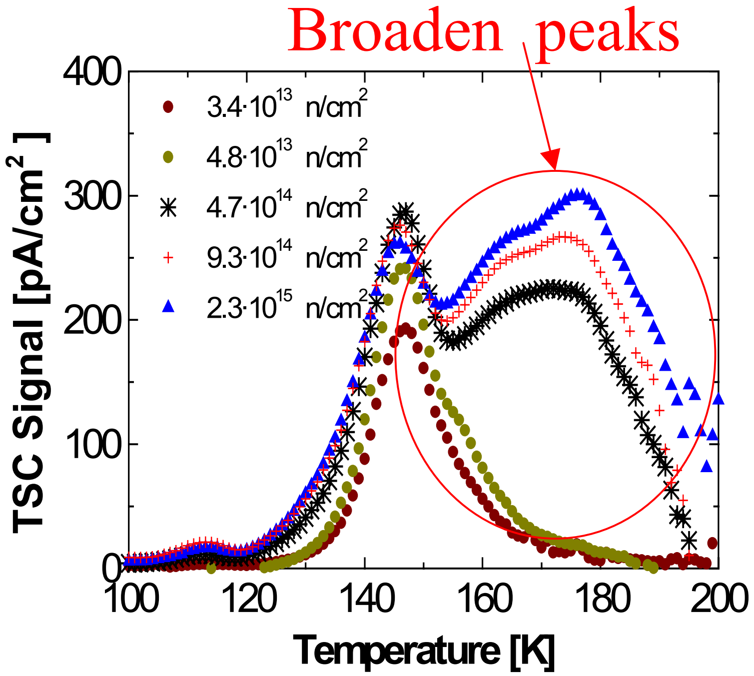

High fluence range

TSC - f =10^{13} -10^{15} cm^{-2}

1MeV neutrons

M. Bruzzi, IEEE TNS (2000)

Gamma-irradiation ⇔ Neutron-irradiation
only point defects ⇔ cluster and point defects

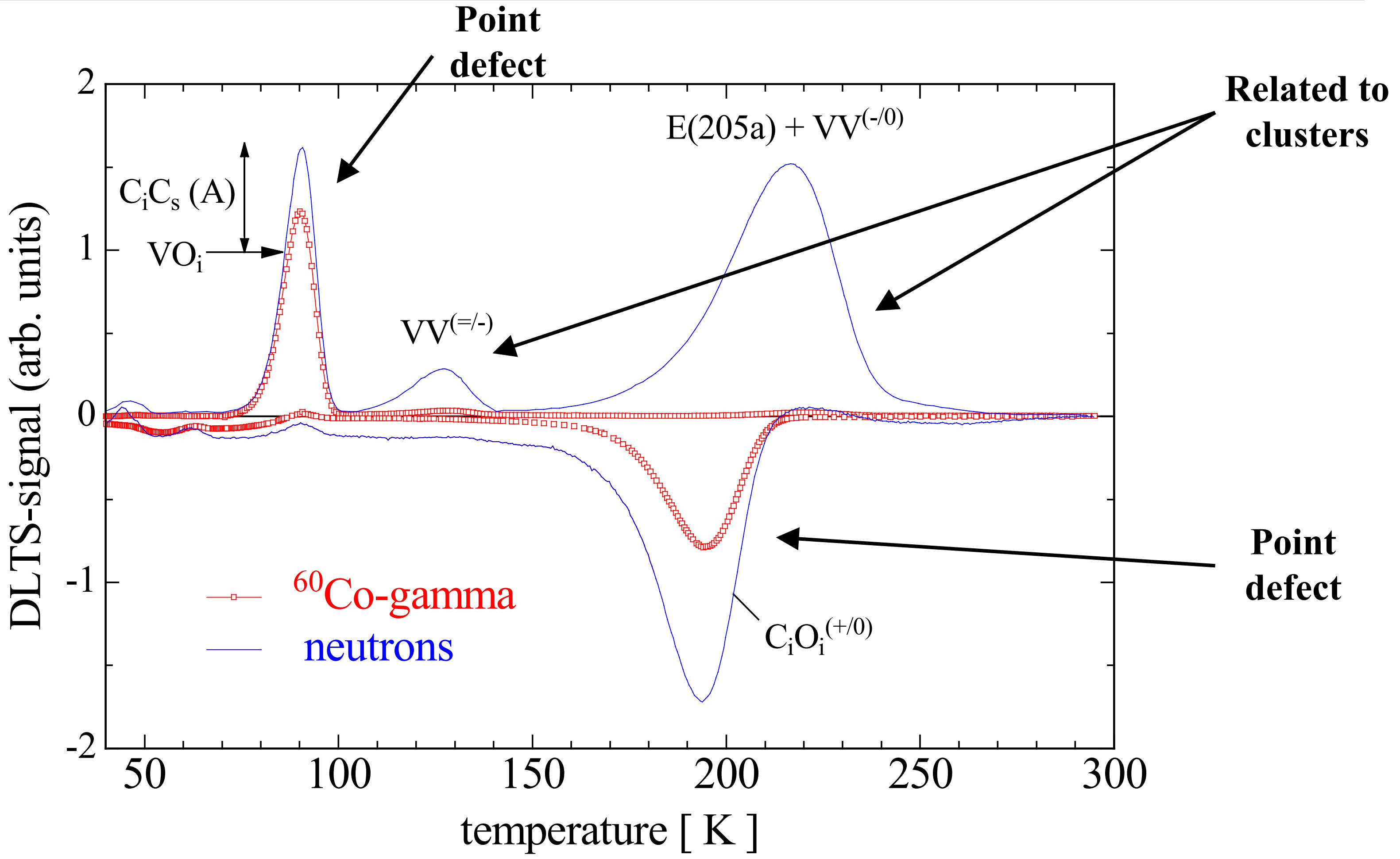

Point defect

Related to clusters

Point defect

Deep Level Transient Spectroscopy, M.Moll et al.

Main Defects in Irradiated Silicon

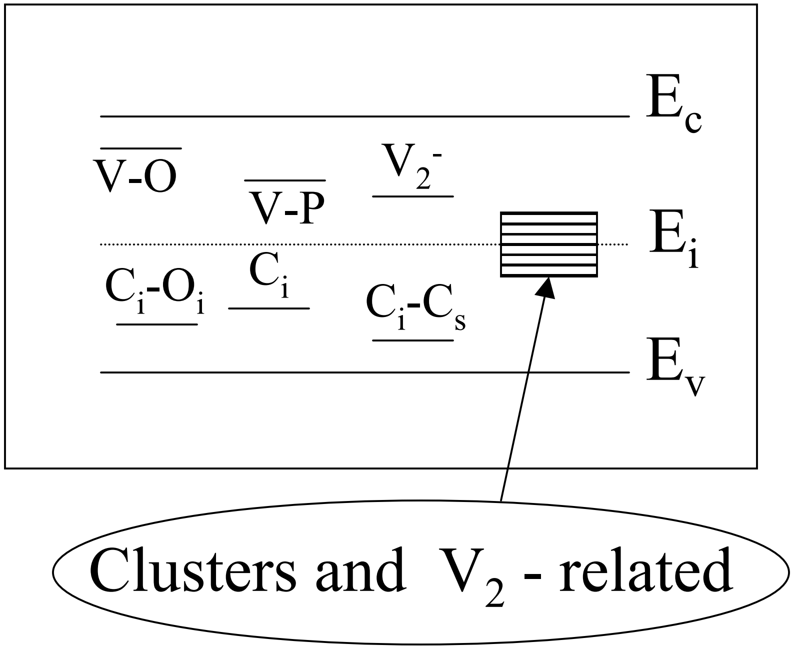

M. Bruzzi, IEEE, Trans. Nucl. Sci. (2000)

Defect Identity	Trap parameters			Annealing parameters	
	method	E_t [eV]	$\sigma_{n,p}$[cm^2]	$E_{ann.}$ [eV]	$T_{ann.}$ °C
V-O_i	DLTS	E_c–0.17	$1.0\text{x}10^{-14}$	2.1	350
C_iC_s	DLTS	E_v+0.17 E_v+0.17	$1.4\text{x}10^{-14}$	1.7	225 250
V_2^+	EPR	E_v + 0.25 E_v + 0.21	$2\text{x}10^{-16}$	1.3	300
$V_2^=$	DLTS TSC	E_c - 0.25 E_c - 0.23	$4\text{x}10^{-16}$ e$^{-.017/KT}$ $2\text{x}10^{-16}$	1.3	300
C_i	DLTS	E_v+ 0.3 E_v+ 0.33	$9\text{x}10^{-14}$	0.74	50
C_iO_i	EPR PL DLTS TCT	E_v+ 0.38 E_v+ 0.36	$2.5\text{x}10^{-15}$ $1.2\text{x}10^{-15}$		400
V_2^-	EPR PL DLTS	E_c – 0.4 E_c – 0.4 E_c – 0.41	$2\text{x}10^{-15}$	1.3	300
P-V	EPR HE DLTS	E_c- 0.4 E_c – 0.46	$3.7\text{x}10^{-15}$	0.94-1.2	150
Si_i	DLTS	E_c– 0.49	$6.6\text{x}10^{-16}$		
No assessed identity	TSC TCT DLTS/ TCT	E_c -0.48 E_c-0.52 E_v+0.48 E_v+ 0.51	$4\text{x}10^{-15}$ $5.5\text{x}10^{-15}$ $1\text{x}10^{-14}$		

Low Temperature TSC-DLTS experimental set-up

-Temperature range: **4.2-300K** (spanned energy range ~0.01-0.50eV)
-Cooling by immersion in liquid He vapors
-Heating (by a resistance) with rates 0.01-0.20K/s.
-Reverse bias: up to 1000 V.
-Excitation:forward bias up to current saturation (3.8 mA).
-Filling Temperature varied by changing distance from
the Liquid He surface
- Several measurements in different T intervals to reduce He evaporation
(10-25 K, 20-80 K, 80-220 K).

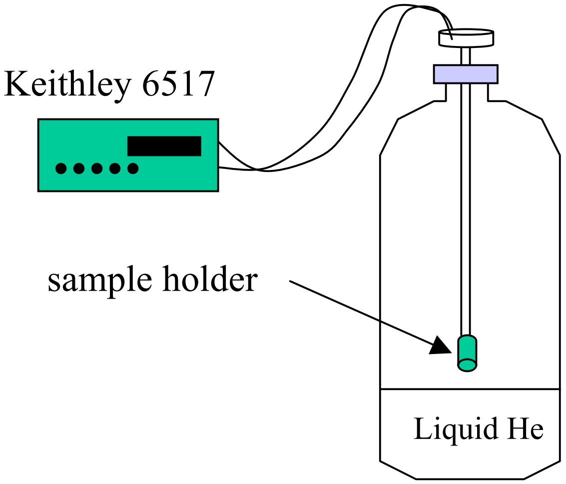

Shallow Donor Removal

Formation of the P-V defect ⟶ P shallow level removal

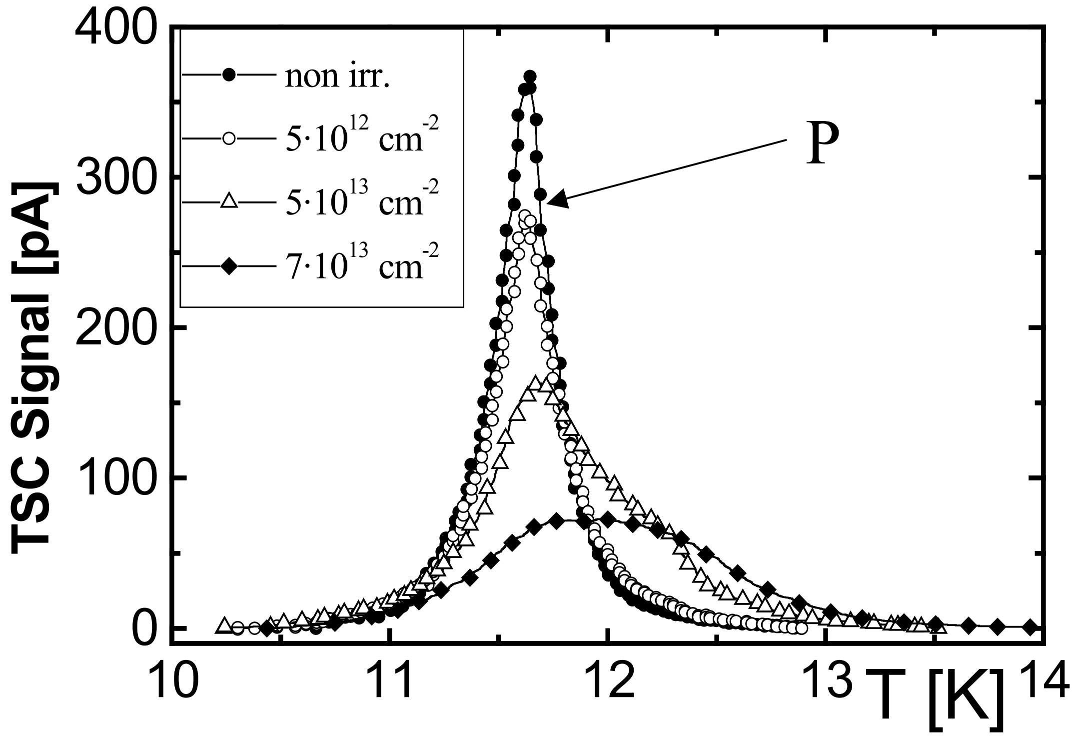

E. Borchi et al., IEEE Trans. Nucl. & Sci and Jour. Phys:D

3. Macroscopic Damage in silicon detectors

Increase of the Leakage Current

Drastic changes in V_{dep} and N_{eff}

Increase of the bulk resistivity and type inversion

Double junction

S/N Decrease →

Decrease of the charge collection efficiency

Increase of the interstrip capacitance

Influence of defects on the material and device properties

Shockley-Read-Hall statistics
(standard theory)

Inter-center charge
transfer model
(inside clusters only)

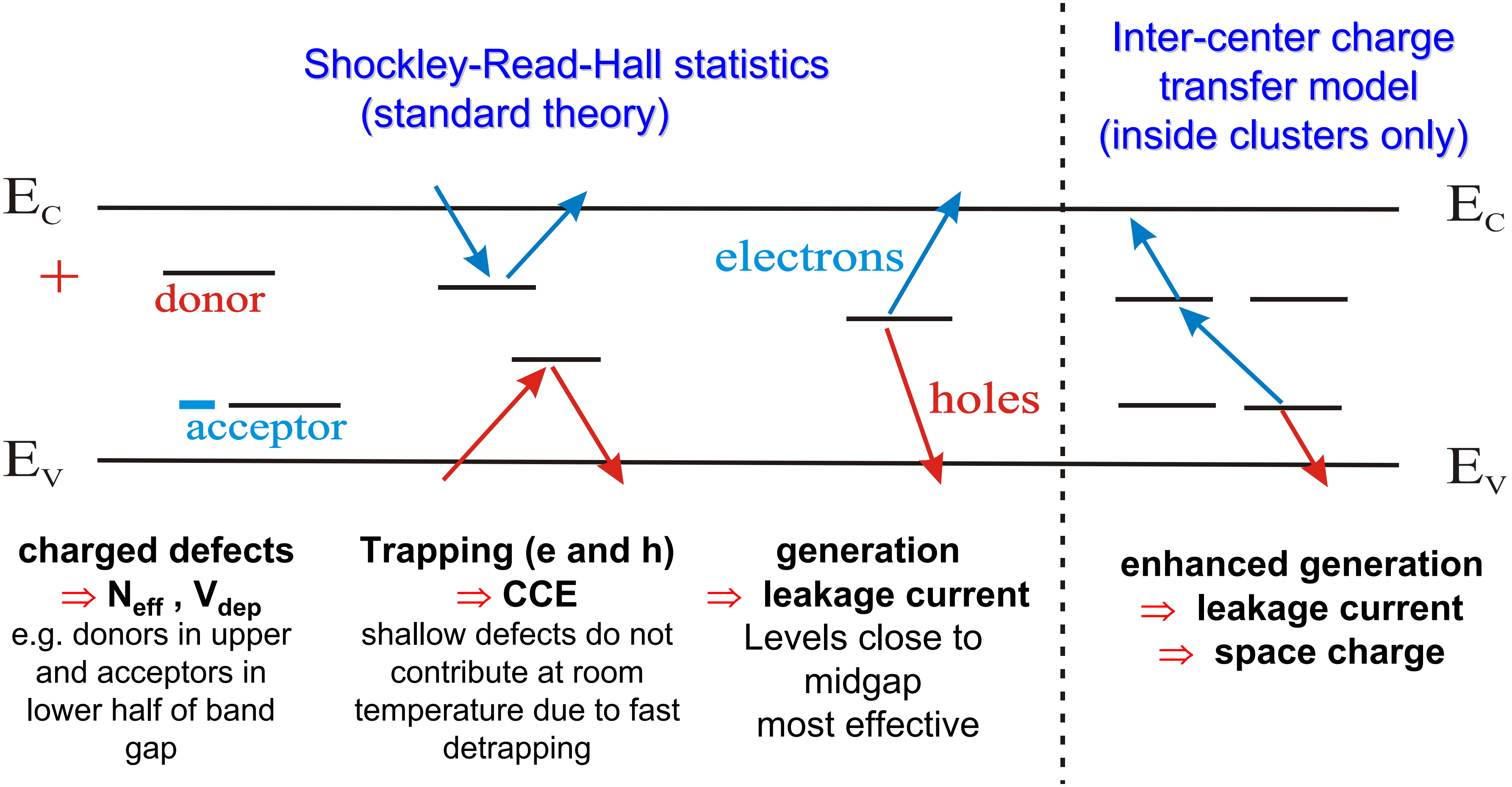

charged defects
⇒ **N_{eff} , V_{dep}**
e.g. donors in upper and acceptors in lower half of band gap

Trapping (e and h)
⇒ **CCE**
shallow defects do not contribute at room temperature due to fast detrapping

generation
⇒ **leakage current**
Levels close to midgap most effective

enhanced generation
⇒ **leakage current**
⇒ **space charge**

Leakage Current

Hadron irradiation

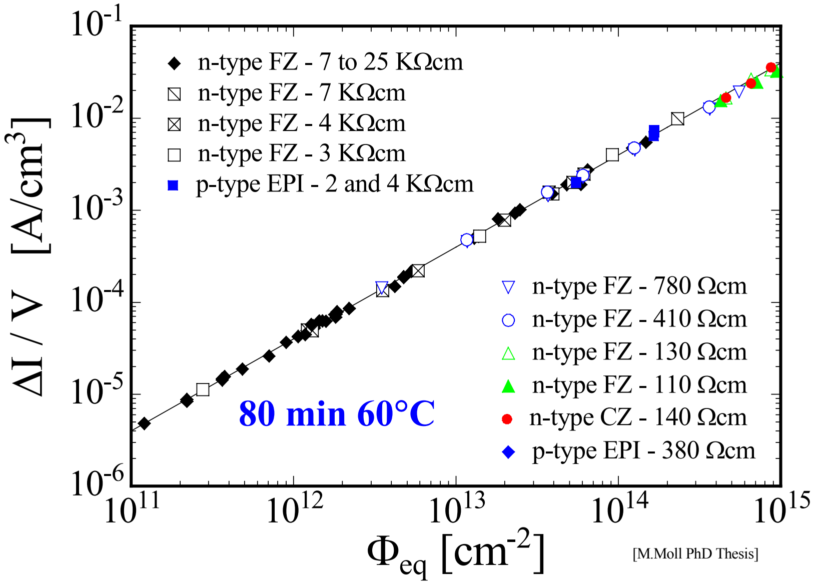

Annealing

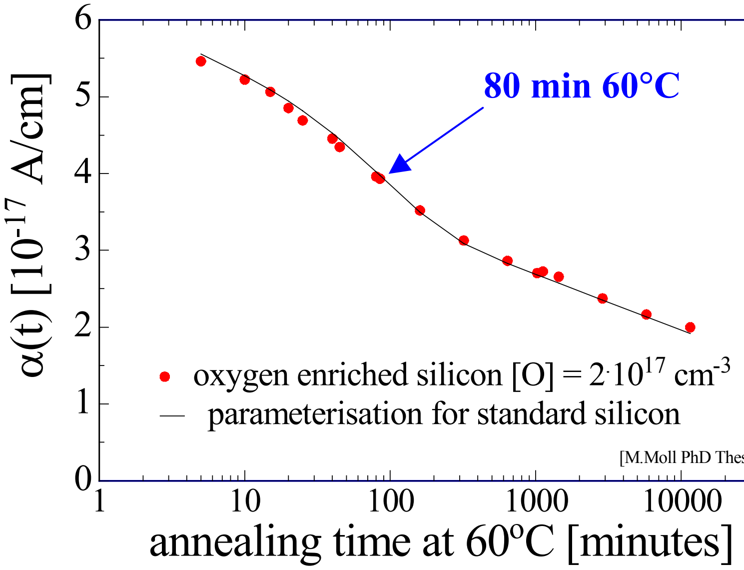

- **Damage parameter α (slope)**

M. Moll, Thesis

$$\boxed{\alpha = \frac{\Delta I}{V \cdot \Phi_{eq}}}$$

- **α independent of Φ_{eq} and impurities**
  α used for fluence calibration (NIEL-Hypothesis)

- **Oxygen enriched and standard silicon show same annealing**
- **Same curve after proton and neutron irradiation**

Depletion Voltage and Effective Space Charge Concentration

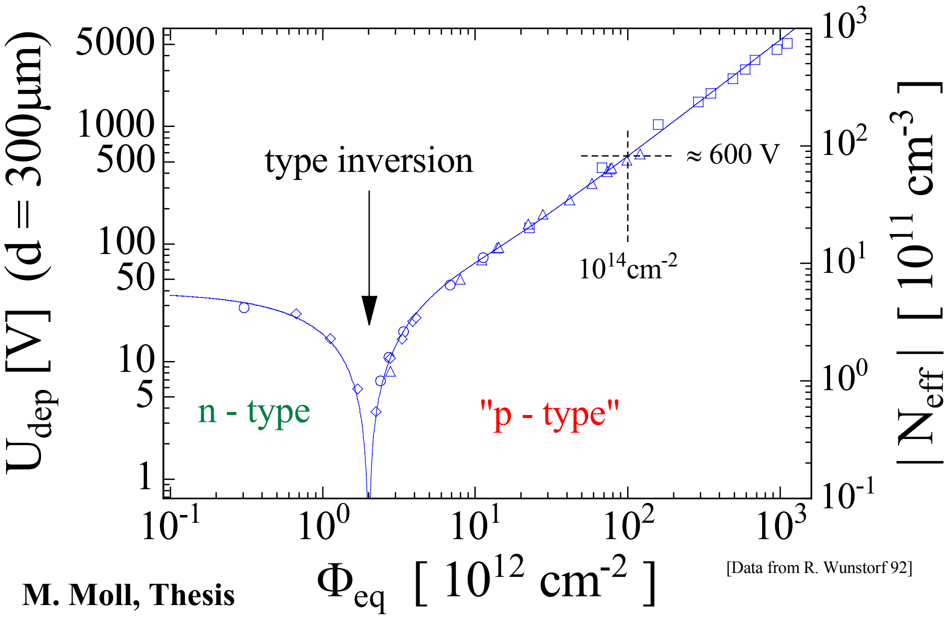

M. Moll, Thesis

[Data from R. Wunstorf 92]

- **Type inversion:**
  SCSI – Space Charge Sign Inversion

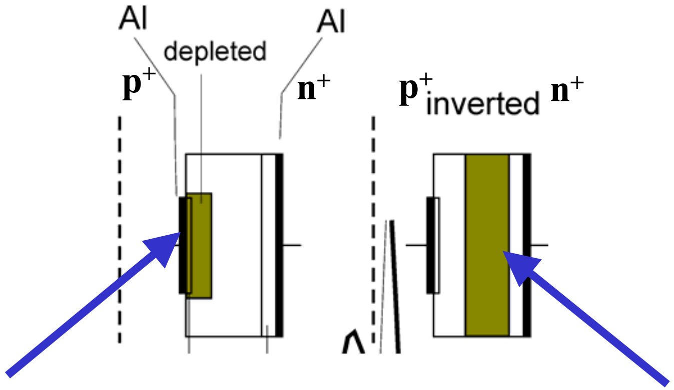

before inversion

after inversion

after inversion and annealing saturation

$$\mathbf{N_{eff}} \sim \beta \cdot \phi$$

Variazione di V_{dep} e N_{eff} con la fluenza : dipendenza dalla resistività iniziale

$$\Delta N_{eff}(f) = | N_{C0}(1 - e^{-cf}) - \beta \cdot f |$$

Produzione di difetti di tipo accettore

Rimozione/compensazione drogante superficiale

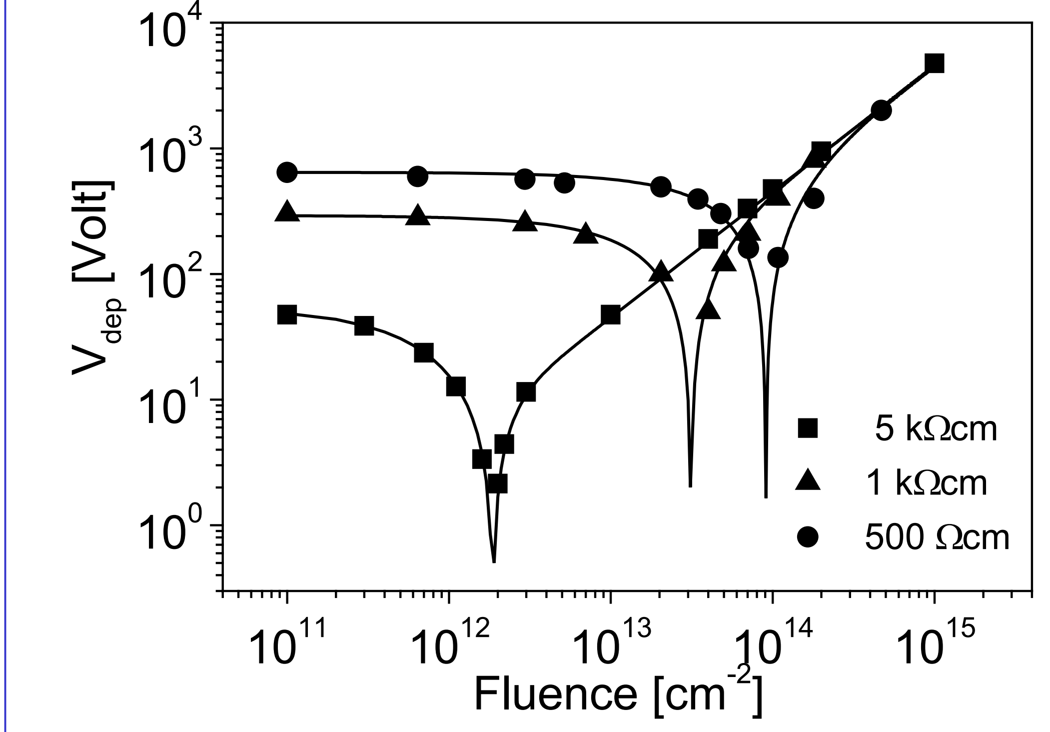

M. Bruzzi, IEEE Trans. Nucl. Sci. 2000

V_{dep} and N_{eff} depends on storage time and temperature

Stable Damage

$$\Delta N_{eff} = N_{C0}(1-e^{-c\cdot f}) + [g_c + g_a e^{-\frac{t}{\tau_a(T)}} + g_y(1-e^{-\frac{t}{\tau_y(T)}})]f$$

ShallowDonor Removal

Beneficial Annealing

Reverse Annealing

- **Short term:** “Beneficial annealing”
- **Long term:** “Reverse annealing”
  time constant : ~ 500 years (-10°C)
  ~ 500 days (20°C)
  ~ 21 hours (60°C)

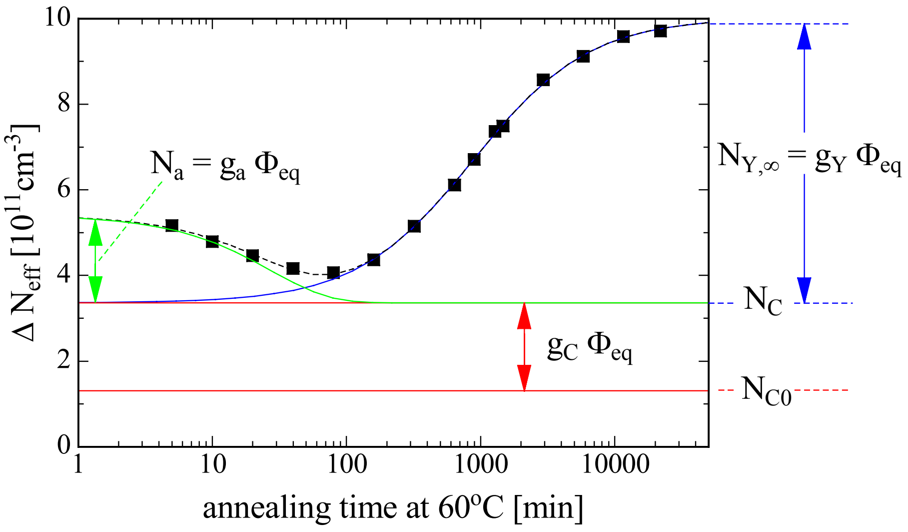

G.Lindstroem et al, NIMA 426 (1999)

3. Aumento della resistività per effetto della rimozione dei droganti superficiali indotta dall'irraggiamento e per la compensazione dovuta ai difetti profondi

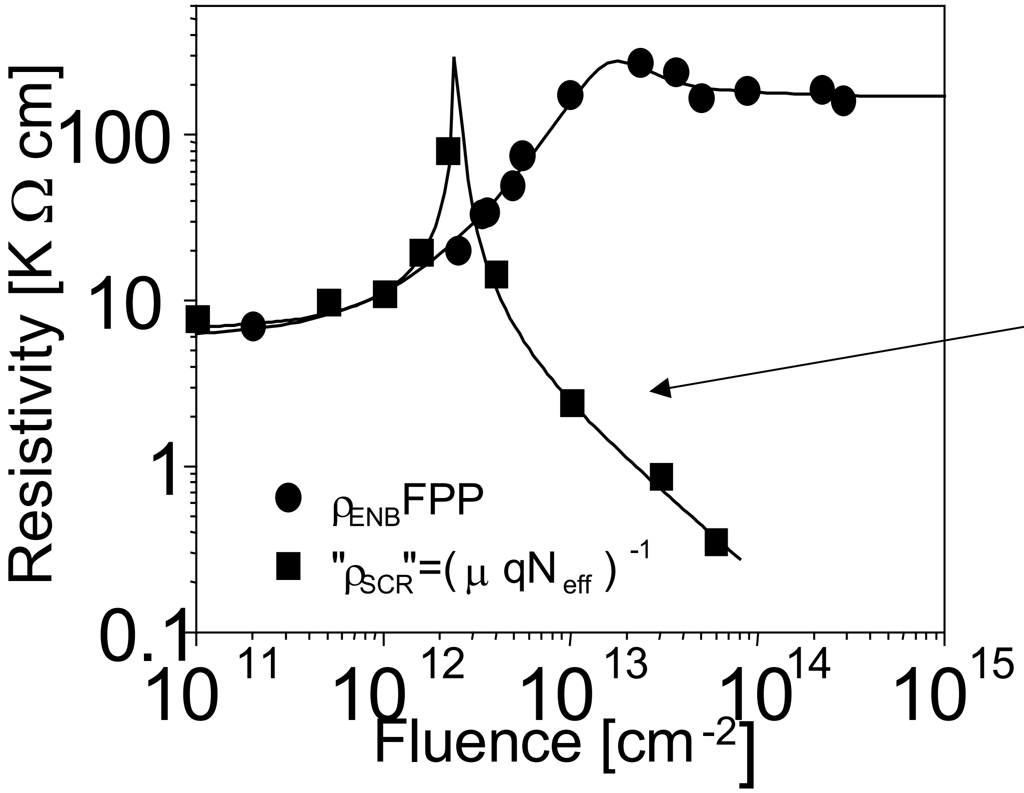

M. Bruzzi, IEEE Trans. Nucl. Sci. 2000

$$\rho_{SCR} = \frac{1}{q\mu N_{eff}}$$

Misura della resistività con tecnica delle quattro punte

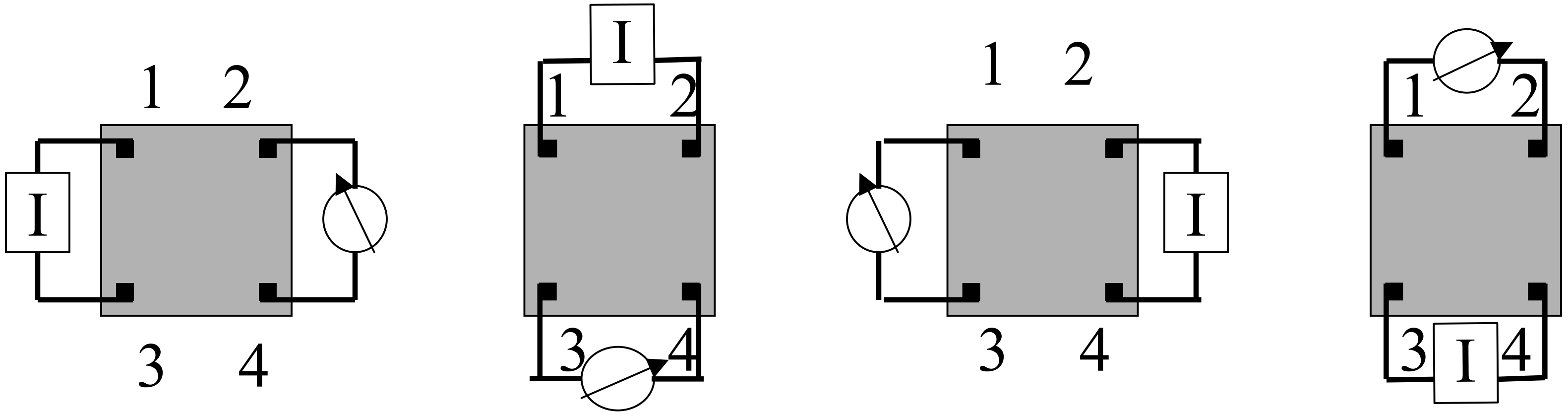

$$\rho = \frac{1}{q\mu_p(p + z \cdot n)}$$

$z = \mu_n/\mu_p$

L'aumento di resistività corrisponde al pinning del livello di Fermi a $E_v + 0.5$ eV

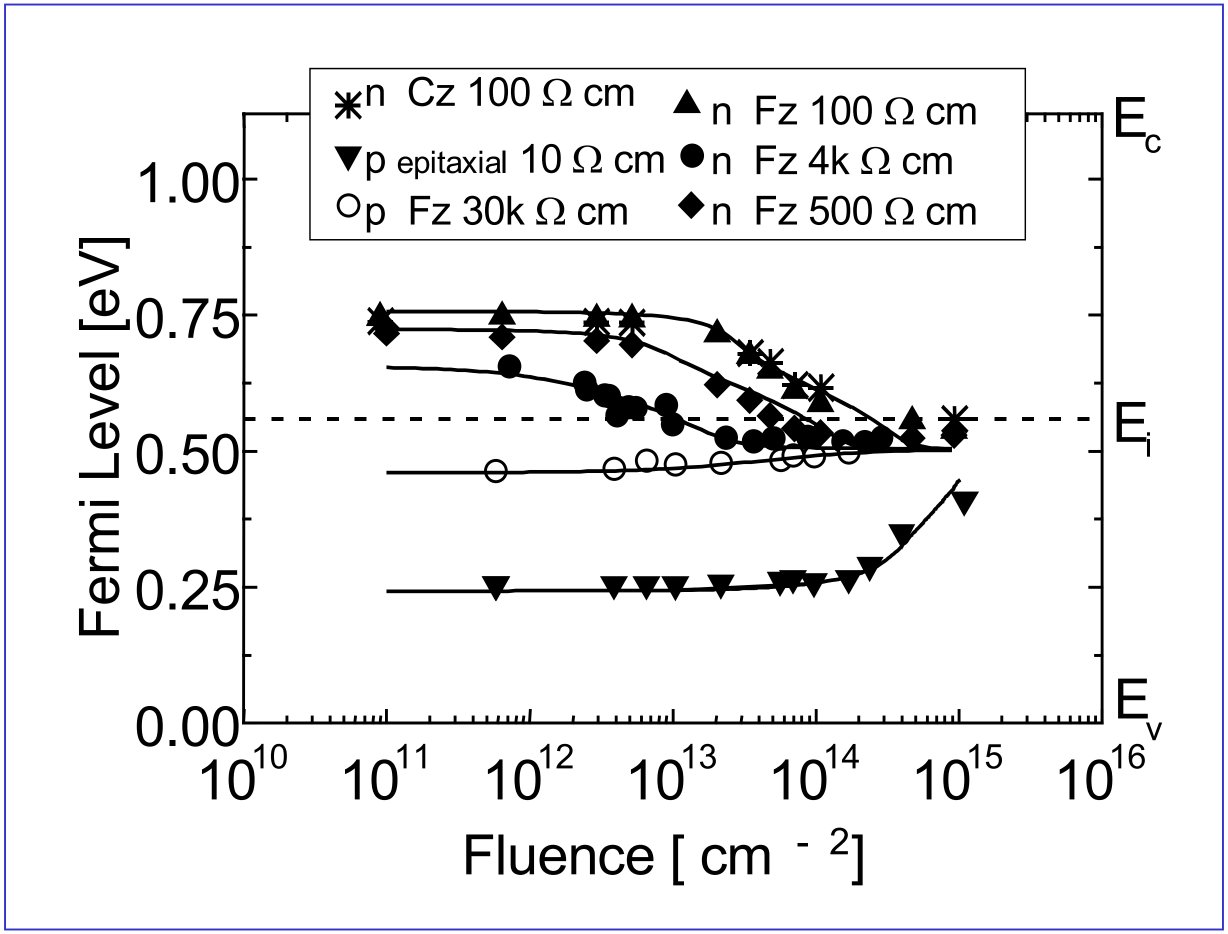

M. Bruzzi, IEEE Trans. Nucl. Sci. 2000

Misura del coefficiente di Hall per la determinazione del tipo di conducibilità

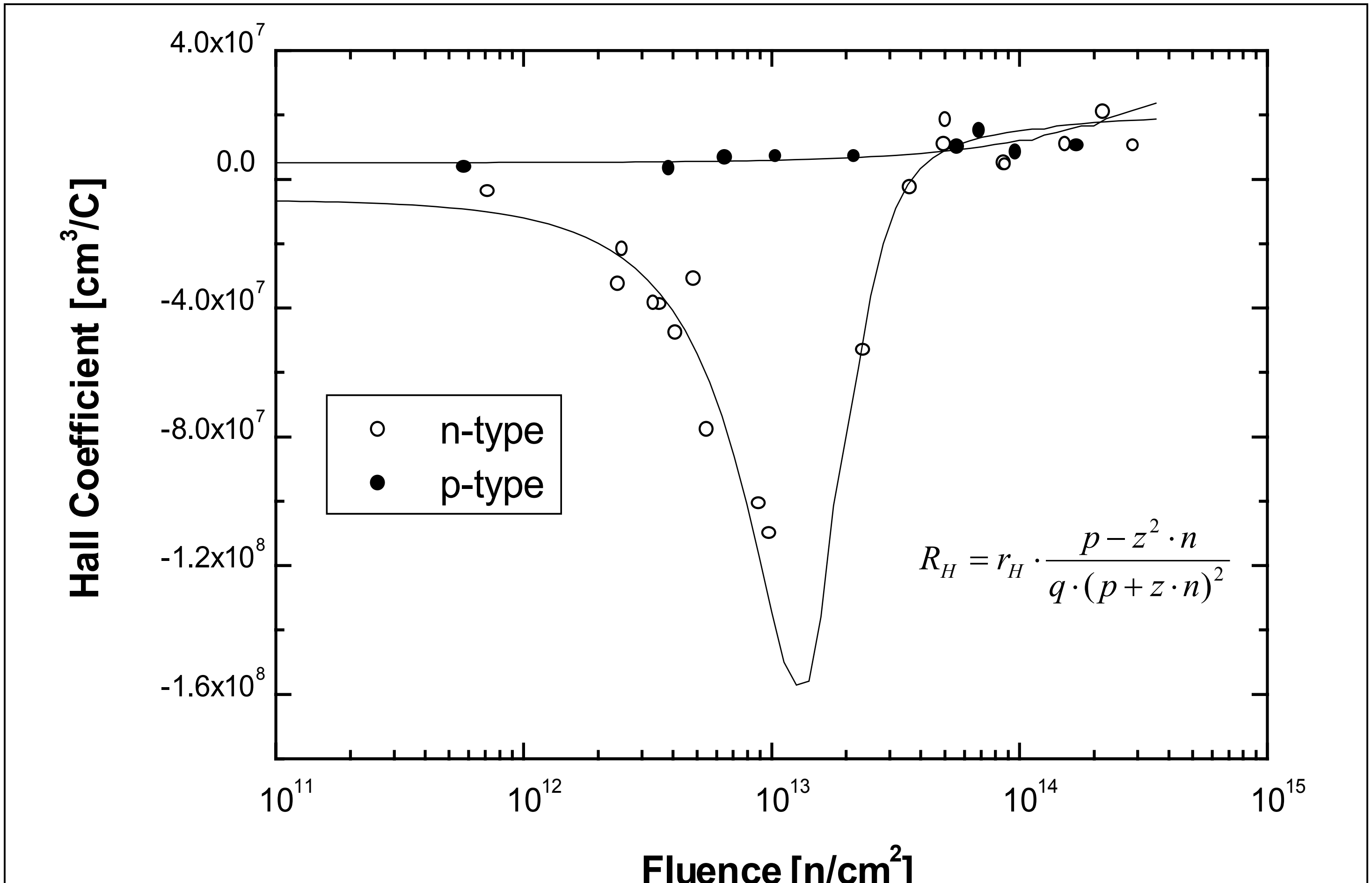

$$R_H = r_H \cdot \frac{p - z^2 \cdot n}{q \cdot (p + z \cdot n)^2}$$

E. Borchi, M. Bruzzi et al.

$$V_{Hall} = R_H J_x B_z h$$

Double junction : observed by TCT analysis

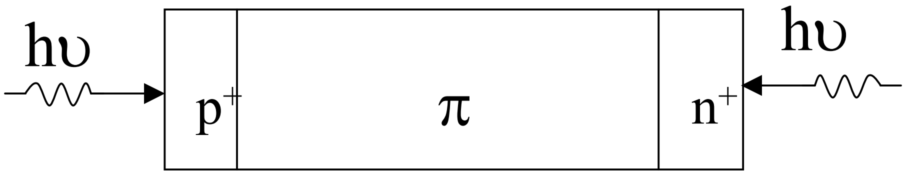

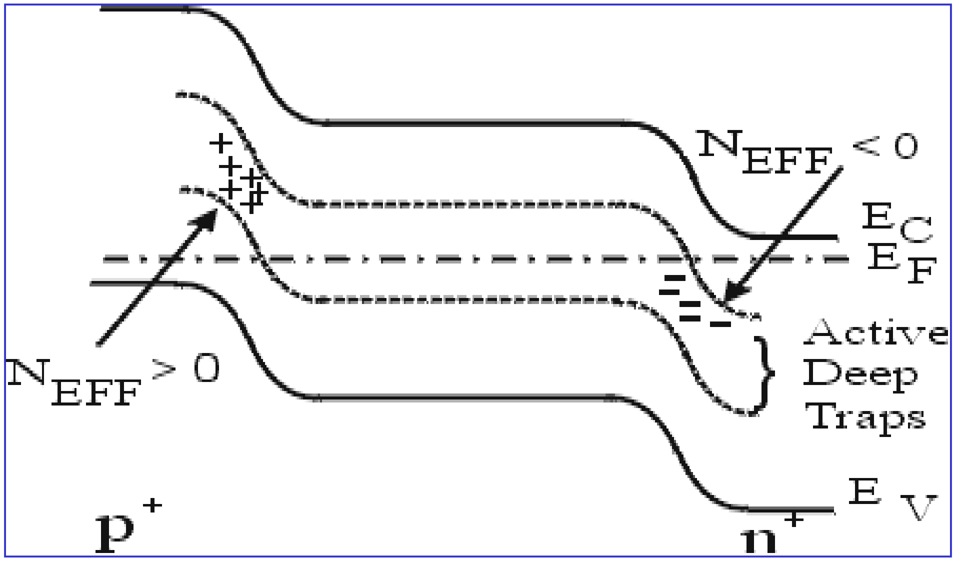

M. Bruzzi, IEEE Trans. Nucl. Sci. 2000

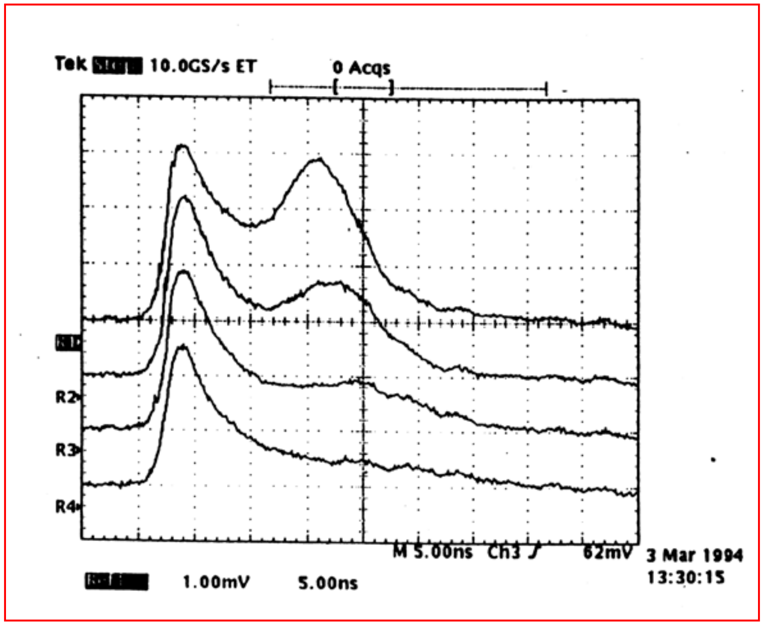

Z.Li et al, 1994

Signal integrated in time, plotted against Vrev to determine the N_{eff} sign

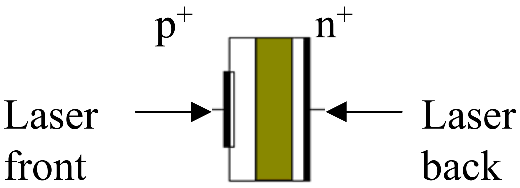

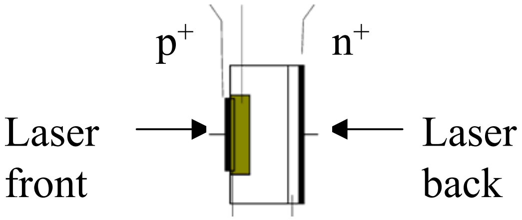

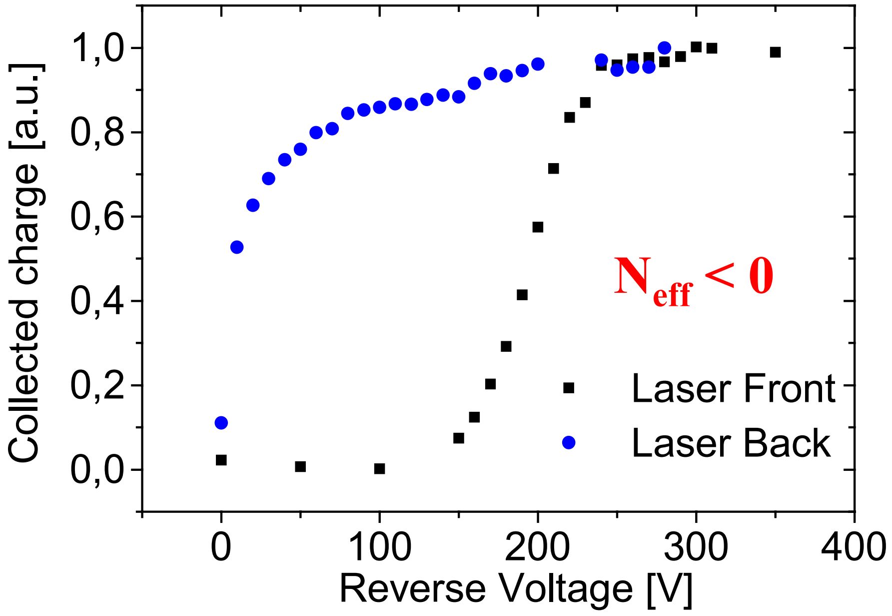

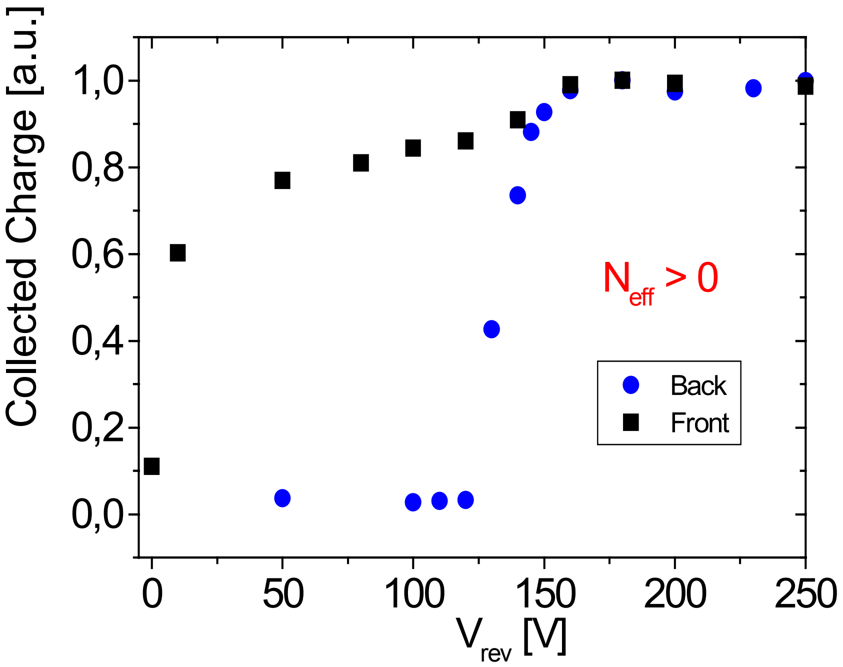

M. Bruzzi, Z.Li, J. Harkonen, presented at the 5th RD50 Workshop, October 2004, Florence

Charge Collection Efficiency

Limited by:

- **Partial depletion**
- **Trapping at deep levels**
- **Type inversion**

Collected Charge: $Q = Q_o \cdot \varepsilon_{\mathrm{dep}} \cdot \varepsilon_{trap}$

$$\varepsilon_{dep} = \frac{d}{W} \qquad \varepsilon_{trap} = e^{-\frac{\tau_c}{\tau_t}}$$

W: total thickness
d: Active thickness
τ_c : Collection time
τ_t : Trapping time

Trapping time reduced by radiation:
Krasel et al. (RD50)
for e/h up to 10^{15} cm^{-2} n- Si:

$1/\tau_t = 5*(\Phi/10^{16})$ ns^{-1}
$\tau_t \sim 1/\Phi$
$\tau_t = 0.2$ ns for $\Phi = 10^{16}$ cm^{-2}

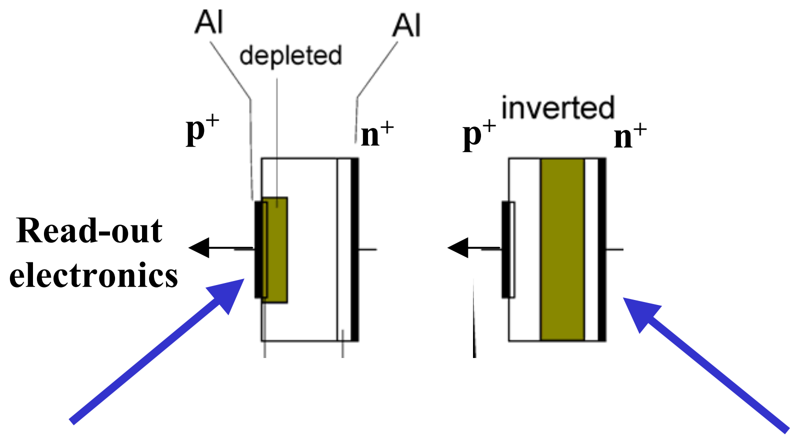

Read-out electronics

before inversion

after inversion
neglecting double junction

Decrease of the Charge Collection Efficiency

Source:
^{106}Ru - ^{90}Sr - laser $\lambda = 1060$nm

$$CCE_{non-irr} \; \alpha \; W = \sqrt{\frac{2\varepsilon V_{rev}}{qN_{eff}}} = \sqrt{\frac{V_{rev}}{V_{dep}}}$$

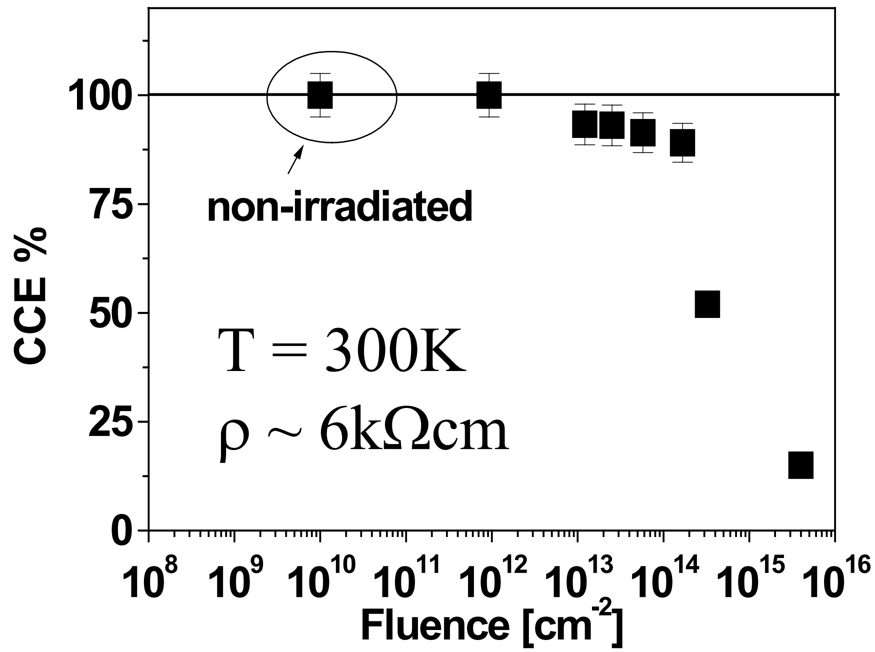

E. Borchi, M. Bruzzi et al. Nucl. Phys. B (1998)

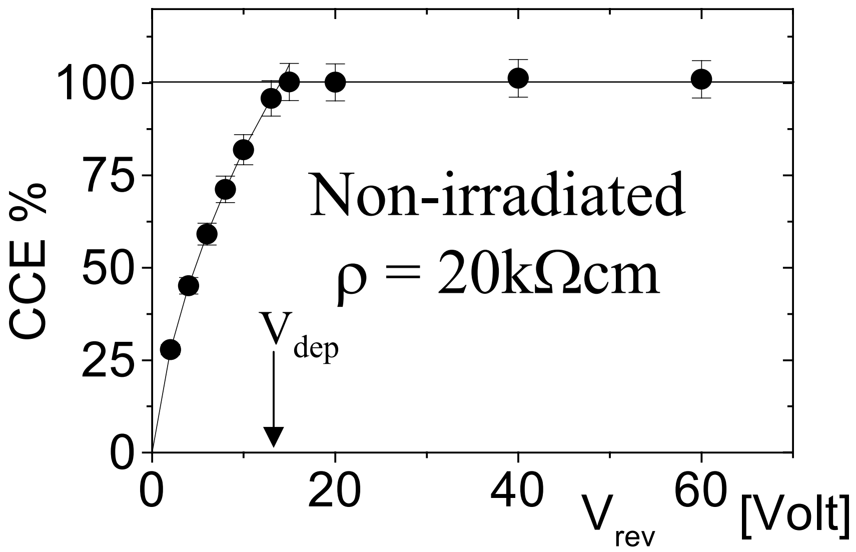

CCE decrease after irradiation:

- **trapping effects**
- **partial depletion due to reverse annealing**

These effects can be minimised by reducing the temperature

I.N.F.M

f=1.1x10^{14}n/cm^2

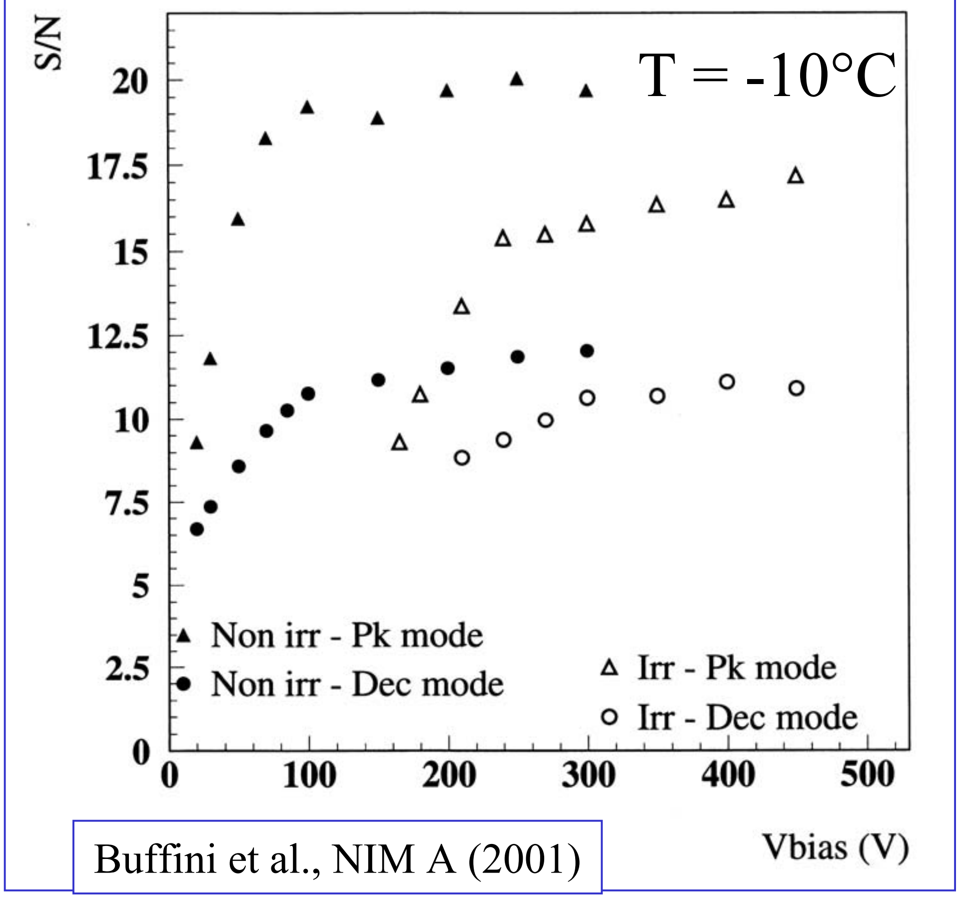

Buffini et al., NIM A (2001)

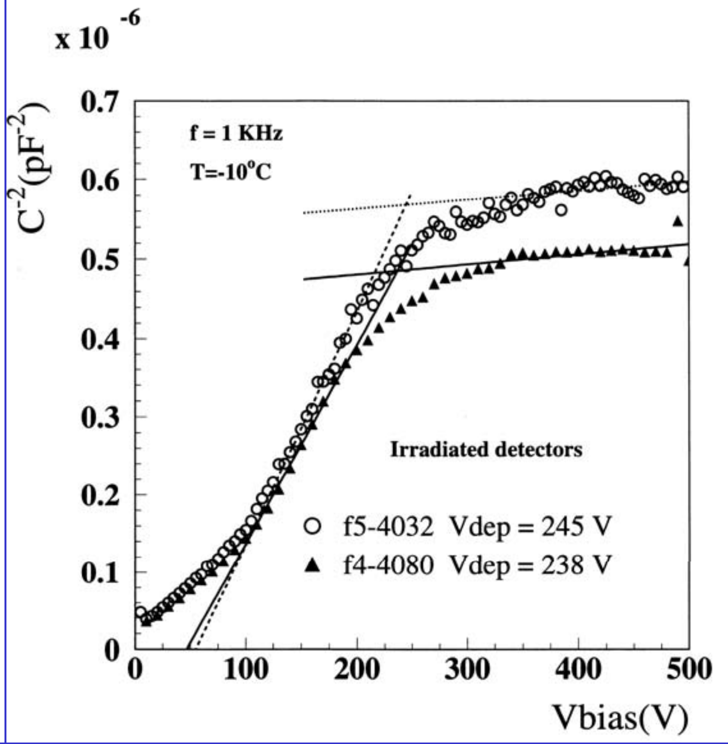

To maximise S/N with <111> it is necessary to overdeplete the detector up to :$V_{rev} \sim 2\ V_{dep}$

Discrepancy between CCE and CV analysis

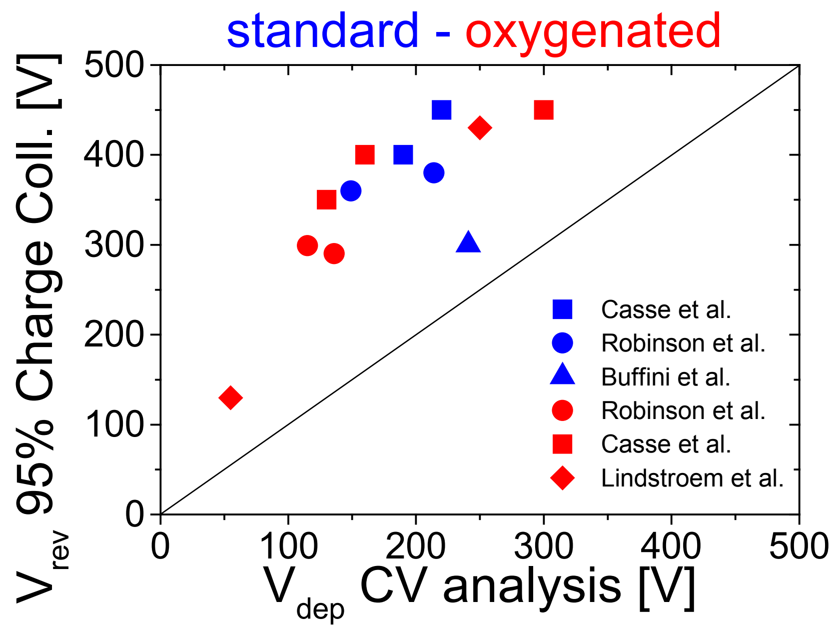

M. Bruzzi presented at ITACPP, Como, 2001

	Author	radiation	Exp.	material
●	Robinson et al., NIM A 461 (2001)	$3\text{x}10^{14}$ 24GeV p/cm^2	ATLAS	Oxygen. + standard
■	Casse et al., NIM A 466 (2001)	$3\text{-}4\text{x}10^{14}$ 24GeV p/cm^2	ATLAS	Oxygen. + standard
◆	Lindström et al., NIM A 466 (2001)	$1.65\text{x}10^{14}$ 24GeV p/cm^2	ROSE	Oxygen. <100>
▲	Buffini et al., NIM A (2001)	$1.1\text{x}10^{14}$ 1MeV n/cm^2	CMS	Standard <111>

Same behavior for standard and oxygenated , <100> and <111> silicon detectors

I dispositivi n-in-n non mostrano necessità di sovrasvuotamento dopo irraggiamento come i p-in-n, quindi risultano maggiormente resistenti alla radiazione (assenza di inversione di tipo).

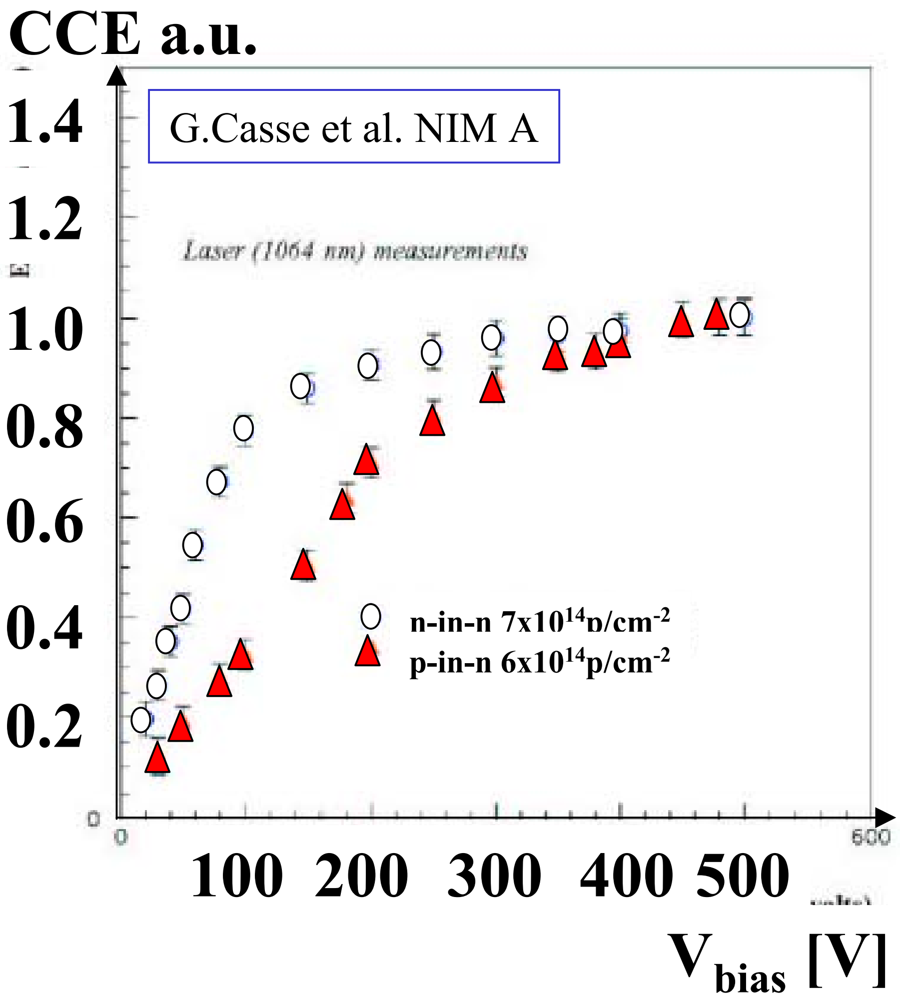

More on charge collection efficiency in n-in-n

- Trapping of generated e-h at defects
- Under-depletion due to high N_{eff}
- SCSI : keeping high electric field

on the read out side will significantly improve charge collection

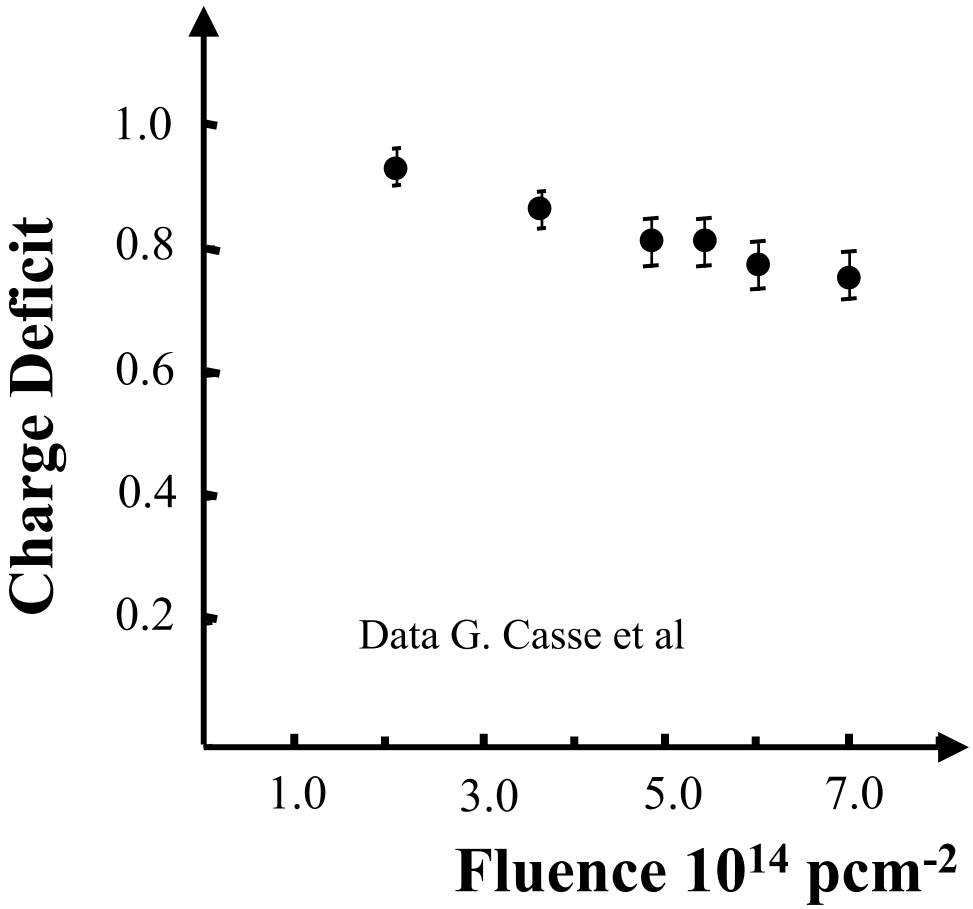

Signal (^{106}Ru ß–source) degradation as a function of fluence in a non-homogeneous irradiated detector (n-in-n).

From: CMS Coll.

Surface Damage and Effect of the crystal orientation

Trap and Oxide charge densities D_{it} and N_{ox} at the Si-SiO$_2$ interface

More available dangling bonds at the crystal surface in <111> than <100> $\Rightarrow D_{it<111>} \gg D_{it<100>}$

$$D_{it} = \frac{1}{q} \cdot \frac{dQ_{it}}{dE}$$

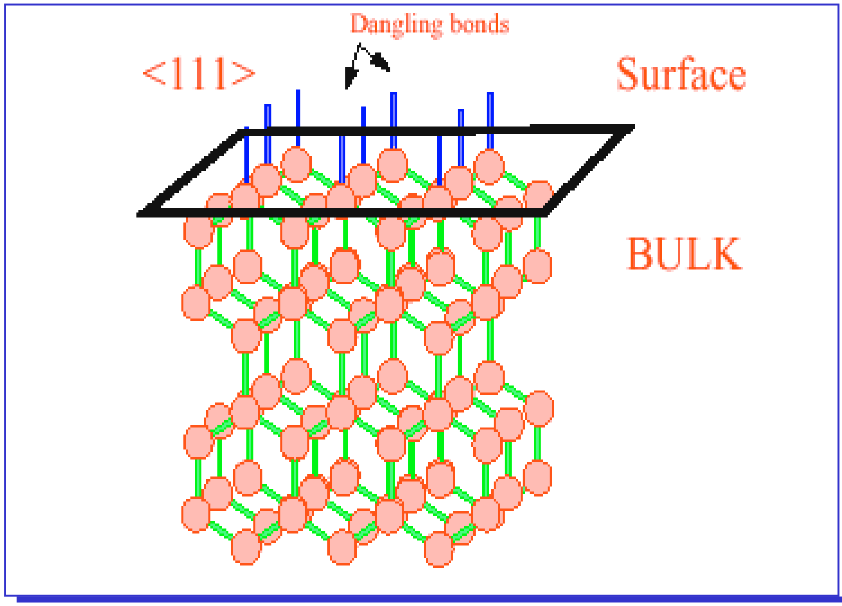

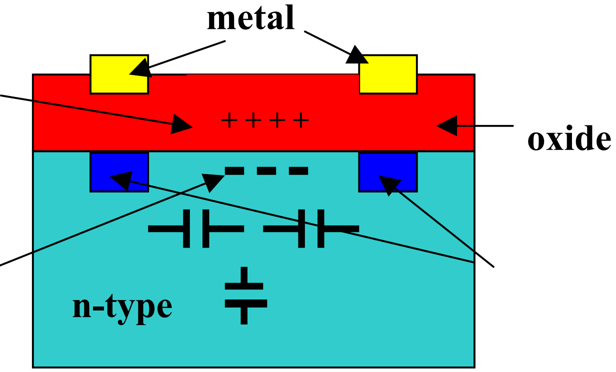

Positive interface charges N_{ox}

Electron layer at the silicon-oxide affecting C_{int} and C_{back}

Noise $ENC = 1000e^{-} + 46e^{-}/pF$

CMS - Deconvoluted mode $\tau = 25ns$

Radiation induced increase in the Interstrip Capacitance in <111> Si; C_{int} unaffected in <100>

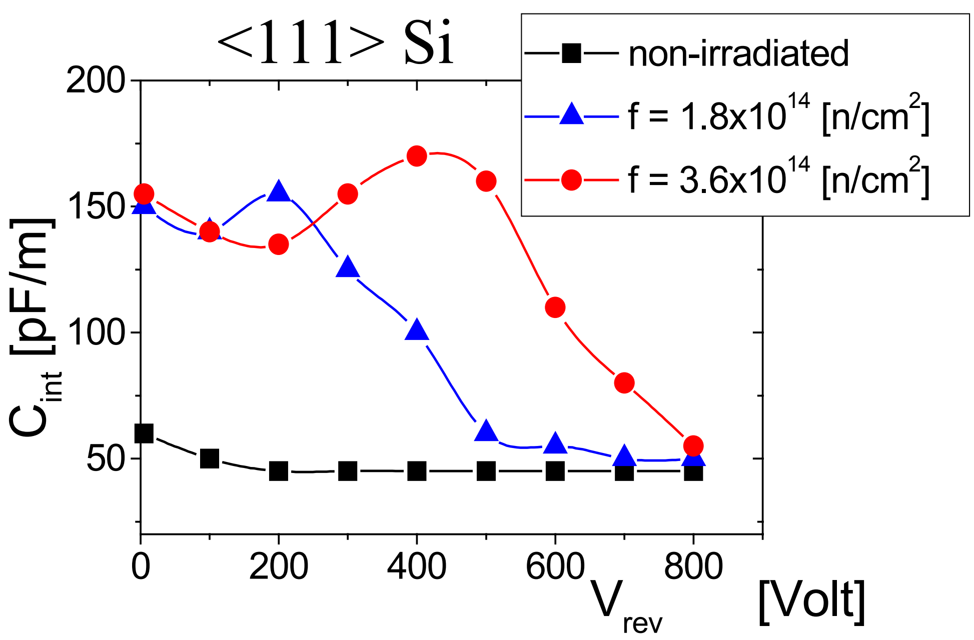

Data from : CMS Coll. NIM A 426 (1999) 16-23

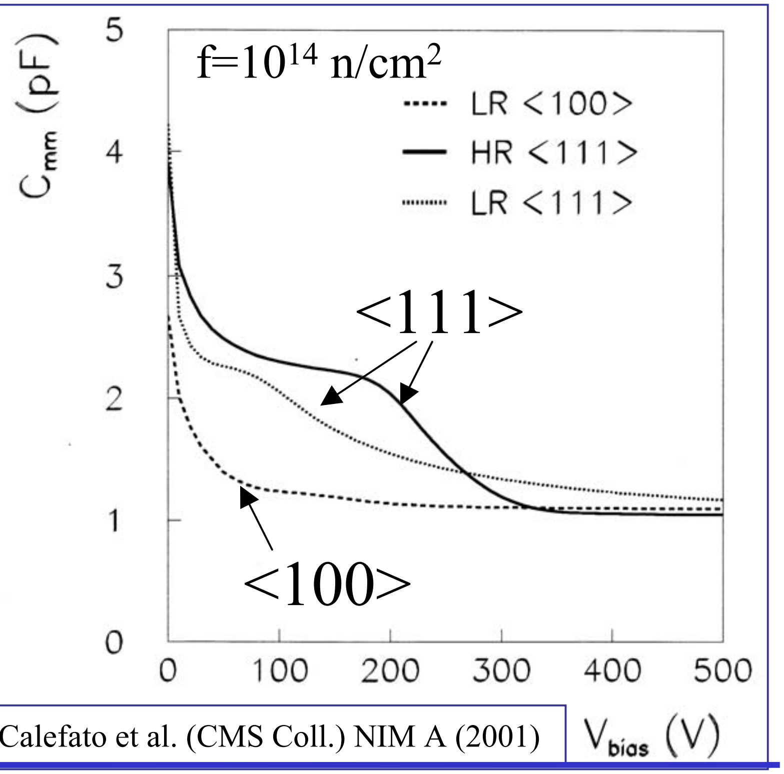

G.Calefato et al. (CMS Coll.) NIM A (2001)

4. Radiation Hardening Technologies

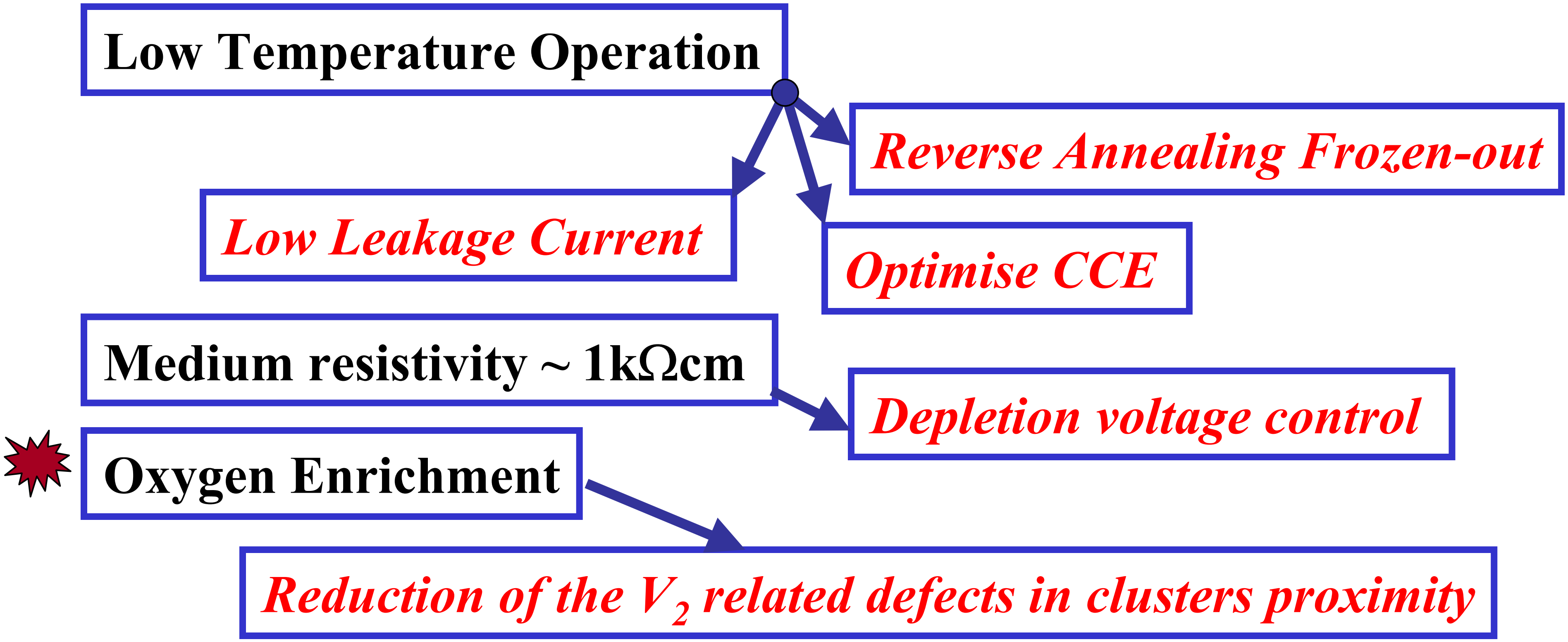

Low Temperature Operation

Reverse Annealing Frozen-out

Low Leakage Current

Optimise CCE

Medium resistivity ~ 1kΩcm

Depletion voltage control

Oxygen Enrichment

Reduction of the V_2 related defects in clusters proximity

Oxygen Enrichment for Radiation Hardening

RD48 (ROSE) CERN Collaboration

Main Hypothesis: Oxygen sink of vacancies

V-O_i complex concentration increase → reduction of deeper levels mainly divacancy related

1964 **Significant radiation hardening for Co^{60} γ-irradiation by increasing the oxygen concentration (CZ Si)**

T.Nakano, Y.Inuishi, effects of dosage and impurities on radiation damage of carrier lifetime in silicon, J.Phys. Soc., 19, 851-858,(1964)

1966 **Neutron-induced degradation independent of the oxygen concentration (CZ Si)**

O.L.Curtis Jr., Effects of oxygen and dopant on lifetime in neutron-irradiated silicon, IEEE Trans. Nucl. Sci. NS-13, 6, 33-40 (1966).

Decrease of N_{eff} and V_{dep} changes after γ and p irradiation
Diffusion oxygenated Float Zone Silicon

Oxygen enrichment at BNL (1992) $[O_i]$ ~5×10^{17} cm^{-3} in pure FZ Si

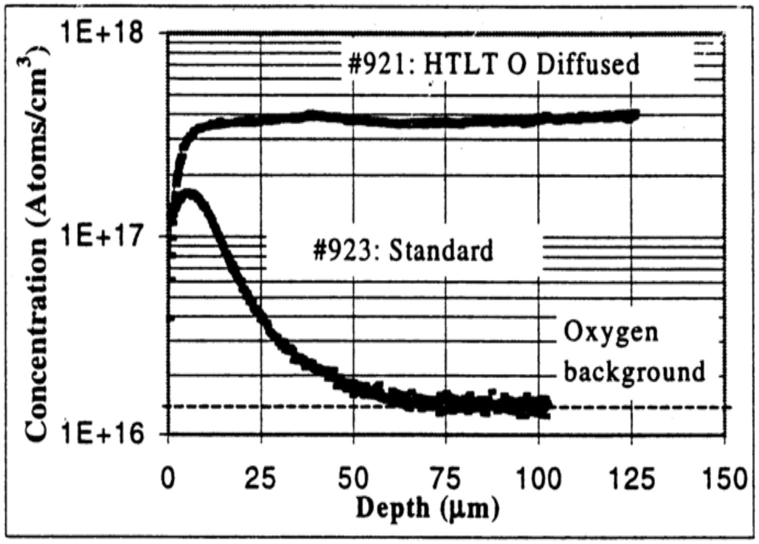

Z.Li et al. IEEE Trans. Nucl. Sci. 42, 4, 219-223 (1995)

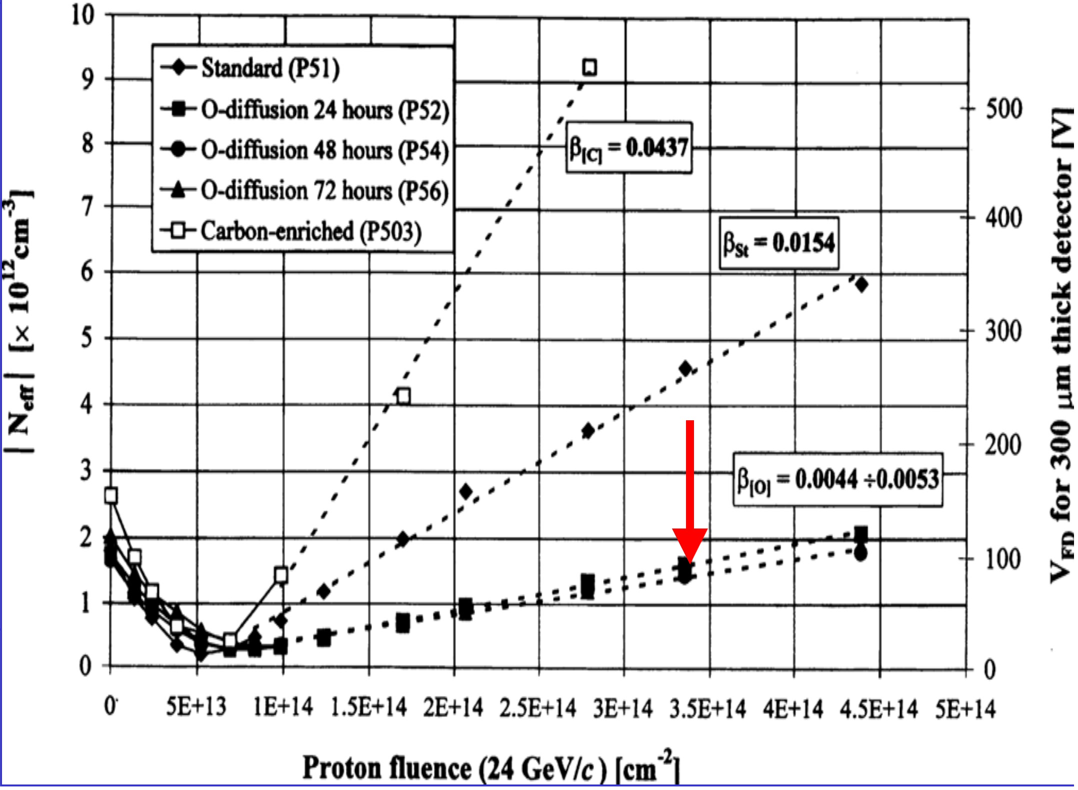

ROSE

RD48

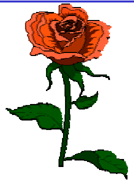

http://cern.ch/rd48

A.Ruzin, Cern RD48 Coll. NIM A 447 (2000), 116-125

The RD50 CERN Collaboration

Development of Radiation Hard Semiconductor Devices for High Luminosity Colliders

- **Collaboration formed in November 2001 - http://www.cern.ch/rd50**
- **Experiment approved as RD50 by CERN in June 2002**
- **Main objective:**

Development of ultra-radiation hard semiconductor detectors for the luminosity upgrade of the LHC to 10^{35} $cm^{-2}s^{-1}$ ("Super-LHC").

Challenges: - Radiation hardness up to 10^{16} cm^{-2} required
- Cost effectiveness

- **Presently 250 Members from 50 Institutes**

Belgium (Louvain), Canada (Montreal), Czech Republic (Prague (2x)), Finland (Helsinki (2x), Oulu), Germany (Berlin, Dortmund, Erfurt, Halle, Hamburg, Karlsruhe), Greece (Athens), Israel (Tel Aviv), Italy (Bari, Bologna, Florence, Milano, Modena, Padova, Perugia, Pisa, Trento, Trieste, Turin), Lithuania (Vilnius), Norway (Oslo (2x)), Poland (Warsaw), Romania (Bucharest (2x)), Russia (Moscow (2x), St.Petersburg), Slovenia (Ljubljana), Spain (Barcelona, Valencia), Sweden (Lund) Switzerland (CERN, PSI), Ukraine (Kiev), United Kingdom (Exeter, Glasgow, Lancaster, Liverpool, London, Sheffield, University of Surrey), USA (Fermilab, Purdue University, Rutgers University, Syracuse University, BNL, University of New Mexico)

Scientific strategies

- Three R&D strategies:
- Material engineering
  - Defect engineering of silicon (oxygenation, dimers, …)
  - New detector materials (SiC, …)
- Device engineering
  - Improvement of present planar detector structures
  (3D detectors, thin detectors, cost effective detectors,…)
- Variation of detector operational conditions
  - Low temperature operation
  - Forward bias operation
- Further key tasks:
- Basic studies
- Defect modeling and device simulation

RD50
Center of gravity

Scientific Organization of RD50

Development of Radiation Hard Semiconductor Devices for High Luminosity Colliders

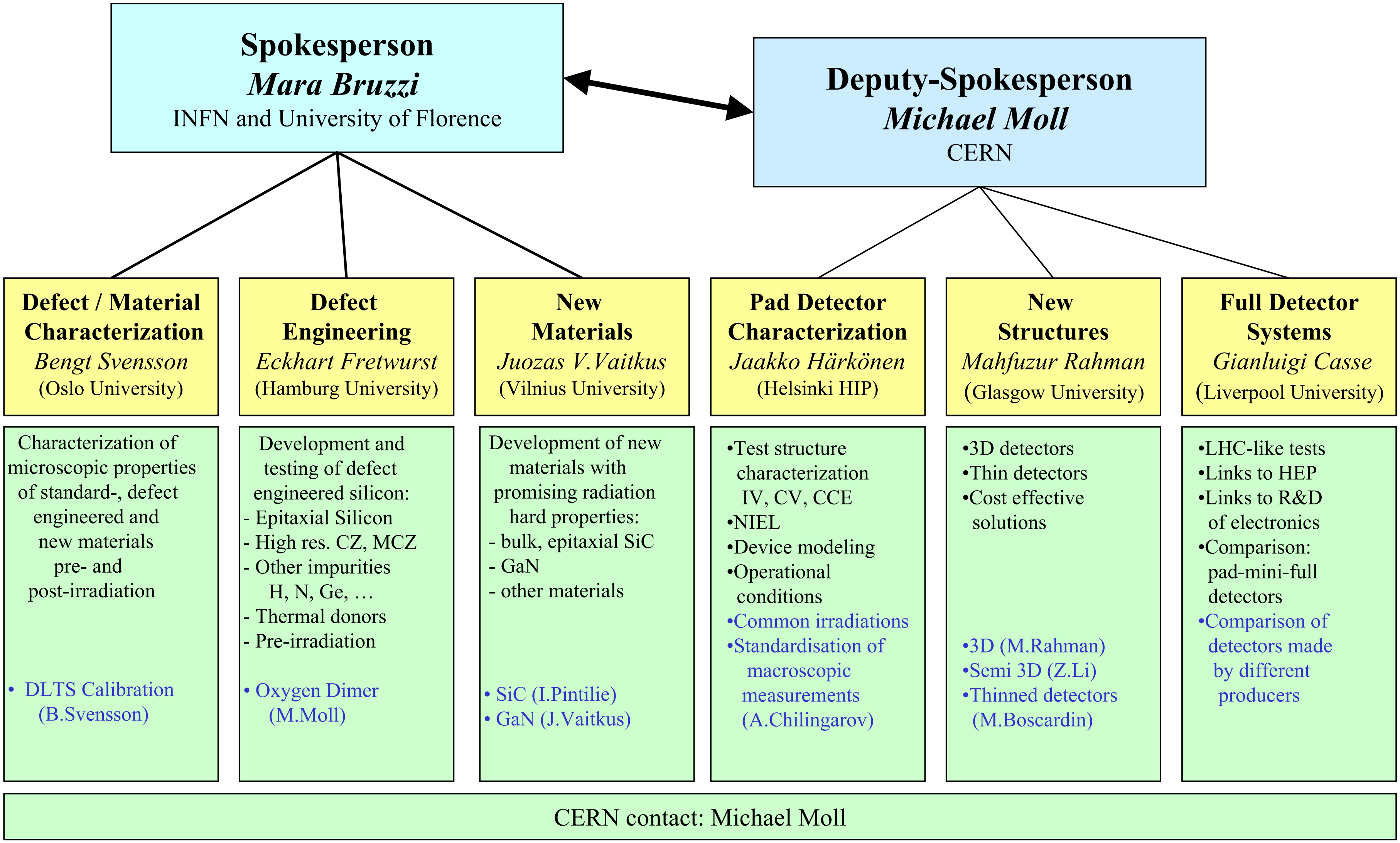

Spokesperson
Mara Bruzzi
INFN and University of Florence

Deputy-Spokesperson
Michael Moll
CERN

Defect / Material Characterization
Bengt Svensson
(Oslo University)

Characterization of microscopic properties of standard-, defect engineered and new materials pre- and post-irradiation

- DLTS Calibration (B.Svensson)

Defect Engineering
Eckhart Fretwurst
(Hamburg University)

Development and testing of defect engineered silicon:
- Epitaxial Silicon
- High res. CZ, MCZ
- Other impurities H, N, Ge, …
- Thermal donors
- Pre-irradiation

- Oxygen Dimer (M.Moll)

New Materials
Juozas V.Vaitkus
(Vilnius University)

Development of new materials with promising radiation hard properties:
- bulk, epitaxial SiC
- GaN
- other materials

- SiC (I.Pintilie)
- GaN (J.Vaitkus)

Pad Detector Characterization
Jaakko Härkönen
(Helsinki HIP)

- Test structure characterization IV, CV, CCE
- NIEL
- Device modeling
- Operational conditions
- Common irradiations
- Standardisation of macroscopic measurements (A.Chilingarov)

New Structures
Mahfuzur Rahman
(Glasgow University)

- 3D detectors
- Thin detectors
- Cost effective solutions

- 3D (M.Rahman)
- Semi 3D (Z.Li)
- Thinned detectors (M.Boscardin)

Full Detector Systems
Gianluigi Casse
(Liverpool University)

- LHC-like tests
- Links to HEP
- Links to R&D of electronics
- Comparison: pad-mini-full detectors
- Comparison of detectors made by different producers

CERN contact: Michael Moll

Approaches of RD50 to develop radiation harder detectors

Material Engineering

- Defect Engineering of Silicon
  - Understanding radiation damage
    - **Microscopic defects**
    - Simulation of defect properties and defect kinetics
  - Oxygen enriched silicon
    - **DOFZ – Diffusion Oxygenated Float Zone Silicon**
    - **CZ – Czochralski Silicon**
    - **MCZ – Magnetic Czochralski**
    - **EPI – Epitaxial silicon grown on CZ substrate**
  - Oxygen dimers
  - Hydrogen enriched silicon
  - Pre-irradiated silicon
- New Materials
  - Silicon Carbide (SiC)
  - Gallium Nitride (GaN)
  - Diamond → **CERN RD42 Collaboration**

Defect engineering strategy

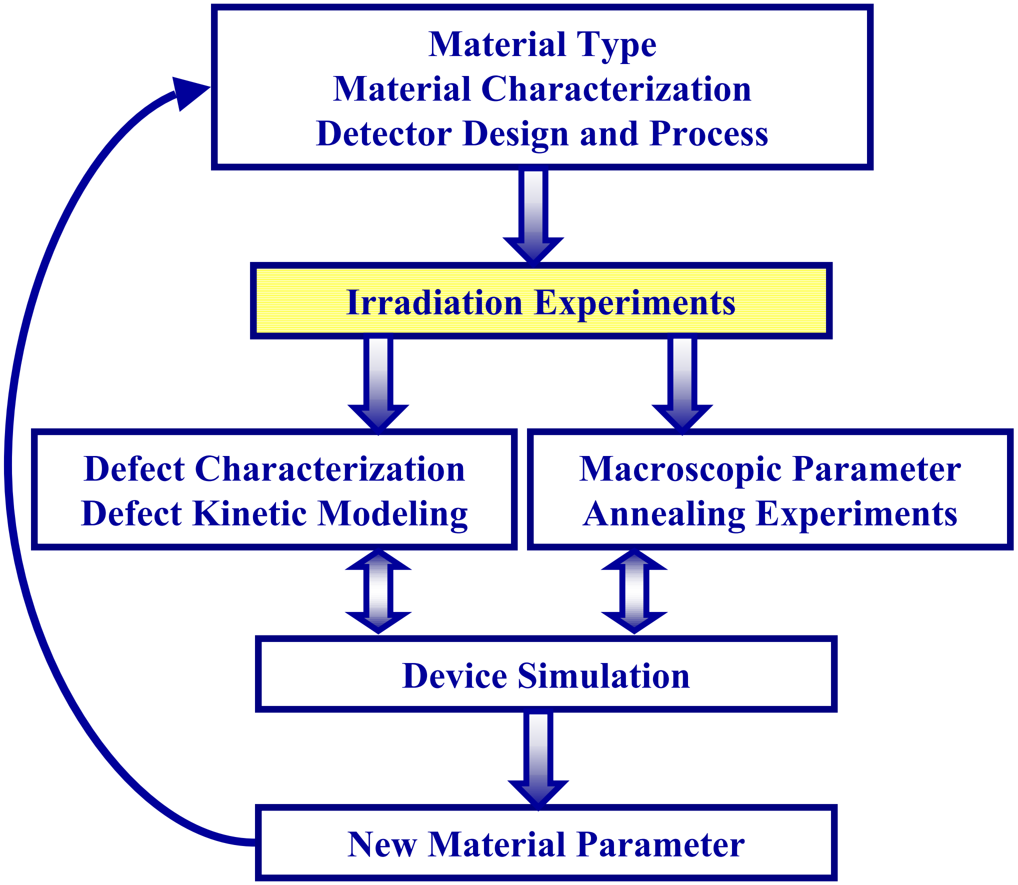

Material Type
Material Characterization
Detector Design and Process

Irradiation Experiments

Defect Characterization
Defect Kinetic Modeling

Macroscopic Parameter
Annealing Experiments

Device Simulation

New Material Parameter

From G. Lindstroem

IRRADIATION EXPERIMENTS in RD50

- **24 GeV/c protons, PS-CERN**
  up to 10^{16} cm^{-2}
- **^{60}Co dose, BNL, USA**
  up to 1.5GRad
- **10-50 MeV protons, Jyvaskyla +Helsinki**
  up to $3x10^{14}$ cm^{-2}
- **TRIGA reactor neutrons, Ljubljana**
  up to $8x10^{15}$ cm^{-2}
- **58 MeV Li ions, Legnaro/ Padova**
- **900 MeV electrons Trieste**
- **15MeV electrons at Oslo**

Defect Engineering of Silicon

- Influence the defect kinetics by incorporation of impurities or defects
- Best example: Oxygen

  Initial idea: **Incorporate Oxygen to getter radiation-induced vacancies ⇒ prevent formation of Di-vacancy (V_2) related deep acceptor levels**
- Observation: Higher oxygen content ⇒ less negative space charge **(less charged acceptors)**
- One possible mechanism: V_2O is a deep acceptor

V → O → VO (not harmful at room temperature)

V → VO → V_2O (negative space charge)

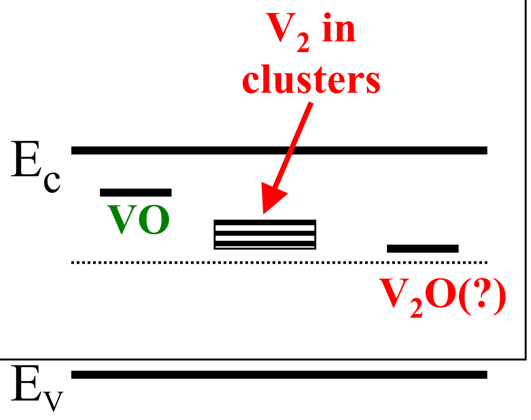

Different kind of Si materials investigated by RD50

Material	Symbol	ρ Ωcm	$[O_i]$ cm^{-3}
Standard n- or p-type FZ	**STNFZ**	$1\text{-}7 \cdot 10^3$	$< 5\ 10^{16}$
Diffusion Oxygenated FZ p or n-type	**DOFZ**	$1\text{-}7 \cdot 10^3$	$\sim 1\text{-}2\ 10^{17}$
Epi-layer 50 µm on CZ n-type ITME	**EPI**	**50-100**	substrate: $1 \cdot 10^{18}$
Czochralski Sumitomo, Japan	**CZ**	$1.2 \cdot 10^3$	$\sim 8\text{-}9\ 10^{17}$
Magnetic Czochralski Okmetic Finland	**MCZ**	$1.2 \cdot 10^3$	$\sim 5\text{-}9\ 10^{17}$

Czochralski Si

- Very high Oxygen content 10^{17}-10^{18}cm^{-3} **(Grown in SiO_2 crucible)**
- High resistivity (>1KΩcm) available only recently **(Magnetic CZ technology)**
- CZ wafers cheaper than FZ **(RF-IC industry got interested)**

DOFZ Si: Spectacular Improvement of γ-irradiation tolerance

Depletion Voltage

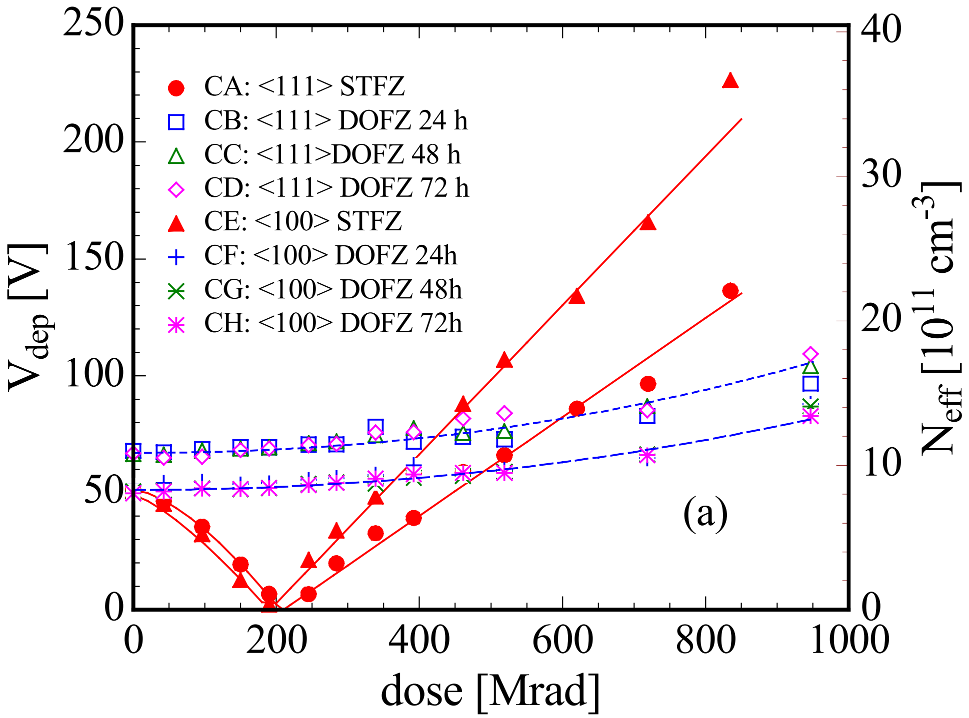

Leakage Current

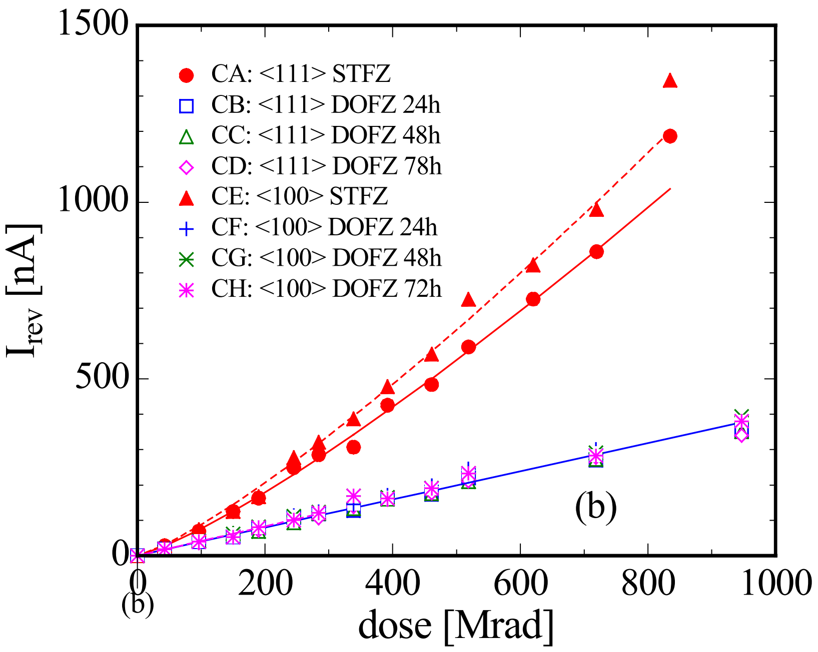

- No type inversion for oxygen enriched silicon!
- Slight increase of positive space charge
  (due to Thermal Donor generation?)
- Leakage increase not linear and depending on oxygen concentration

[E.Fretwurst et al. 1st RD50 Workshop]
See also:
- Z.Li et al. [NIMA461(2001)126]
- Z.Li et al. [1st RD50 Workshop]

Oxygen enriched silicon - DOFZ

Data From G.Lindstrom et al.

Reverse Annealing

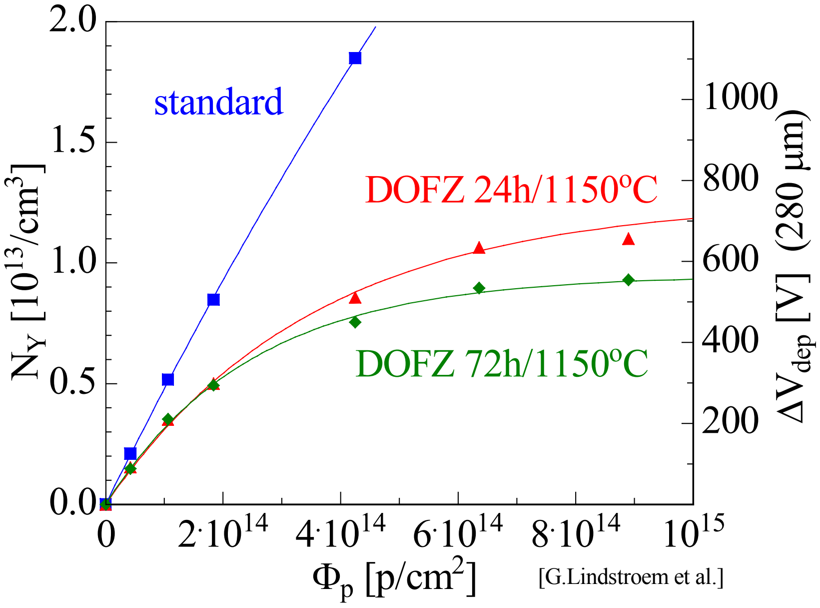

[G.Lindstroem et al.]

Saturation of amplitude

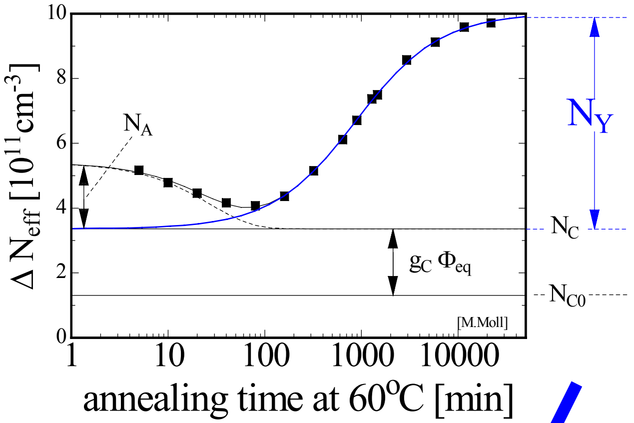

delayed reverse annealing

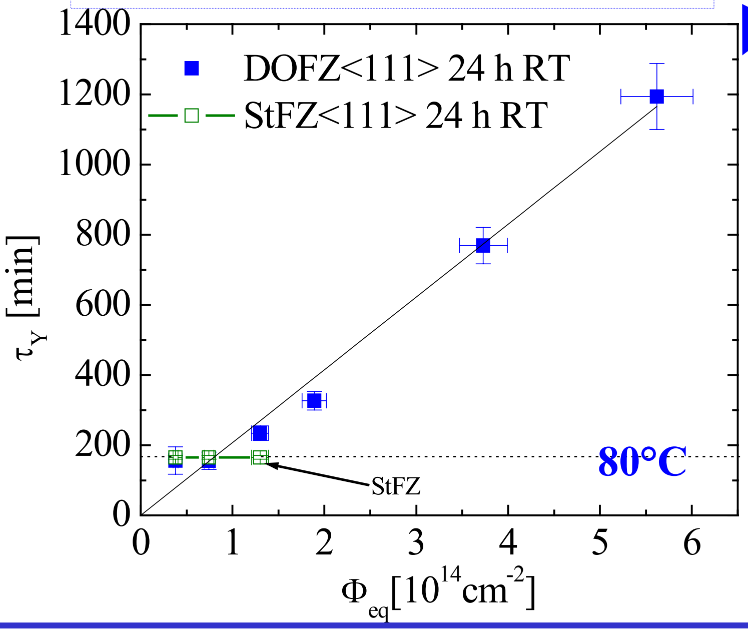

- Saturation of reverse annealing

  (24 GeV/c p - only little effect after neutron irradiation observed !)
- No big difference between 24h and 72h oxidation at 1150°C
- time constant depending on fluence

Il difetto responsabile del danno da radiazione nel Si standard FZ è stato identificato

- “I defect” Acceptor + Donor E_c- 0.545 eV + E_v+0.23 eV

[I.Pintilie et al., APL 82 (13), 2169 (2003)]

E’ tuttora controverso se esso corrisponde al difetto V_2O

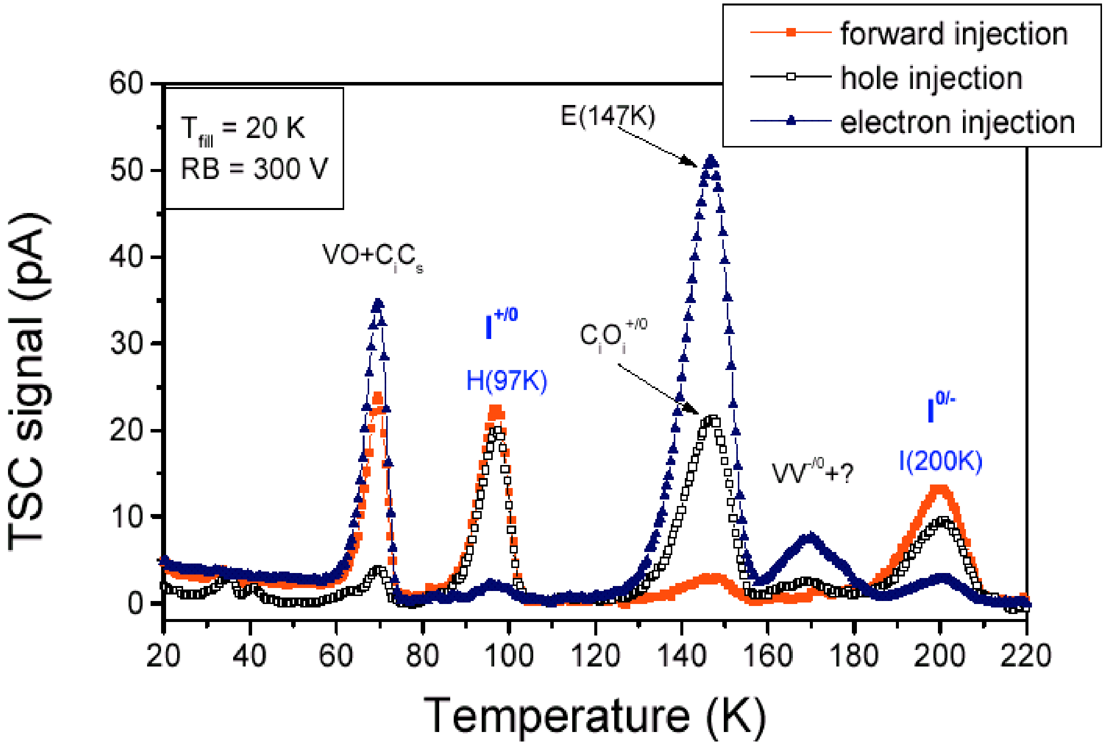

I defect responsible for type inversion in Standard FZ Si after ^{60}Co γ–irradiation and for increase of leakage current with dose. It appears in oxygen lean Si.

Microscopic defects ⇔ Macroscopic properties
- Co^{60} γ-irradiated silicon detectors -

- Comparison for effective doping concentration (left) and leakage current (right) for two different materials
  - as predicted by the microscopic measurements (open symbols)
  - as deduced from CV/IV characteristics (filled symbols)

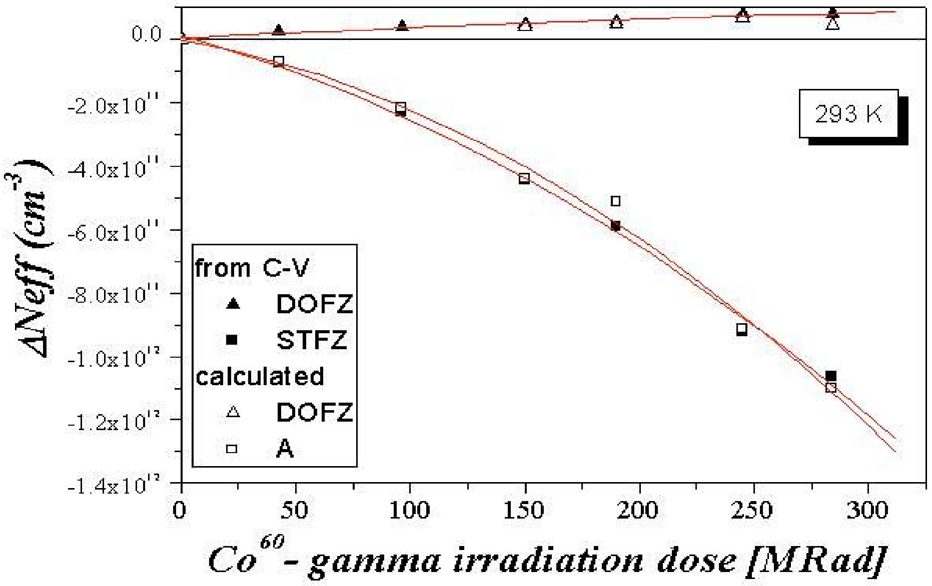

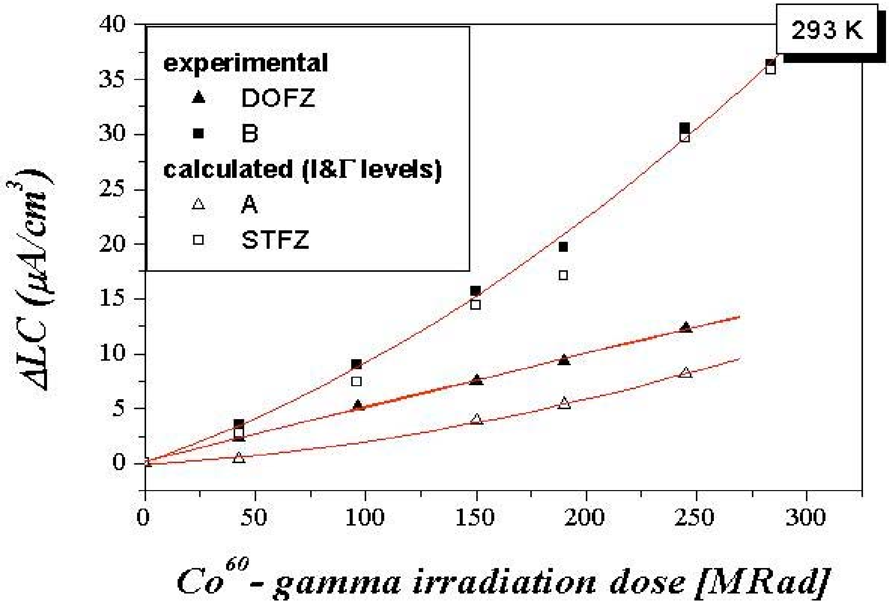

[I.Pintilie et al.,Applied Physics Letters,82, 2169, March 2003]

Czochralski Si

190 MeV π irradiation Villigen
Cz from Sumitomo Sitix, Japan

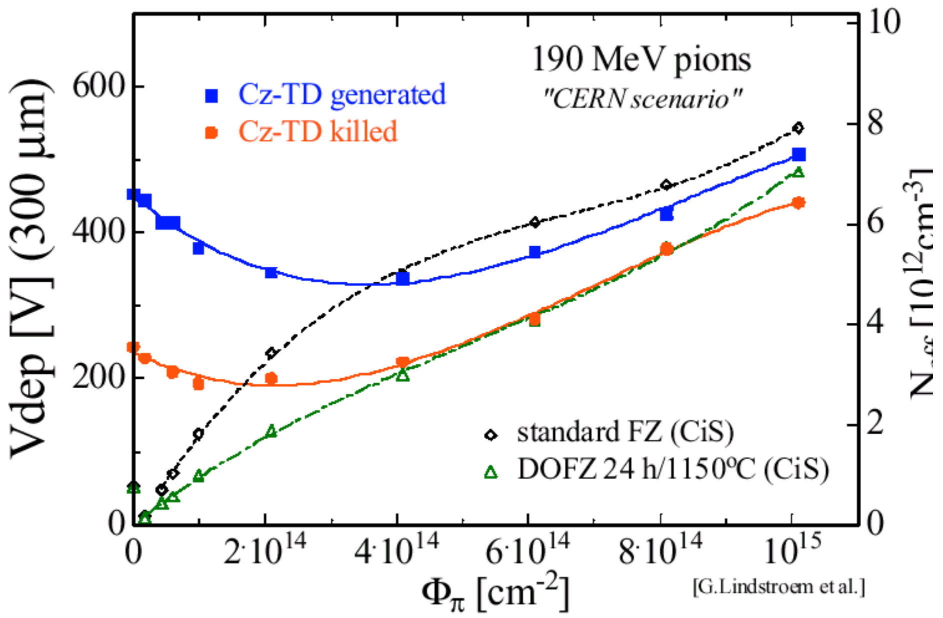

24 GeV/c p irradiation CERN
Cz from Sumitomo Sitix, Japan

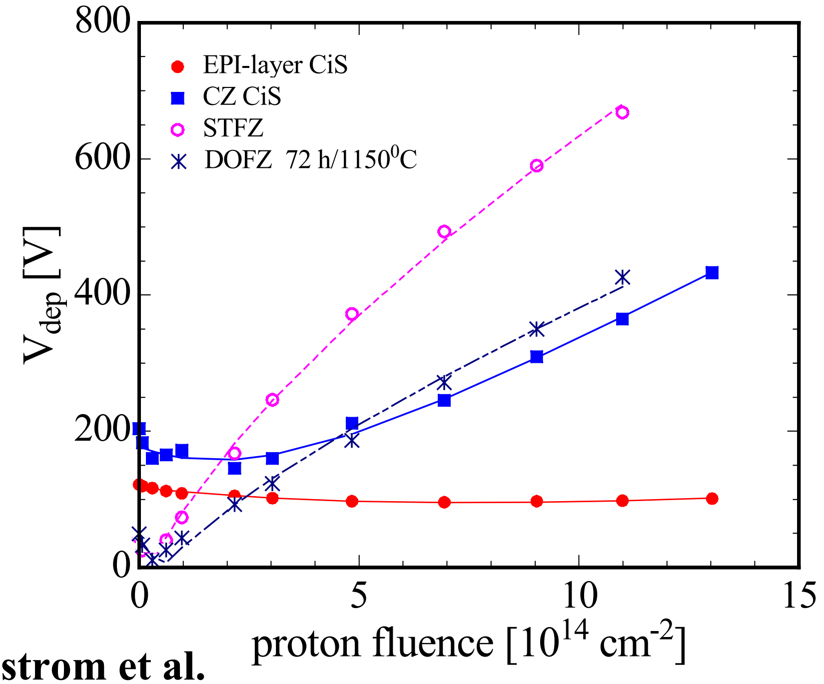

Data From G.Lindstrom et al.

- ♦ **No type inversion (SCSI)**
- ♦ **Reverse current and charge trapping comparable to FZ silicon**

Magnetic CZ, Okmetic, Finland

10 MeV proton irr. at Jyväskylä, Finland

- Improvement in V_{dep}, N_{eff}
- Observed SCSI – Space Charge Sign inversion
- Reduction of reverse current ??

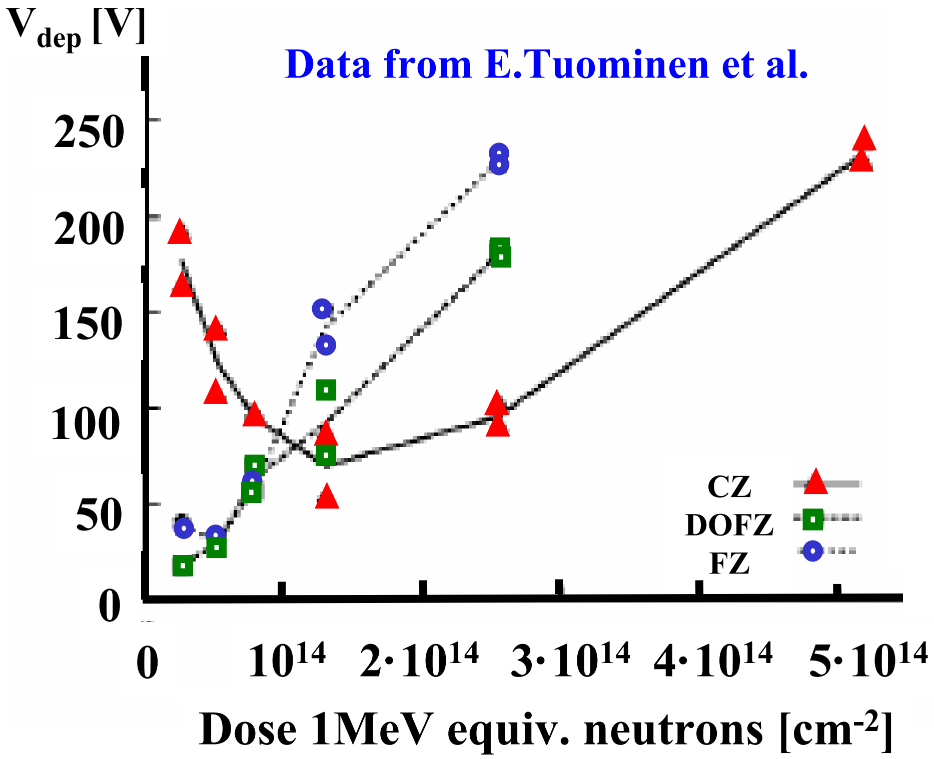

Only small change in V_{dep}

- $1•10^{15}$ (190 MeVπ)/cm^2
- $1•10^{15}$ (24 GeV/c p)/cm^2
- $5•10^{14}$ (10 MeV p)/cm^2

- No type inversion (Sumitomo CZ)
  type inversion observed for Okmetic MCZ after $5•10^{14}$ (10 MeV p)/cm^2
- Leakage current and charge trapping as for FZ silicon
- Very high oxygen content: Beware of thermal donors !

From J. Harkonen et al.

Epitaxial silicon

Motivation: After 1 MeV neutron irradiation to 10^{15} cm^{-2}
the effective drift length for e is ~150μm and for h ~50μm

⇒ use thin detectors (50-100μm) from the beginning, with low resistivity Epitaxial Si
50μm, 50Ωcm on CZ Si made by ITME (Warsaw)

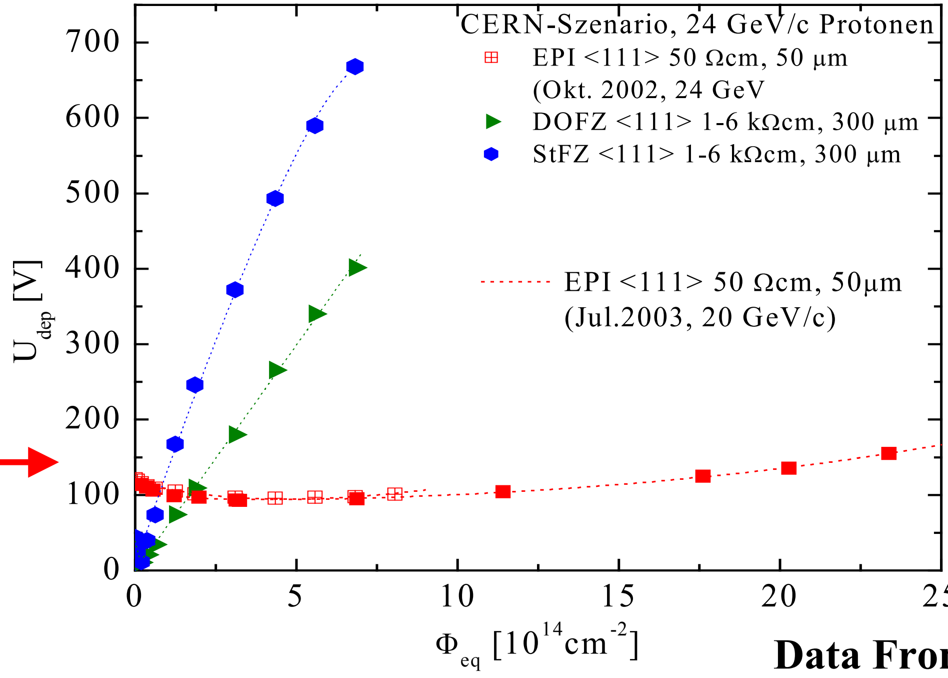

120 V

160 V

Data From G.Lindstrom et al.

- Leakage current almost identical to CZ, FZ, DOFZ detectors

COMPARISON STFZ-, DOFZ-, Cz- and EPI-SI

24 GeV/c PROTONS

CERN-SCENARIO MEASUREMENTS (4min/80°C treatment after each step)

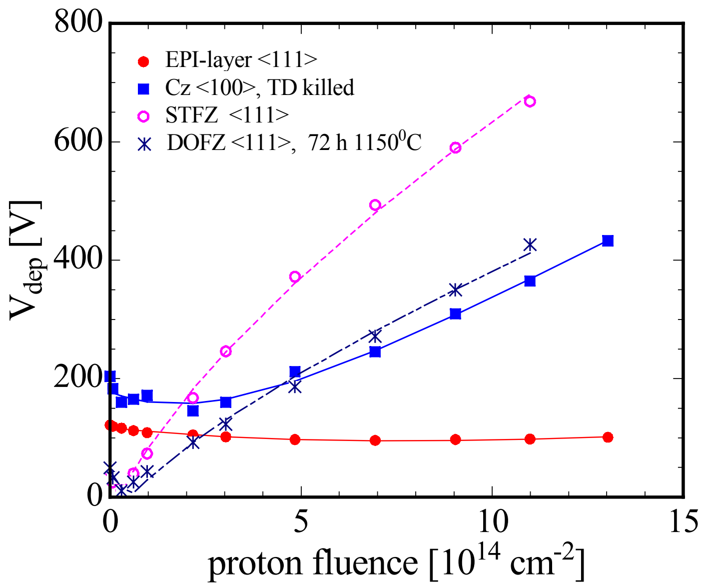

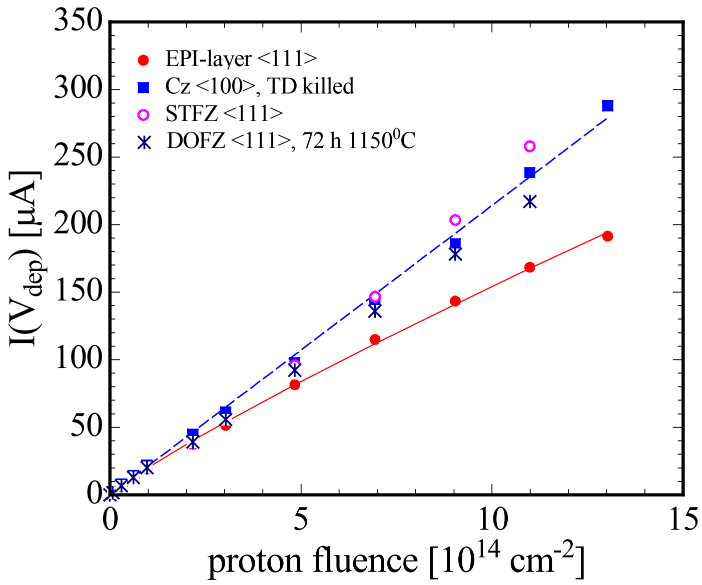

Data From G.Lindstrom et al.

EPI-silicon:

- **No type inversion**
- **Small change in depletion voltage up to $1.3 \cdot 10^{15}$ p/cm²**

- **No difference in reverse current between STFZ, DOFZ & Cz**
- **Small reduction for EPI-silicon at high fluences**

Recent results with n-in-p microstrip detectors

Liverpool & CNM-Barcelona within RD50
Data presented by G. Casse at Vienna Conference, February 2004

- ❑ **Miniature n-in-p microstrip detectors (280µm thick) produced by CNM-Barcelona using a mask-set designed by the University of Liverpool.**

- ❑ **Detectors read-out with a SCT128A LHC speed (40MHz) chip**

- ❑ **Material: standard p-type and oxygenated (DOFZ) p-type**

- ❑ **Irradiation: 24GeV protons up to 3 10^{15} p cm^{-2} (standard) and 7.5 10^{15} p cm^{-2} (oxygenated)**

CCE ~ 60% after 3 10^{15} p cm^{-2} at 900V(standard p-type)

CCE ~ 30% after 7.5 10^{15} p cm^{-2} 900V (oxygenated p-type)

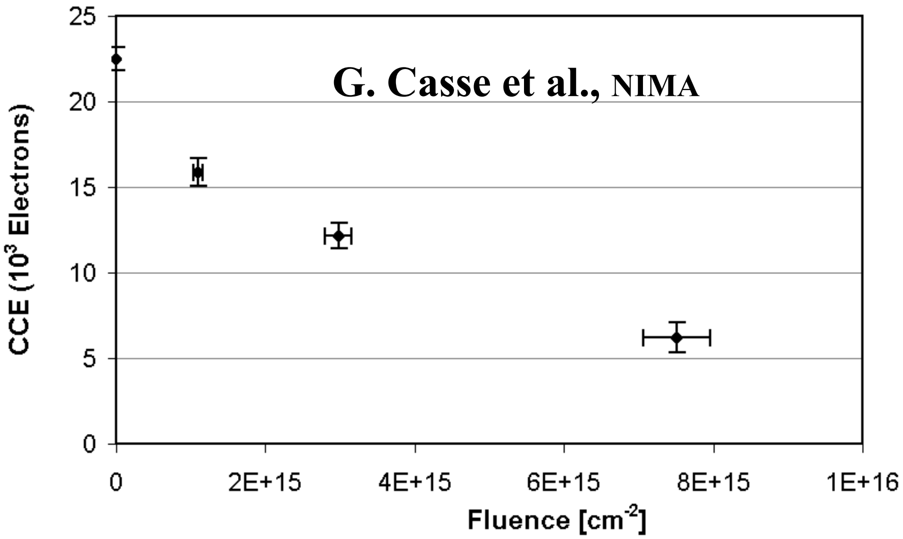

At the highest fluence Q~6500e at V_{bias}=900V corresponding to: ccd~90µm

Towards p-type Si detectors

n-on-p batch IRST – SMART INFN

#	sub-type	comments
3	FZ 525	p-spray 3E12
3	FZ 525	p-spray 5E12
3	FZ 200	p-spray 3E12
3	FZ 200	p-spray 5E12
6	MCz	no OG; p-spray 3E12
5	MCz	no OG; p-spray 5E12

→ **FZ <100>**
p-type
>5000Ωcm
525μm

→ **FZ <100>**
p-type
>5000Ωcm
200μm

→ **MCz <100>**
p-type
>1.8kΩcm
300μm

C. Piemonte, presented at 5th RD50 Workshop, October 2004, Florence

n-on-p – CV on diodes

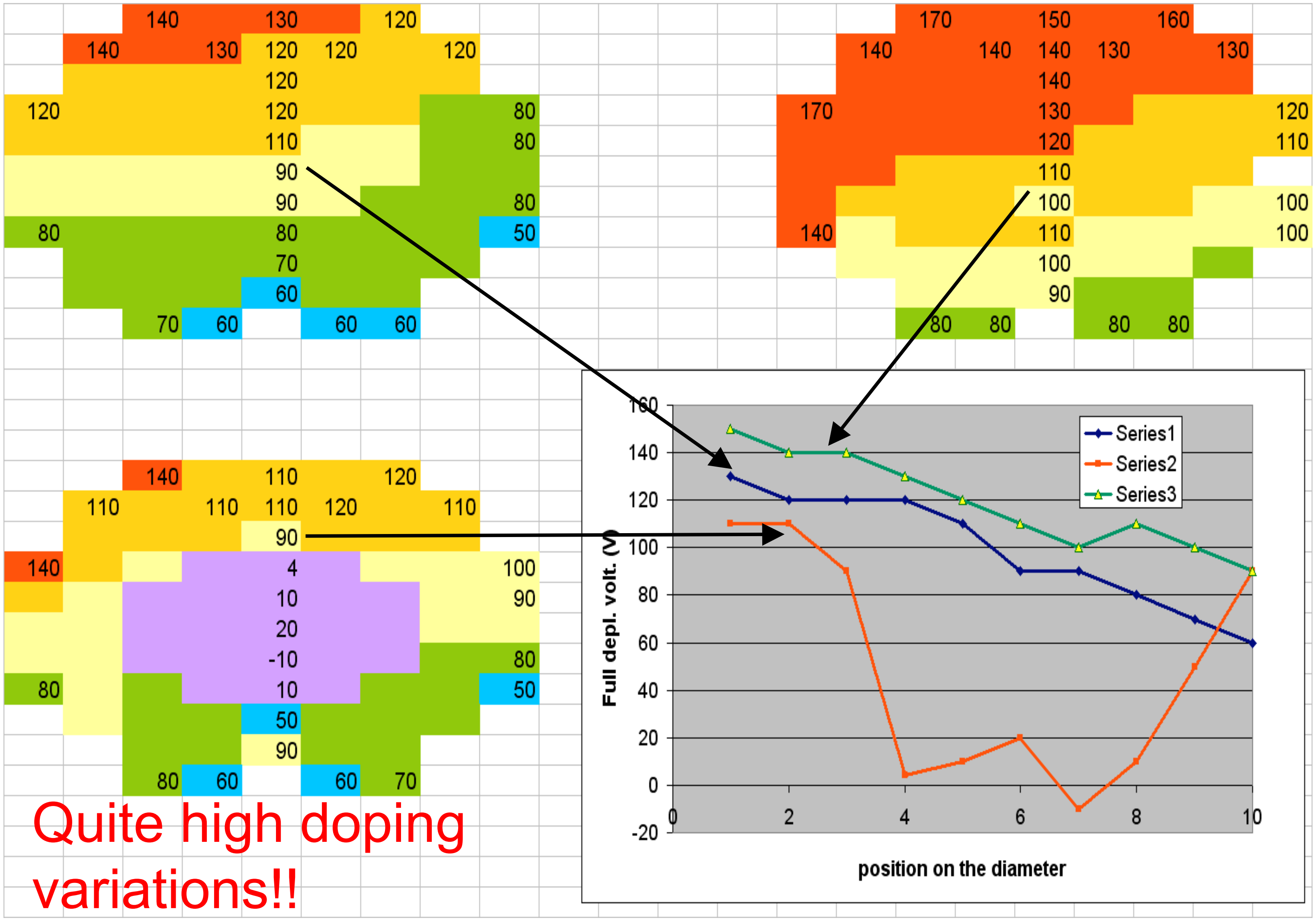

		140		130		120		
	140		130	120	120		120	
				120				
120				120				80
				110				80
				90				
				90				80
80				80				50
				70				
				60				
		70	60		60	60		

		170		150		160		
	140		140	140	130		130	
				140				
170				130				120
				120				110
				110				
				100				100
140				110				100
				100				
				90				
		80	80		80	80		

		140		110		120		
	110		110	110	120		110	
				90				
140				4				100
				10				90
				20				
				-10				80
80				10				50
				50				
				90				
		80	60		60	70		

Quite high doping variations!!

N. Zorzi, presented at the RD50 Meeting on p-type detectors, February 2005, Trento, Italy

Probably due to fluctuations of the oxygen concentration.

Activation of thermal donors in p-type Cz Si

- ☐ Six $p^+/p/n^+$ diodes (active area 0.25cm^2, thickness 300µm) manufactured on p-type Cz Si Okmetic wafers (nominal resistivity 5kΩcm) at the Helsinki University of Technology, Finland .
- ☐ Devices studied at BNL by Transient Current Technique using a pulsed infrared laser (660nm) beam placed close either front or back electrodes. Collected charge measured in the range 0-400V, to determine full depletion voltage and sign of the effective space charge concentration N_{eff}.
- ☐ An isothermal annealing cycle has been performed at 430°C with different time interval from 45min to 120min. TCT has been measured before and after each annealing step.

M. Bruzzi, Z.Li, J. Harkonen, presented at the 5th RD50 Workshop, October 2004, Florence

Full depletion voltage (V_{fd}) and effective concentration (N_{eff}) as determined by TCT before annealing

Sample	V_{fd} [V]	N_{eff} [10^{12}cm^{-3}]
P7	262,00	- 3.86
P8	226,65	- 3.34
P17	229,05	- 3.37
P46	232,95	- 3.43
P57	237,15	- 3.49
P58	214,75	- 3.16

No correlation between N_{eff} and position in wafer

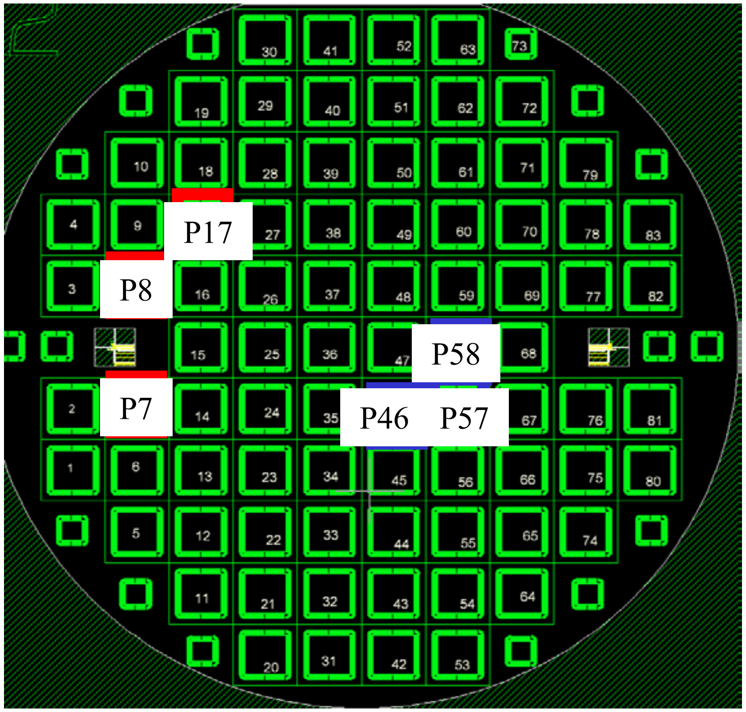

M. Bruzzi, Z.Li, J. Harkonen, presented at the 5th RD50 Workshop, October 2004, Florence

The generation rate for N_{eff} is not correlated to the initial N_{eff} value, but depend on the position of the diode inside the wafer → O_i concentration or other impurity involved

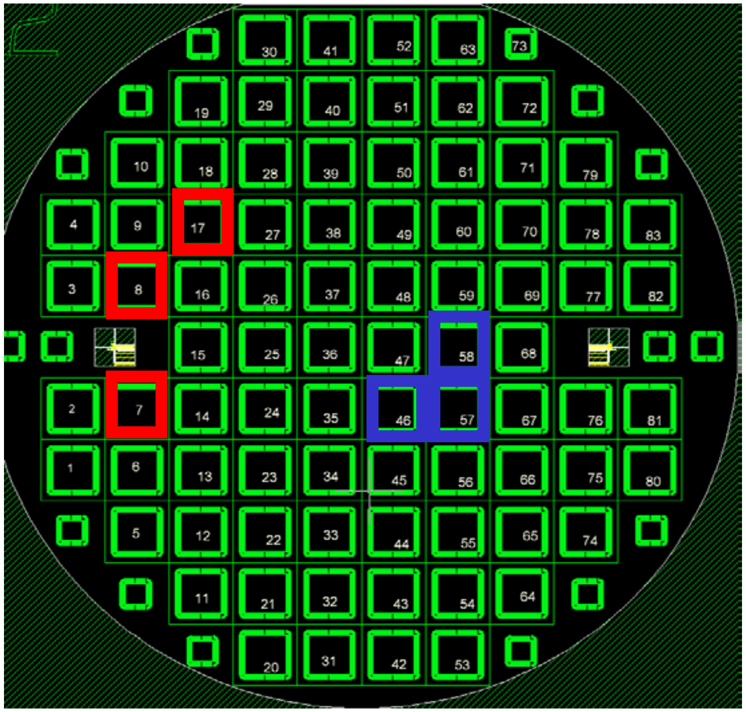

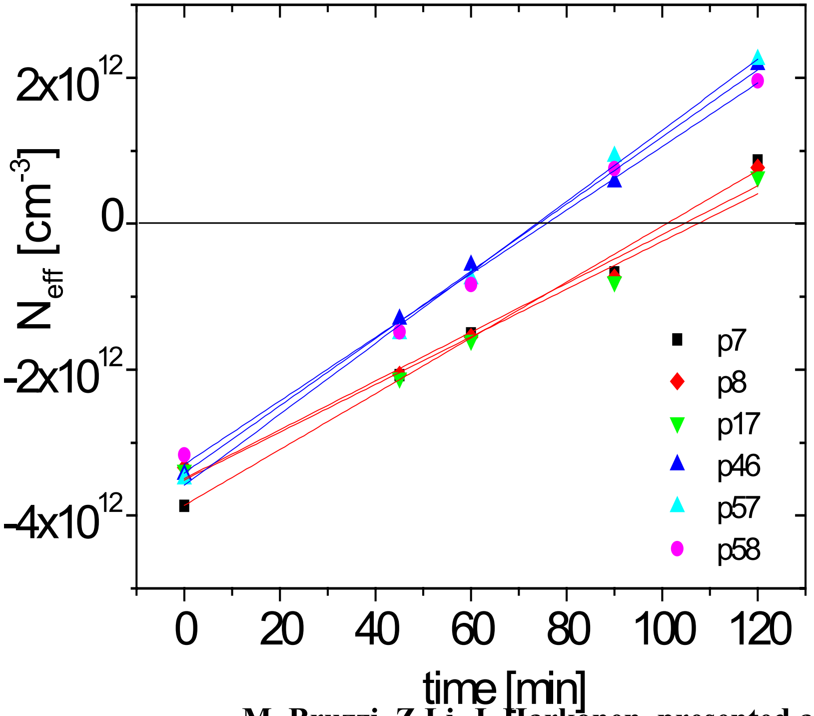

Initial N_{eff} (🟥)/N_{eff} (🟦) = 1.05

Final N_{eff} (🟥)/N_{eff} (🟦) = 2.8

In the simple hypothesis:

$$N_{eff} = N_{eff}(0) + b(T)^{*}\ t$$

$b = (3.48 \pm 0.30) \times 10^{10}$ cm^{-3}/min

$b = (4.61 \pm 0.25) \times 10^{10}$ cm^{-3}/min

M. Bruzzi, Z.Li, J. Harkonen, presented at the 5th RD50 Workshop, October 2004, Florence

Comparison of TSC spectra before and after thermal treatment at 430°C

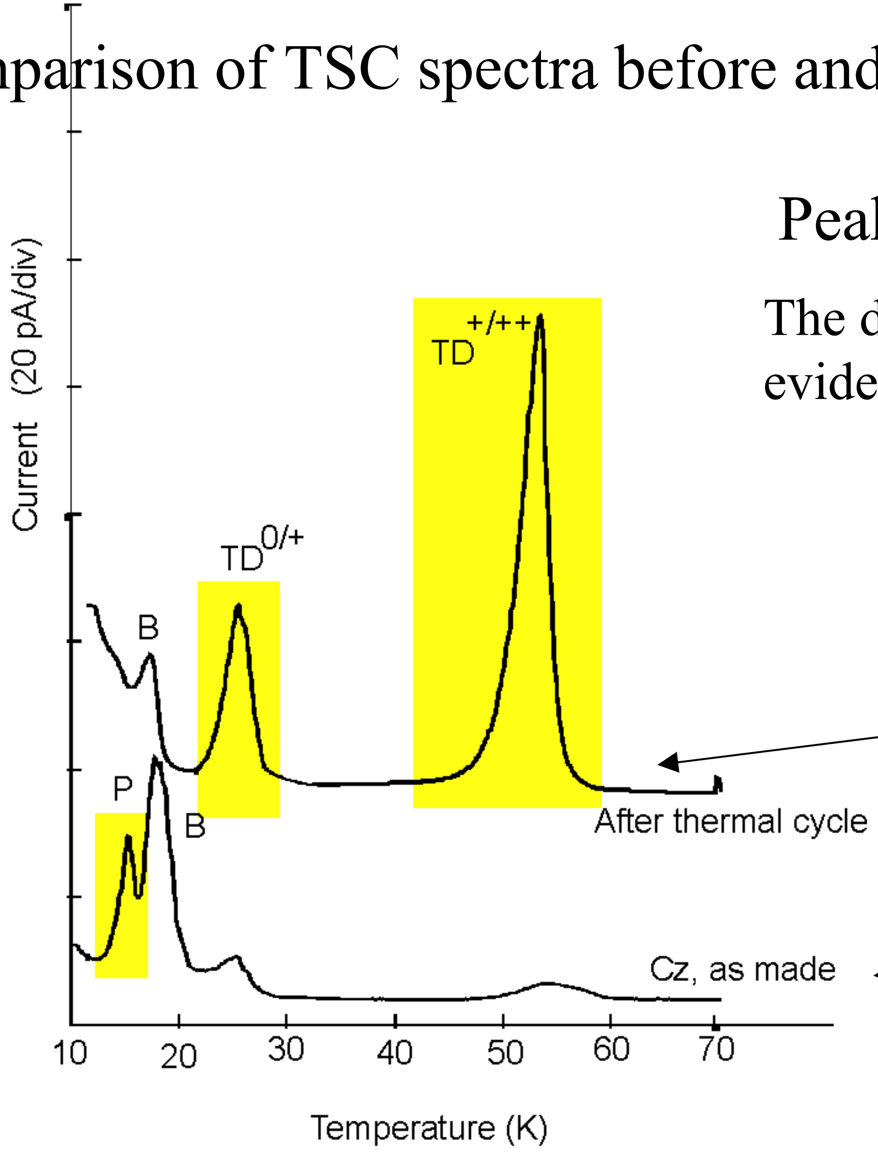

Peaks in yellow are donors

The donor-like behaviour was proved by evidence of Poole-Frenkel effect

Helsinki diodes $p^+/p/n^+$ after thermal treatment

before

M. Bruzzi, D. Menichelli, M. Scaringella, presented at the RD50 Meeting on p-type detectors, February 2005, Trento, Italy

3. TD activation by irradiation

p-on-n IRST
no LTO and sintering at 380°C
24GeV/c p up to 4x10^{14}p/cm^2
annealing of 1260min at 60°C
Full depletion voltage 93V.

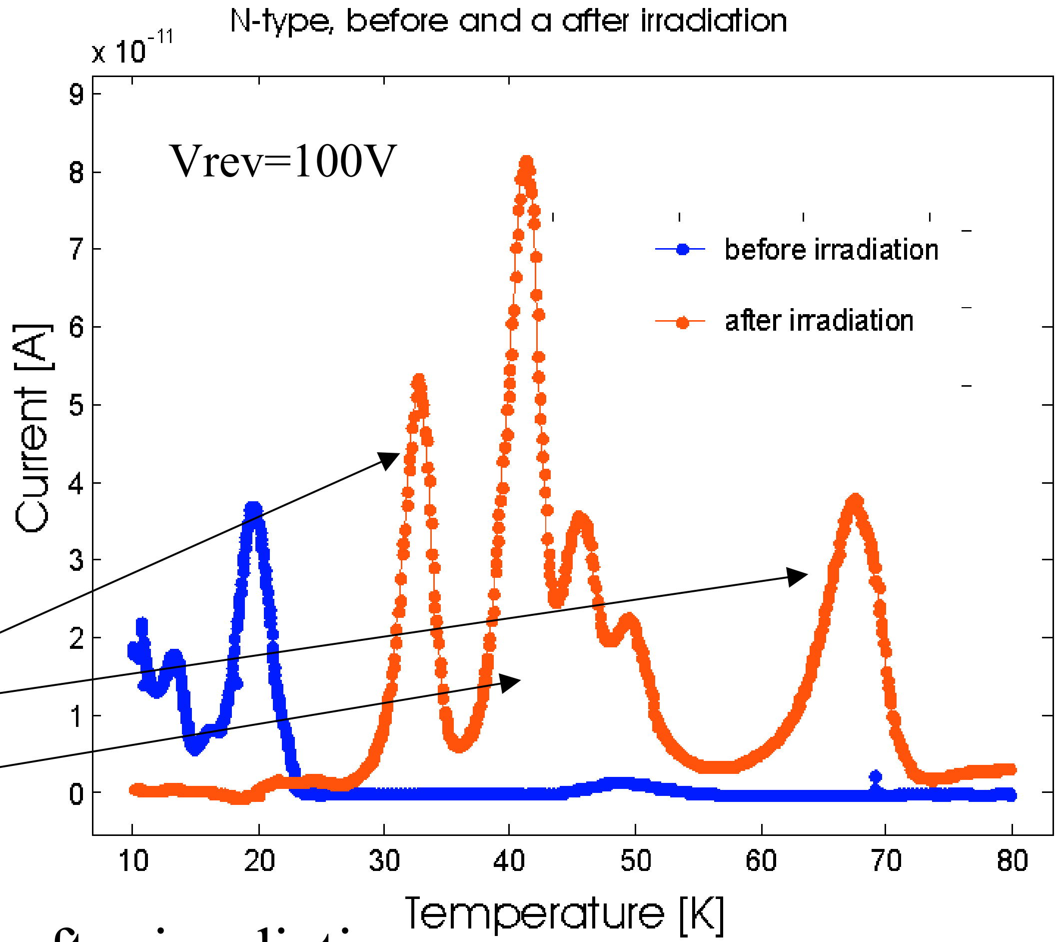

Main results

Removed : P and peak at 20K
Formed: peak at 30K – donor
CiCs – VO
group at 40-50K

No evidence of TD activation after irradiation

M. Bruzzi, D. Menichelli, M. Scaringella, presented at the RD50 Meeting on p-type detectors, February 2005, Trento, Italy

The radiation-induced peak at 30K is a donor (not a TD)

Shallow TSC peaks observed in a MCZ Si diode after irradiation with a 24GeV proton irradiation up to 4x10^{14} cm^{-2}. In the inset, the Pool-Frenkel shift observed on peak at 30K when the applied voltage is 100V (black line) and 200V (light line) is shown. This effect evidences the donor-like nature of the related energy level.

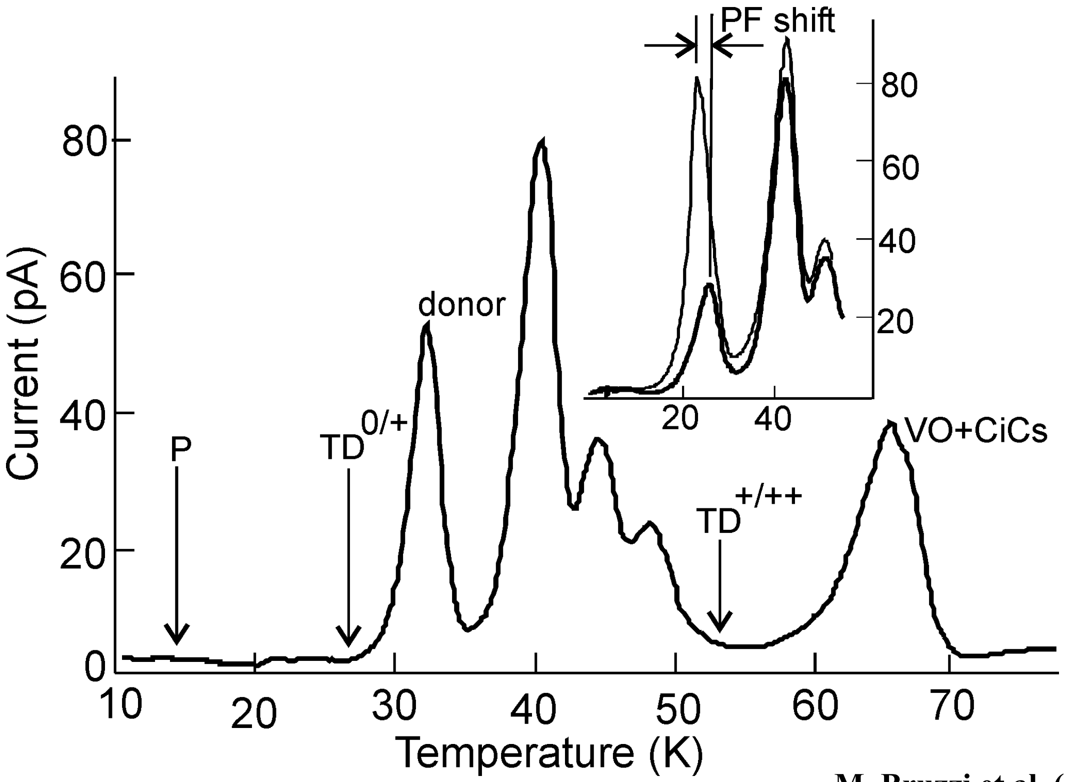

M. Bruzzi et al. (2005) in press on NIM A

Comparison p- and n-type MCZ after irradiation

n-on-p IRST
p-spray dose of $5x10^{12}cm^{-2}$
24GeV/c p up to $4x10^{14}p/cm^2$
annealing of 180min at 80°C
Full depletion voltage 337V.

Main results:

Same peaks formed
Lower 50K peak IO_2?

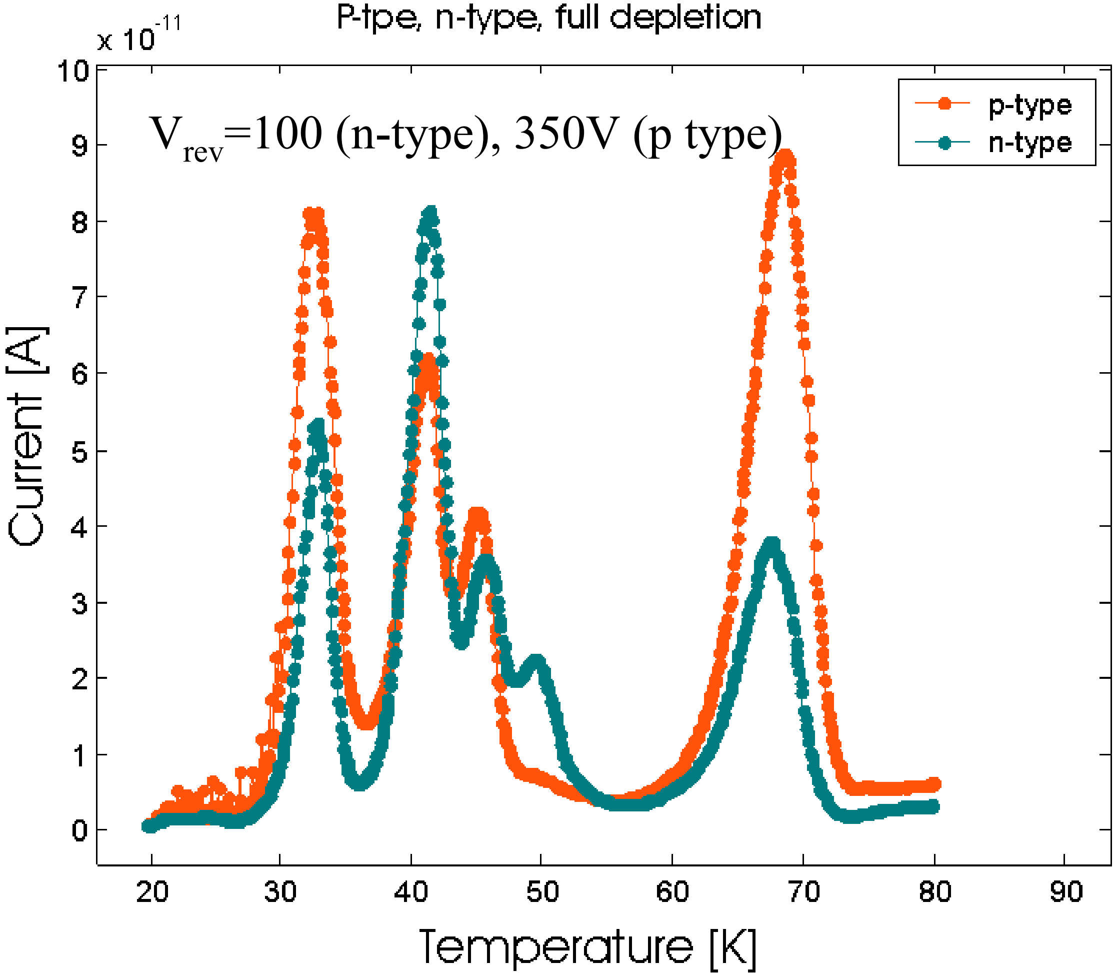

M. Bruzzi, D. Menichelli, M. Scaringella, presented at the RD50 Meeting on p-type detectors, February 2005, Trento, Italy

Improved radiation hardness of Cz Si seems to be due to a a radiation induced shallow donor

❑Thermal Donors can be activated by thermal treatment at 430°C, they compensate B dopant in p-type MCz Si and provoke type inversion.

❑A process at 380°C and no LTO is sufficient to keep TDs within negligible amounts

❑Irradiation does not activate thermal donors. A shallow donor level at 30K is produced by irradiation both in p-type and n-type MCz Si.

❑ while in n-type Si P is removed, B is not removed in p-type !

❑Other defects as C_iC_s, VO, V_2 C_iO_i are produced in p- and n-type MCz Si by irradiation.

M. Bruzzi, D. Menichelli, M. Scaringella, presented at the RD50 Meeting on p-type detectors, February 2005, Trento, Italy

Device Engineering - Thin Detectors

Motivation for using thin detectors:

- Smaller leakage current: $I_{leak} \propto W$, W sensitive detector thickness
- Smaller voltage for total depletion: $V_{dep} \propto W^2$
- Charge collection at very high fluences is limited by carrier trapping

  Extrapolated mean free drift length (G. Kramberger) at 10^{16} n/cm^2:

  $\lambda e \approx 20\ \mu m$, $\lambda_h \approx 10\ \mu m$
- **Drawback:** mip signal ~ 3500e-h pairs

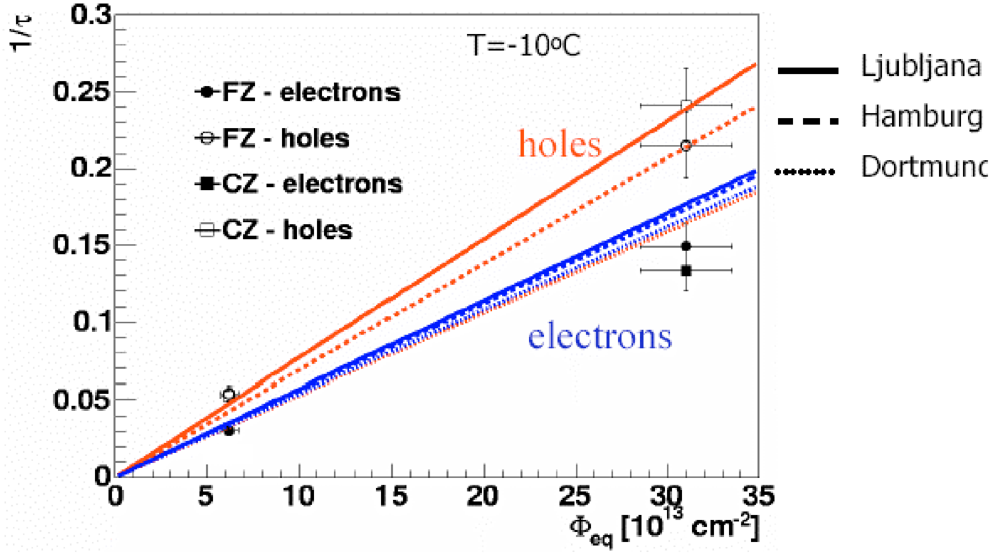

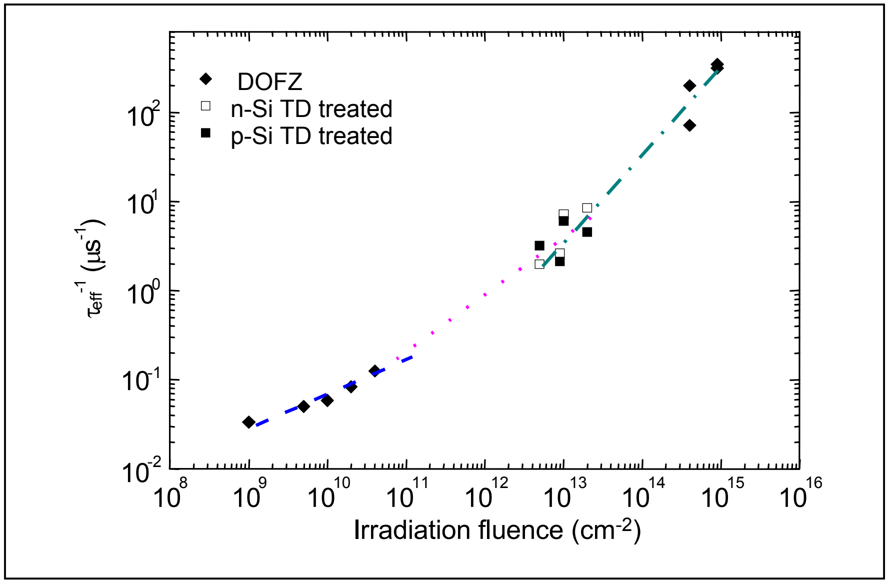

(*G. Kramberger, 4-th RD50 Workshop, May 2004*)

(*J.Vaitkus et al., IWORID-6, July 2004, Glasgow*)

E. Fretwurst, Univ. Hamburg, RESMDD04, Florence, October 10.-13. 2004

Device Engineering - Thin Detectors

Technical Approaches

ITC-IRST, Trento, Italy

Thinning with chemical attacks

Cross section of a thinned silicon detector

IRST: SEM of a silicon wafer thinned by TMAH

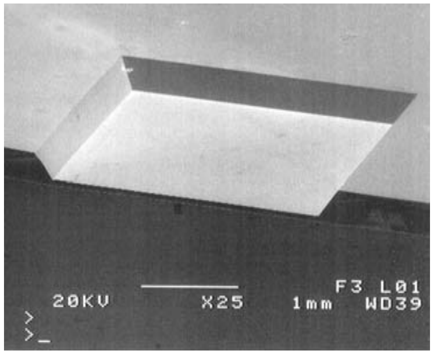

(E. Ronchin et al., NIM A 530 (2004) 134)

MPI-Munich, Germany

Wafer bonding technology

b) wafer bonding and grinding/polishing of top wafer

d) anisotropic deep etching opens "windows" in handle wafer

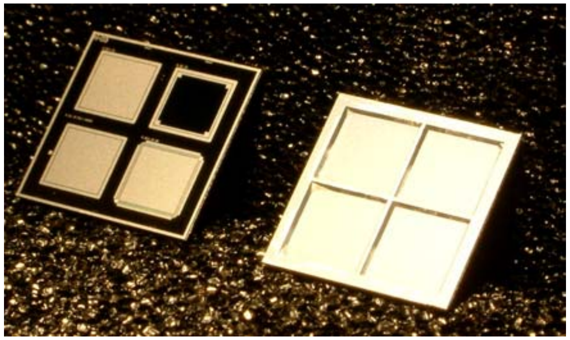

Photo:
front (left) and
back (right) view
of thinned devices

(L.Andricek, 1st ECFA Workshop, Montpellier, Nov. 2003)

Device Engineering: 3D detectors

proposed by Sherwood Parker

- Electrodes:
  - **narrow columns along detector thickness-“3D”**
  - **diameter:** 10μm **distance:** 50 - 100μm
- Lateral depletion:
  - **lower depletion voltage needed**
  - **thicker detectors possible**
  - **fast signal**
- Hole processing :
  - **Dry etching, Laser drilling, Photo Electro Chemical**
  - **Present aspect ratio (RD50) 13:1, Target: 30:1**
- Electrode material
  - **Doped Polysilicon (Si)**
  - **Schottky (GaAs)**
- Irradiation tests
  - **$1\cdot10^{15}$ p/cm^2 (55 MeV, 23GeV)**
  - **$2\cdot10^{14}$ π/cm^2 (190 MeV)**
- Possible application
  - **LHCb Velo – Glasgow University**
  - **TOTEM edgeless detectors – Brunel, Hawaii (not RD50)**

Present size up to ~1cm^2

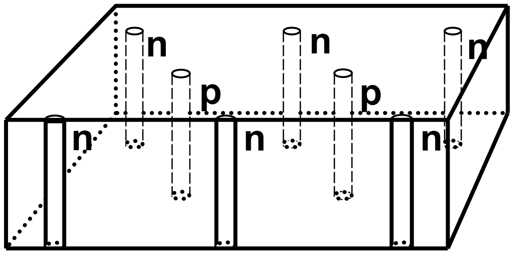

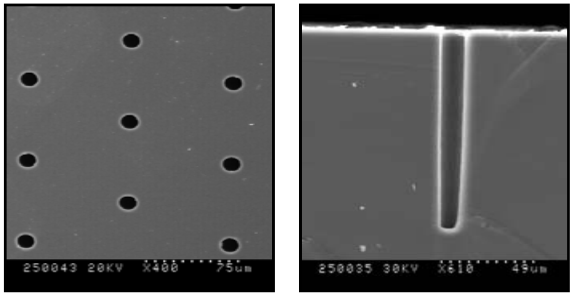

α spectroscopy

[P. Roy, Glasgow, 2nd RD50 Workshop]

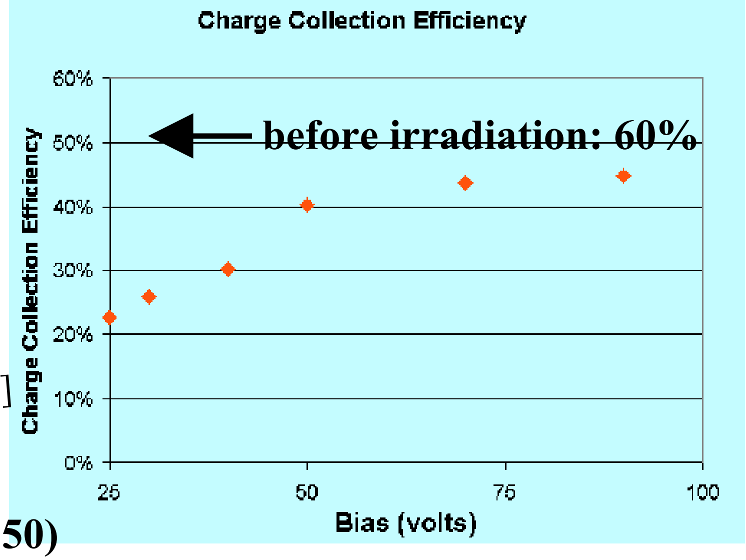

Device Engineering –Semi-3D Detectors

Semi 3-D devices proposed by Z. Li, BNL.

- Planar technology easier to process than 3D sensors
- Single-sided processing
- Large reduction in detector full depletion voltage after type inversion
- Processing of first prototype completed (presently under test).

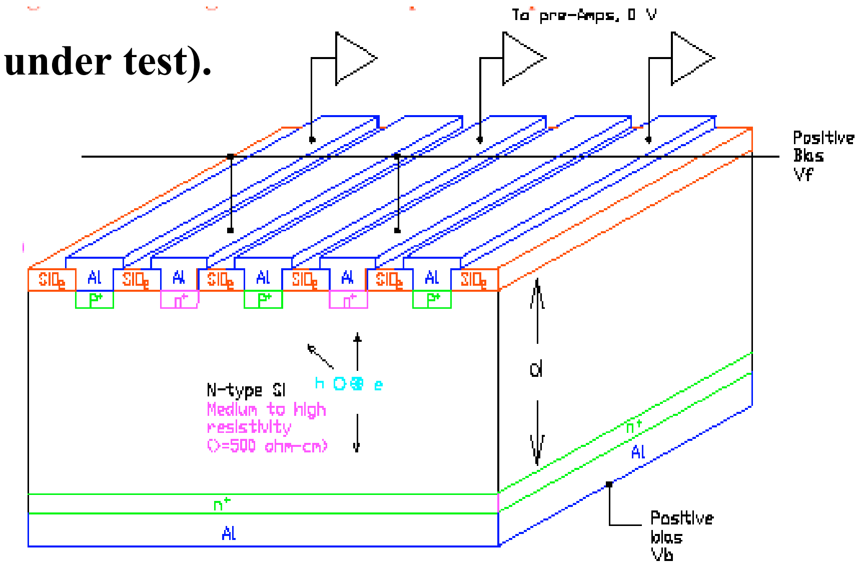

Z. Li et al. NIMA478, (2002), 303-310

n+(150V) p+(0 V) n+(150V)

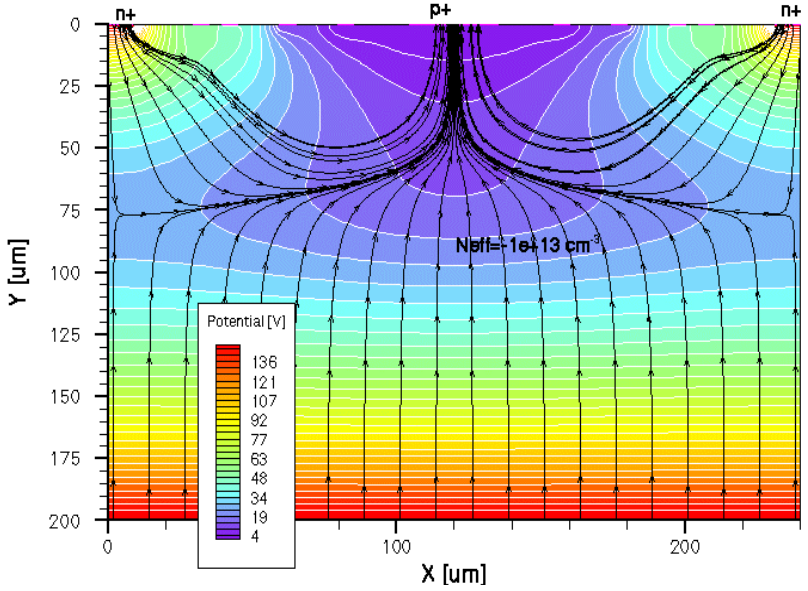

n+(150V)

Simulation of electric profile in semi 3D after irradiation to $5x10^{14}$ n/cm^2.

E. Fretwurst, Univ. Hamburg, RESMDD04, Florence, October 10.-13. 2004

Summary

- Different Si materials and new device concepts allowed to imrpove the radiation resistance of Si detectors. The challenge is the development of tracking detectors for SLHC-experiments, under study by the CERN-RD50 collaboration.

- In different tracking areas different detector concepts and materials have to be optimized:
  Outer layers exposed up to 10^{15} hadrons/cm^2: Change of the depletion voltage and the large area to be covered are the major problems.
  High resistivity Cz detectors might be a cost-effective radiation hard solution.
  Inner layers exposed up to 10^{16} hadrons/cm^{-2} : The sensitive detector thickness is strongly reduced due to carrier trapping. Two promising options are:
  Thin/EPI detectors; drawback: radiation hard electronics for small signals needed
  3-D detectors; drawback: complicated technology which has to be optimized

- Miniature micro-strip and pixel detectors on defect engineered Si were fabricated by RD50. First tests with LHC like electronics are encouraging: CCE ≈ 6500 e for n-in-p oxygenated microstrip detectors irradiated up to 7×10^{15} cm^{-2} (23 GeV protons)

- A microscopic model of the radiation damage of Si detectors is in progress. The key idea is to consider the shallow donor production in Cz Si as a way to compensate the deep acceptor concentration created during irradiation.